Towards national estuarine modeling and characterization/classification systems: a pilot study for Coos Bay

Nate Hyde

A thesis presented to the faculty of the OGI
School of Science and Engineering at
Oregon Health and Science University in
partial fulfillment of the requirements for the
degree of

Master of Science
in
Environmental Science and Engineering

June 2007

The thesis "Towards National Estuarine Modeling and Characterization/ Classification Systems: A Pilot Study for Coos Bay" by Nathaniel Hyde has been examined and approved by the following Examination Committee:

António Baptista, Ph.D., Thesis Advisor
Professor

Karen H. Watanabe, Ph.D.
Assistant Professor

Parker MacCready, Ph.D.
Associate Professor
University of Washington

Steven S. Rumrill, Ph.D.
Assistant Professor
University of Oregon

Dedication

To Timory and my Motu Ram

Acknowledgements

I would like to thank my advisor Antonio Baptista, whose patience, guidance and vision were instrumental to this thesis. I count myself extremely fortunate to have had the opportunity to learn from this rare man whose first rate intellect and dedication are matched by his integrity and good humor.

I would also like to thank the rest of my thesis committee, Parker MacCready, Steve Rumrill and Karen Watanabe, both for their substantial contributions and for taking the time to evaluate and comment upon this thesis.

I could not have completed this thesis with my sanity intact without the support of my family and friends. I would like to thank my wonderful parents, Barney and Roberta Hyde, for blessing me with their love, wisdom and DNA. I would especially like to thank my wife, Maruti Gupta, whose unflagging faith in my abilities pulled me through the rough patches. She makes my life happier and easier in countless ways, and is a treasure beyond reckoning. Most of all I would like to acknowledge my sister Timory, whose character, love, adventurous nature and outrageous sense of humor shaped me in more ways than I can count.

Generous grants from the National Science Foundation (ACI-0121475, OCE-0424602), National Oceanic and Atmospheric Administration (NA04NOS4730156) and Bonneville Power Administration (23677, 28143) provided financial support for this research. Any statements, opinions, findings, conclusions or recommendations expressed in this material are those of the authors and do not necessarily reflect the views or policies of the sponsors, and no official endorsement should be inferred.

Contents

Signatures page ii
Dedication iii
Acknowledgements iv
Contents v
List of Tables vii
List of Figures viii
Abstract xi
1. Introduction 1
1.1. IOOS and a National Estuarine Modeling System 1
1.2. Literature Review 2
1.2.1. Integrated Ocean Observing System 2
1.2.2. Estuarine Phenomena 3
1.2.3. Coos Bay Circulation 4
1.2.4. Estuary Classification 5
1.3. Thesis Objectives 10
1.4. Semi-implicit Eulerian Lagrangian Finite Element model 11
2. An exploration of new concepts in estuarine modeling systems, with application to Coos Bay 15
2.1. Introduction 15
2.2 The Coos Bay EMS pilot: Purpose and Plan 17
2.2.1 Grid and Bathymetry 18
2.2.2 Atmospheric and Ocean Boundary Conditions 19
2.2.3 River Flow Data 20
2.2.4 Calibration and Validation Data 21
2.3 Coos Bay Model Skill Assessment 22
2.3.1 Methodology 22
2.3.2 Coos Bay RDFS Results 23
2.3.3 Summary of Coos Bay Results 27
2.4 Implications for the Rapid Deployment Forecasting System 29
Chapter 2 Figures and Tables 33
3. Model-Based Estuarine Characterization and Classification Systems: Concept and Pilot Application 81
3.1 Introduction: The vision for a model-based estuarine characterization and classification system 81
3.1.2 Characterizing flushing times in estuaries 82
3.1.3 Characterizing baroclinic circulation and density stratification 83
3.2 Methods 84
3.2.1 From EMS to MECCS 84
3.2.2 Parameter Definitions and Descriptions 85
3.3 Characterizing Coos Bay 91
3.3.1 Introduction 91
3.3.2 Flushing Time Parameters 92
3.3.2 Circulation Related Parameters 93

3.4 Discussion 96
3.5 Conclusion 100
Chapter 3 Figures and Tables 102
4. Conclusion 134
5. References 136
Biographical Information 141

List of Tables

Table 2.1: Data sources 74
Table 2.2 RMS error and index of agreement for all stations with elevation for all runs 75
Table 2.3 Amplitude, phase and model-data differences for K1 and M2 tidal constituents for all stations with elevation data lasting more than 4 weeks. 76
Table 2.4 Along channel velocity model-data comparison of RMS error, index of agreement and data and model tidal excursion for all 1982 NOAA stations..... 77
Table 2.5 Salinity RMS error and Index of Agreement 78
Table 2.6 Standard deviation and mean elevation for the NOAA tide gauge at Charleston, ccho3 and the SSNERR stations..... 79
Table 2.7 Calibration runs for determining source and solutions for velocity and salinity errors 80
Table 3.1: Flow ratio numbers for typical spring and neap prisms and river flows. 132
Table 3.2: Fraction saltwater correlations to river flow and tidal amplitude. 133

List of Figures

Figure 2.1: Components of an Environmental Modeling System (EMS)..... 33
Figure 2.2: The estuarine modeling systems vision..... 34
Figure 2.3a: Grid and ocean bathymetry. 35
Figure 2.3b: Grid transition from ocean to mouth..... 36
Figure 2.3c: South Slough grid. 37
Figure 2.3d: Grid from Empire to Isthmus Slough..... 38
Figure 2.4: Total Coos Bay freshwater input based on 1954-1981 West Fork of the Millicoma data from USGS. 39
Figure 2.5: Coos Bay tributaries used as model inputs..... 40
Figure 2.6: 1982 (top) and 2003 (bottom) model freshwater inputs..... 41
Figure 2.7: Primary calibration/validation sites..... 42
Figure 2.8: Periods of data for NOAA82 stations. 43
Figure 2.9a: Index of Agreement for different error types against a sine wave. 44
Figure 2.9b: Index of Agreement vs. a range of errors for different error types. 45
Figure 2.10a: NOAA Charleston tide gauge model-data comparison for 1982 model run 46
Figure 2.10b: NOAA Charleston tide gauge model-data comparison for 2003 model run 46
Figure 2.11: Model/data elevation harmonic analysis comparison of major constituents for SSNERR stations and for the NOAA Charleston station during the Summer 1982 Winter-Spring 2003 model runs..... 47
Figure 2.12: Low pass filter (7 day Butterworth filter) on the NOAA Charleston tide gauge data and the model-data error. 48
Figure 2.13 a-b: Elevation at station epa01 and epa02..... 49
Figure 2.13 c: Elevation at station epa01, epa02 and epa0C for an August 2005 calibration run. 50
Figure 2.14 a-b: Model-data comparisons of along channel velocity from the NOAA82 data. 51
Figure 2.14 c-d: Model-data comparisons of along channel velocity from the NOAA82 data. 52
Figure 2.14 e-f: Model-data comparisons of along channel velocity from the NOAA82 data..... 53
Figure 2.14 g-h: Model-data comparisons of along channel velocity from the NOAA82 data. 54
Figure 2.14 h-j: Along-channel velocity plots stations at the head of the estuary. 55
Figure 2.15: Comparison of velocity: reference model, calibration model with the stray node removed and increased grid resolution and data. 56
Figure 2.16 a-b: Salinity plots for the summer 1982 run 57
Figure 2.16 c-d: Salinity plots for the summer 1982 run of stations near North Bend. .. 58
Figure 2.16 e: Salinity plots for the summer 1982 run of another stations near North Bend 59
Figure 2.16 f-g: Salinity plots for the summer 1982 run for a station near the city of Coos Bay 60
Figure 2.16 h-i: Salinity plots for the summer 1982 run of stations at the head 61

Figure 2.17: Salinity scatter plots for all depths at all NOAA82 stations 62
Figure 2.18: Comparisons between observations and the model at various depths. 63
Figure 2.19 a-b: Salinity sensitivity to calibration runs, with observed data 64
Salinity sensitivity to calibration runs at noa02 and noa06, with observed data 65
Figure 2.19 e-f: Salinity sensitivity to calibration runs at noa03 and noa09m, with observed data. 66
Figure 2.19 g-h: Salinity sensitivity to calibration runs at noa09b and noa10, with observed data 67
Figure 2.19 i-j: Salinity sensitivity to calibration runs at noa04 with observed data. 68
Figure 2.20 a-b: Salinity sensitivity to reductions in freshwater flow for the 1982 run, with observed data 69
Figure 2.21 a-b: Salinity time series for each depth at the SSNERR stations near the head of South Slough 70
Figure 2.21 c-d: Salinity time series for each depth at the SSNERR stations near the head of South Slough..... 71
Figure 2.22: Model vs. data scatter plot for SSNERR salinity 72
Figure 2.23: Harmonic analysis of salinity for the 2003 SSNERR stations 73
Figure 3.1: Coos Bay plotted on the classic Hansen and Rattray (1966) stratification diagram. 102
Figure 3.2: Diagram of the Model-based Estuarine Characterization and Classification System. 104
Figure 3.3a: Regions and points for the classification parameters. 105
Figure 3.3 b: Regions and points for the Columbia River Estuary..... 106
Figure 3.4a: Tidal exchange vs. tidal prism for the estuary and for the South Slough . 107
Figure 3.4b: The correlation between tidal amplitude and prism and tidal exchange... 108
3.5: Filling time vs. mean flow for the entire estuary and for the South Slough..... 109
Figure 3.6a: Freshwater flushing time vs. river flow for two regions in the Coos Bay estuary 110
Freshwater flushing time vs. river flow for two regions in the Columbia River estuary. 111
Figure 3.6 b: Freshwater flushing time vs. tidal amplitude in Coos Bay. 112
Figure 3.6 c: Freshwater flushing time vs. tidal amplitude in the Columbia River Estuary 113
Figure 3.7a: Summer 1982 Fraction of Saltwater vs. river flow and amplitude, by region. 114
Figure 3.8b: Winter 2003 Fraction of Saltwater vs. river flow and amplitude, by region. 115
Figure 3.9a: Coos Bay winter 2003 Fraction saltwater vs. tidal amplitude at the mouth 116
Figure 3.9b: Coos Bay winter 2003 fraction saltwater vs. net river flow..... 117
Figure 3.10 a: Path of the transect used to make the images in **Figure 3.10-11,** as well as the points for the interfacial Froude number calculations in **Figure 3.12** and **3.13** 118
Figure 3.10b: The time averaged (2 tidal periods: 24.8 hrs) salinity, residual velocity and mean velocity magnitude transects for a period when the interfacial Froude number > 1 (9/15)..... 119

Figure 3.10c: The time averaged (2 tidal periods: 24.8 hrs) salinity, residual velocity and mean velocity magnitude transects for a period when $F_i < 1$ (9/28)..... 120
Figure 3.11a: Time averaged (2 tidal periods: 24.8 hrs) salinity, residual velocity and mean velocity magnitude transects for a period when F_i is relatively low (2/6). 121
Figure 3.11b: Time averaged (2 tidal periods: 24.8 hrs) salinity, residual velocity and mean velocity magnitude transects for a period when F_i is relatively high..... 122
Figure 3.12 a: Coos Bay summer 1982 interfacial Froude number correlation with river flow 123
Figure 3.12 b: Coos Bay summer 1982 interfacial Froude number correlation with tidal amplitude..... 124
Figure 3.13a: 2003 Interfacial Froude number vs. net river flow..... 125
Figure 3.13b: Coos Bay winter 2003 interfacial Froude number vs. tidal amplitude ... 126
Figure 3.14: Interfacial Froude # and F_{SW} in the mouth 127
Figure 3.15: Filling rate from river flow (using the total Coos watershed river input 50th percentile climatology) and the regression equation in **Figure 3.6a** 128
Figure 3.16 a: Sample locations for Salt and Temperature diagrams..... 129
Figure 3.16 b: Model salinity vs. temperature plots for the summer 1982 model run show moderately distinctive mixing characteristics in the mouth, South Slough and estuary head. 130
Figure 3.16 c: Model salinity vs. temperature plots during the winter 2003 run show significantly distinctive mixing characteristics in the mouth, South Slough and estuary head, especially between the Valino Island and Winchester Creek stations 131

Abstract

Coastal ecosystems are inadequately understood in the context of increasing stresses from a combination of anthropogenic sources, natural variability and global climate change. Estuarine Modeling Systems (EMS) seek to advance knowledge of estuarine and near-shore circulation by combining observations, 3D numerical simulations, and data products. The Rapid Deployment Forecasting System (RDFS) has been conceived in order to facilitate the expansion of EMS. RDFS involves the quick deployment of model-based forecasting systems, which can be then be leveraged into high quality EMS. A pilot Coos Bay Estuary RDFS has been launched and developed towards a full fledged EMS. Through this development the opportunities and obstacles in the RDFS to EMS process are investigated.

With the spread of EMS comes the opportunity to re-visit and expand fundamental understanding of estuarine processes, including extended ability to conduct comparisons across estuaries. A newly conceived model-based estuarine characterization and classification system (MECCS) uses EMS to provide effective logistical means to hypothesize, to classify and to contrast estuarine behavior. At the core of MECCS is the filtering of simulation EMS databases, using mostly classical definitions of a range of dimensionless numbers and classification parameters. A pilot MECCS associated with the pilot Coos Bay EMS has been developed. Initial characterization and classification numbers focus on traditional parameters associated with stratification and circulation, as well as parameters associated with estuarine flushing.

1. Introduction

1.1. IOOS and a National Estuarine Modeling System

The oceans bordering the United States play critical roles in our weather, climate and national security, provide an important medium for commerce, and are a rich source of natural resources. About 41.45% of the U.S. population lives within 100 km of the coast (Socioeconomic Data and Applications Center). Furthermore, the population in coastal counties is 53% of the total US population, but coastal counties cover only 17% of the total area (not including Alaska). With coastal and interior county populations expected to increase at roughly the same rate, coastal county population densities will grow significantly faster than interior county densities (Crossett, 2004). This increasing population density places increasing stress on the economically valuable and ecologically sensitive coastal drainage basins (Malone, 2003). In addition to providing homes, the coastal regions are magnets for tourists. The US travel and tourism industry contributes ~$1.2 trillion to the Gross Domestic Product, of which roughly 85% is spent in coastal states (Houston, 2002). Simultaneous to the large and increasing anthropogenic effects, coastal ecosystems experience natural variability that is not adequately understood under normal conditions, and even less understood in the context of global climate change. The combination of anthropogenic uses and stresses with natural variability make it increasingly important to develop a broad and detailed understanding of coastal systems.

In 1998 an Integrated Ocean Observing System (IOOS) was proposed. IOOS is structured as two interdependent components: a global ocean component and a national coastal component. The coastal component has been further sub-sectioned into regional organizations. The regional organizations take advantage of existing ocean observing systems (OOS), and involve a broad spectrum of stakeholders who can make effective contributions to, and use of, the OOS, as well as generate state and local financial support. The basic components of IOOS are a foundation of observations, upon which rests an integrated data communication and management system, which then feeds data

products and analysis to the various user groups (Oceans.US 2003). At all stages it is important that the IOOS systems be integrated and sustained, as well as be highly responsive to user needs.

Predictive models form an important part of the analysis role of IOOS. A high-skill circulation model can provide useful scientific data, and together with proper analysis and translation tools it can also aid management decisions in such areas as harbor maintenance and expansion, regulation of seafood harvests due to pollution, and maintenance and expansion of healthy habitats. The Columbia River Ecosystem (CORIE) observation and modeling system (Baptista, 2006) is an example of a well developed Estuarine Modeling System (EMS). CORIE provides the foundation for the expansion of EMS to other estuaries, thereby enhancing the observation and analysis components of IOOS.

Despite their utility, few continuous EMS have been developed that link multiple estuaries with the near-shore ocean waters. In the past, it has required considerable investments in time, expertise and environmental sensing infrastructure to build, calibrate, validate, maintain and apply estuarine circulation models. To help overcome this barrier to wide-scale model use the Rapid Deployment Forecasting System (RDFS) was recently developed. RDFS seeks to apply advances over the last decade to quickly deploy estuarine circulation models and easily access model results, eventually forming the backbone of a National Estuarine Modeling System (NEMS). The expansion of high-skill EMS brings the opportunity to expand fundamental understanding of estuarine processes, including extended ability to conduct comparisons across estuaries. To that end, the first steps towards a model based estuarine characterization and classification system have been taken.

1.2. Literature Review

1.2.1. Integrated Ocean Observing System

Malone (2003) presents the motivation, goals and methods for development and implementation of the Integrated Ocean Observing System (IOOS). Two trends make detailed knowledge of coastal systems increasingly more important: human migration into coastal regions and unprecedented changes in coastal ecosystems. Many individual

efforts have been undertaken to understand the causes and impacts of these changes, but from a national perspective they suffer from redundancy, scarcity, inaccessibility, and lack of timeliness of raw data and analysis. IOOS seeks to integrate and fund existing and new systems so that redundancies are reduced, coverage and access are increased, and data and useful analysis are quickly available. The system is envisioned as having three broad components: a monitoring subsystem, a communications network, and a modeling and applications subsystem. Implementation of IOOS is facilitated by a federation of regional observation systems, which develop sustained state, regional and federal financial support. The implementation plan for IOOS also includes oversight of the design and implementation of the regional observing systems, and guidance to ensure that the systems are driven by local priorities, include existing programs, and engage stakeholders at all stages.

1.2.2. Estuarine Phenomena

In a widely used tome on estuaries, "Estuaries: A Physical Introduction," Dyer (1997) states that possibly the most satisfactory definition of an estuary is: "a semi-enclosed coastal body of water which has free connection to the open sea, extending into the river as far as the limit of tidal influence, and within which sea water is measurably diluted with fresh water derived from land drainage." A great variety of complex phenomena occur within estuaries. The basic dynamics of the estuarine salt balance is discussed in papers from the estuary classification section of the literature review (section 1.2.4), while the possible effects of the deep channels and extensive tidal flats found in Coos Bay are discussed here.

Section 2 of this thesis argues that current Coos Bay EMS errors are to a significant degree due to unknown bathymetry in, and assumptions made in constructing, Coos Bay's tidal flats and peripheral inlets. The basis for that analysis comes from the work of Speer and Aubrey (1985), who construct a 1D circulation model to investigate the affect of tidal amplitude to channel depth ratio and tidal flat volume on producing M2-M4 phase shifts in the tidal harmonics, which then produce ebb/flood asymmetries. They find that estuaries with smaller amplitude/channel depth ratios and high volume tidal flats produce "ebb dominant" systems: system in which flood tides are slowed and

lengthened by friction over tidal flats, while ebb tides speed out the deep channel. This combination of small amplitude/channel depth ratio and large tidal flats and inlet volume exist in Coos Bay.

Blanton (2001) describes some of the possible effects of ebb dominance in the Mira Estuary, Portugal. The Mira, like Coos Bay, is a mesotidal coastal plain estuary. Blanton finds that the Mira's first 10 km are ebb-dominant, and that ebb-flood asymmetries between parts of the estuary can lead to salt trapping that reduces the tendency for freshwater inputs to flush salt form the estuary. While the Mira's precise morphological characteristics are different from those of Coos Bay, the paper describes an example, and some of the mechanics, of how salt intrusion is enhanced in ebb dominant portions of estuaries.

1.2.3. Coos Bay Circulation

Meaningful investigation of the utility of RDFS requires choosing an estuary that presents an instructive mix of opportunity and challenge. Coos Bay, a mesotidal coastal plain estuary located on the south-central Oregon coast, provides both. Opportunities come from the existence of significant industry using or affecting the estuary, attendant regulatory agencies, and two local research agencies (the South Slough National Estuarine Research Reserve and the Coos Watershed Association), all of which can potentially provide assistance in developing a RDFS instance into a high skill EMS. Challenges include limited model input and calibration data outside the South Slough, and an estuary whose circulation has received relatively little detailed scientific scrutiny.

In one of the few papers discussing Coos Bay circulation, Blanton (1969) uses Coos Bay to analyze the tidal energy lost as a tidal wave progresses up the estuary, and compares it to the potential energy gain required to mix ocean water with the fresh water inflow. He finds that during the April 1963 observation period (river flow approximated as 50 m^3/s), Coos Bay has a tidal dissipation (G_m) to potential energy deficit (J) ratio of 520, which makes it a very well mixed estuary during this period. In addition to providing some background on Coos Bay circulation, this study provides an example of a type of classification that could be added to a Model-based Estuarine Characterization and Classification System (MECCS).

More recently, Hickey and Banas (2003) presented a survey of estuaries in the Pacific Northwest focusing on estuary-ocean interaction and the implications for coastal ecology. They note that the smaller estuaries (generally everything except the Columbia River) can be seen as extensions of the ocean in the summer due to extremely low river flows and high flushing. Coos Bay is a mesotidal (mean tidal range of 1.7 m) coastal plain estuary with highly variable seasonal river flows with monthly means ranging from 2.8 m^3/s in the summer to 190 m^3/s in the winter. The wet surface area of the estuary at mean sea level is around 34 km^2. Temperatures and salinities at the mouth during spring-fall of 1999 were around 9-11 °C and ~33 psu during upwelling (north to south) winds and around 11-13 °C and ~31 psu during downwelling (south to north) winds (Hickey and Banas, 2003). Upwelling and downwelling conditions correlated fairly well between the Washington estuaries (Grays Harbor and Willapa Bay) and Coos Bay. Due to low summer river inputs, nutrient supplies during the summer growth season are derived primarily from upwelling.

1.2.4. Estuary Classification

The classification numbers presented in section 3 focuses on estuarine circulation and flushing. Both topics have been the subject of copious research papers. This survey focuses a few highly relevant papers in the circulation category, and a few general and representative papers in the flushing time category.

1.2.4.1. Classification Numbers Related to Circulation and Stratification

Pritchard (1952) presents one of the earliest discussions of estuarine classification, much of which remains relevant today. Estuaries may be generally classified according to the rate of evaporation vs. the rate of freshwater input (negative vs. positive estuaries), geomorphological structure (fjord, coastal plain and bar built) and dominant cause of mixing (tides, wind and river). Pritchard describes the general circulation pattern and salinity distribution in (geomorphologically defined) coastal plain estuaries: high salinity at the mouth decreasing towards the head, increasing salinity with depth, and a two layer net flow that is seaward towards the surface and landward near the bottom.

Henry Simmons (1955) discusses the general hydraulic and shoaling characteristics of estuaries under a range of tidal and river discharge regimes. He notes that density stratification from the interaction of salty and fresh water result in distinct flow characteristics. Mixing is a key component for determining these characteristics, and Simmons was one of the first to separate estuaries into three broad mixing categories: highly stratified, partly mixed and well mixed (noting that the transition from one to the other is gradual and ambiguous). In stratified or partially mixed estuaries ebb flows are faster in the upper, fresh water zone, while flood flows are faster in the lower, salty zone. He finds that mixing changes with upland discharge and tidal prism, and uses the ratio of the two (flow/prism) for categorization. He found that flow ratios above 1 indicate a highly stratified estuary, ratios around 0.25 indicate a partially mixed estuary, and ratios below 0.1 indicate a well mixed estuary.

Hansen and Rattray (1965) investigated estuarine circulation and salt flux processes. Differential equations and boundary conditions for velocity and salinity in an idealized 2D (length and depth, with rectangular cross section) estuary are presented. The equations assume a balance between downstream salt flux through river flow and upstream salt flux through diffusion (which includes various methods of tidal dispersion) and advection. The three processes are found to be characterized by three dimensionless parameters: T (dimensionless wind stress), Ra (an estuarine analog of the Rayleigh number, with larger values indicating greater baroclinic circulation and smaller values indicating greater diffusive circulation), and M (the ratio of tidal mixing to river flow). The authors use the constant v (the fraction of salt advected seaward by river discharge that is balanced by diffusion, as opposed to advection) to tie together the relationships between T, Ra and M and salinity structure and circulation. These relationships form a foundation for the theoretical understanding of the non-linear interaction between estuarine salinity and circulation.

Having demonstrated the complexity of, and formed a theoretical basis for, the interaction between circulation and stratification, Hansen and Rattray (1966) developed a general estuary classification system based on quantified circulation and stratification characteristics. They found that the essential features of the determining bulk parameters from Hansen and Rattray (1965) (vRa, M/v and T, where v is the percentage of upstream

salt flux due to diffusion) can be expressed by three quantities having the dimensions of velocity: the freshwater velocity U_f (river discharge/cross sectional area), the rms tidal current speed U_t, and the densimetric velocity $U_d = \sqrt{gD\Delta\rho/\rho}$, where $\Delta\rho$ is the density difference between river and sea water and D is the mean depth. Their main categorizations are by type: type 1 with net flow seaward at all depths, type 2 where net flow reverses at depth and both advection and diffusion contribute to upstream salt flux, type 3 where net flow reverses at depth and advection dominates upstream salt flux, and type 4 which is a traditional salt wedge estuary. Types 1-3 are further subcategorized as type a, with little stratification, and type b, with significant stratification.

MacCready (1999) built upon the work of Hansen and Rattray and others by constructing 2D analytical and numerical models to analyze estuarine salinity responses to changes in tidal and river forcings. Significant simplifications, including using a rectangular estuary with 2 equal depth vertically averaged levels, were made to simplify the numerical model while retaining time dependence, two-layer exchange flow and along channel salinity and velocity variations. Analytical solutions were derived for exchange and diffusion-dominated estuaries. From these two models the response time and fraction of ocean water (sensitivity) from steady state to new steady state were calculated. It was found that response times and sensitivities were greatest in the estuaries with "intermediate" depth (generally between 15 and 30 m). Response times were greatest at the intermediate depths and decreased towards the shallow/deep extremes. Shallow estuaries responded to forcing changes more significantly than deeper estuaries, but the intermediate depth estuaries displayed the highest sensitivity. Increased river flow always resulted in some decrease in salinity. At depths deeper than intermediate, increases/decreases in tidal mixing tended to decrease/increase salinity intrusion. At shallower depths increases/decreases in tidal mixing tended to increase/decrease salinity intrusion. At the intermediate depths the transition between responses to tidal mixing were based on the amount of the change, with larger decreases/increases producing a transition from shallow to deep behavior at lesser/greater depths.

1.2.4.2. Characterization Numbers Related to Flushing Time

There have been numerous efforts to calculate flushing times in estuaries, as well as many studies in which flushing time estimates are integral to the study's conclusions. The following papers are chosen to provide examples of the different types of flushing time calculations that have been made, and variations in their application.

Tidal prism models estimate estuarine flushing due to tidal motions. At their simplest tidal prism models are calculated quite easily (by comparing estuary volume to tidal prism sizes), but include large assumptions about the amount of mixing during each flood tide and the amount of return flow after each ebb tide. Sanford (1992) created a tidal prism model to be applied to small, well mixed estuaries: just the sort of estuary for which tidal prism models are ideal. Sanford develops a basic model that accounts for four factors of effluent concentration *c*: source, decay, tidal flushing, and net inflow. The tidal flushing term equals $\frac{1}{T_E}\frac{1}{T}$, where T_E is the tidal exchange (equation {3.1}). The bulk of the paper is concerned with calculating the return flow factor *b*.

Wang et. al. (2004) created a model to estimate the residence time of the Danshuei River in Taiwan, where residence time is the average amount of time the water in the estuary at a given time stays in the estuary. Noting that there is little primary production despite high nutrients and low zooplankton, they conclude that the low concentrations of phytoplankton must be due to a low residence time or high toxicity. They note that residence and flushing times are essentially opposite perspectives on the transport time. They define the flushing rate as the e-folding time (the time for the effluent concentration to reduce by a factor of 1/e) for the flushing of a mass from the estuary. A laterally integrated 2D hydrodynamic eutrophication model is used to simulate the Danshuei. Residence times were calculated for a variety of river flow conditions, and the suitability of applying the calculation of flushing time (defined as full flushing rather than average residence time) by tidal prism (similar to equation {3.1}: $T_f = \frac{(V+P)T}{P}$) and fraction freshwater methods (identical to equation {3.3}) for the Danshuei are investigated. The river flow is found to have only moderate affect on residence time, with full, half and 0 flow residence times of 1.08, 1.55 and 2.23 days.

The tidal prism method with adjustments to account for return flow and river flow showed good agreement with the modeled (through particle tracking) residence times, and the fraction freshwater method for flushing time showed good agreement without adjustments.

Garcon et. al. (1986) studied the implications of tidal flushing in an estuarine embayment on dinoflagellate blooms. The researchers expected the shallow (max depth of 4.5 m at high tide) embayment with small (ungauged) fresh water input to be well mixed, and that tidal flushing would be inefficient. A dye study showed that tidal flushing was actually 70% of the tidal exchange (T_E), and the dye and salinity data showed evidence of significant baroclinic circulation. Because the flushing rate was near the dinoflagellate growth rate, they concluded that the dinoflagellates must move vertically away from the outgoing surface waters. This conclusion was supported by data from a period of drought, where the salinity (and presumably mixing) increased and the dinoflagellate count decreased, suggesting that the dinoflagellates were less able to avoid flushing.

Monsen et. al. (2002) illuminates some of the assumptions and pitfalls common to the use of various flushing or residence time calculations. She notes that the use of transport time scales is "pervasive in biological, hydrologic and geochemical studies," and identifies "flushing time, age and residence time as three fundamentally different concepts of transport time leading to three different approaches for calculating this scale." Flushing time, defined as $T_f = \frac{V}{Q}$ where V is the volume of a defined system and Q is the volumetric flow rate through it, suffers from not always knowing the values of these parameters and thus being treated as a continuously stirred tank reactor (CSTR) that allows flushing time to be calculated from observed outflow concentrations. The CSTR assumption that an introduced mass is instantly and evenly distributed throughout the volume is its major assumption. The tidal prism method is defined as $T_f = \frac{VT}{(1-b)P}$ where T is the tidal period, b is the return flow and P is the tidal prism. It requires that the system be well mixed, river flow must be small compared to tidal flow and the receiving body must be large enough to dilute the effluent. The residence time is the

amount of time a parcel of water starting at a specified location in the estuary will remain inside it. It is dependent on the specification of the entrance and exit boundaries, the time of release (in tidal systems), and generally assumes no re-entry once a particle leaves. The uses and drawbacks of each of these methods are then illustrated using data from Mildred Island, a tidal lake in the Sacramento-San Joaquin River Delta.

1.3. Thesis Objectives

The first half of this thesis presents the results of the Coos Bay pilot Rapid Deployment Forecast System/Estuarine Modeling System (RDFS/EMS). A numerical hydrodynamic model, the Semi-implicit Eulerian Lagrangian Finite Element model (SELFE), was applied to Coos Bay. In accordance with the RDFS concept, the Coos Bay model was brought on-line quickly and at little cost, with much of the model inputs and calibration/validation data contributed by local stakeholders. Enough data was collected to engage in a meaningful calibration/validation cycle and move significantly toward a model accurate enough to inform management decisions. The process of acquiring input data, and the methods used to estimate unknown input data, is covered. Model calibration and validation are discussed in the context of the difficulties inherent in achieving high model skill from a rapidly deployed model in a sparse data environment. From this pilot effort we justify the aptness of RDFS as a foundational component in the creation of an EMS.

The second half of this thesis is an investigation into, and initial development of, one of the potential advantages of a successful EMS system. Raw model results and simple plots (e.g. time series and transects) represent only the most basic of data products. For general science and management purposes it is useful to distill model results into metrics that meaningfully characterize aspects of estuary behavior. Physical oceanographers have been generating circulation and stratification classification numbers since at least the 1950s, when Simmons (1955) defined the flow ratio. Since then many more refined classification numbers have been developed, and access to a fully 3D data set creates the possibility for many more. Additionally, characterization numbers can provide useful information about the estuary to scientists in other fields as well as to resource management agencies, with flushing time estimates representing an important

example. The second half of this thesis describes early steps towards a Model Based Estuarine Characterization and Classification System (MECCS), with a focus on parameters relating to density stratification and effluent flushing rates. It uses the example of the Coos Bay model to illustrate the numbers, as well as to further characterize the Coos Bay Estuary.

1.4. Semi-implicit Eulerian-Lagrangian Finite Element model

Model runs were performed using SELFE, an unstructured grid, semi-implicit Eulerian-Lagrangian finite-element model for cross-scale ocean circulation, with hybrid S-Z vertical coordinates (Zhang and Baptista, 2007). SELFE is a primitive equation model solving for elevation, 3D velocity, salinity and temperature based on the Reynolds-stress averaged Navier-Stokes equations and the continuity equation, and closed with the equation of state. The governing equations solve for six independent variables: surface elevation η, salinity S, temperature T and velocities u, v and w. The equations make use of the hydrostatic and Boussinesq approximations. S vertical coordinates are an improvement on traditional σ coordinates (in which vertical coordinates are a ratio of the distance from bottom to surface) by allowing for increased resolution at the boundary layers. Z coordinates (in which vertical coordinates are absolute) at deeper levels are used to avoid the hydrostatic inconsistency, as described in (Zhang and Baptista, 2007).

The governing equations, with a brief descriptive sentence, are listed below.

Continuity equation:

$$\frac{\partial u}{\partial x}+\frac{\partial v}{\partial y}+\frac{\partial w}{\partial z}=0 \qquad \{1.1\}$$

Depth integrated continuity equation:

$$\frac{\partial \eta}{\partial t}+\nabla\bullet\int_{-h}^{\eta}\mathrm{u}dz=0 \qquad \{1.2\}$$

Momentum Equation:

$$\frac{D\mathrm{u}}{Dt} = \mathrm{f} - g\nabla\eta + \frac{\partial}{\partial z}\left(\kappa\frac{\partial \mathrm{u}}{\partial z}\right);$$

$$\mathrm{f} = -f\mathrm{k}\times\mathrm{u} + \alpha g\nabla\psi - \frac{1}{\rho_0}\nabla p_A - \frac{g}{\rho_0}\int_z^\eta \nabla\rho d\zeta + \nabla\bullet(\mu\nabla\mathrm{u}) \qquad \{1.3\}$$

Transport equations for salinity and temperature:

$$\frac{DS}{Dt} = \frac{\partial}{\partial z}\left(\kappa\frac{\partial S}{\partial z}\right) + F_s \qquad \{1.4\}$$

$$\frac{DT}{Dt} = \frac{\partial}{\partial z}\left(\kappa\frac{\partial T}{\partial z}\right) + \frac{\dot{Q}}{\rho_0 C_p} + F_h \qquad \{1.5\}$$

Density equation of state:

$$\rho = \rho_0(1 + \beta\Delta S - \gamma\Delta T) \qquad \{1.6\}$$

where

(x,y)	horizontal Cartesian coordinates, in [m]
z	vertical coordinate, positive upward, in [m]
∇	$\left(\frac{\partial}{\partial x}, \frac{\partial}{\partial y}\right)$
$\frac{D()}{Dt}$	$\frac{\partial}{\partial t} + u\frac{\partial}{\partial x} + v\frac{\partial}{\partial y}$
t	time [s]
$\eta(x,y,t)$	free-surface elevation, in [m]
$h(x,y)$	bathymetric depth, in [m]
$\mathrm{u}(x,y,z,t)$	horizontal velocity, with Cartesian components (u,v), in [ms^{-1}]
u	velocity in the x direction, in [ms^{-1}]
v	velocity in the y direction, in [ms^{-1}]
w	vertical velocity, in [ms^{-1}]
f	Coriolis factor, in [s^{-1}]
k	unit velocity vector in the z direction [ms^{-1}]
g	acceleration of gravity, in [ms^{-1}]
$\psi(\varphi,\lambda)$	earth tidal potential, in [m]
α	effective Earth elasticity factor
$\rho(x,t)$	water density; by default, reference value ρ_0 is set as 1025 $kg\ m^{-3}$
p_A	atmospheric pressure at the free surface, in [Nm^{-2}]
S,T	salinity and temperature [*practical salinity units (psu)*, ^oC]

κ	vertical eddy viscosity, in $[m^2 s^{-1}]$
μ	horizontal eddy viscosity, in $[m^2 s^{-1}]$
κ	vertical eddy diffusivity, for salt and heat, in $[m^2 s^{-1}]$
F_s, F_h	horizontal diffusion for transport equations (neglected in SELFE)
$\dot{Q}$	rate of absorption of solar radiation $[W\, m^{-2}]$
C_p	specific heat of water $[JKg^{-1}K^{-1}]$
β, γ	coefficients of expansion and contraction

Numerically SELFE is inspired on lessons learned from the ELCIRC model (Zhang et. al., 2004), which differs from SELFE by using finite-difference/finite-volume numerical solutions, and using a Z coordinate system in the vertical. The change to finite elements in SELFE allows higher-order solutions, which is especially important when applied to single derivatives. The hybrid vertical coordinates allow better resolution of the bottom boundary layer inside the estuary (a property of the S coordinates), while maintaining the correct representation of surface features such as the plume (a property of the Z coordinates). This flexibility is central to the model's ability to perform well in both oceanic and estuarine depth scales. The boundary between S and Z vertical coordinates was set at 100 m depth from MSL, above which the vertical grid consists of 20 σ levels of 4% of the total height from surface to bottom (up to 100 m).

The version of SELFE used in the bulk of this thesis solves advection using a Eulerian-Lagrangian method that reduces stability requirements but introduces a diffusion-like truncation error that can degrade model accuracy if the time step is too small relative to the grid size.

$$\mathrm{E} \sim \frac{\Delta_L{}^2}{\Delta t}[Cu](1-[Cu]) \qquad \{1.7\}$$

where Δ_L is the horizontal length scale, Δ_t is the time step in seconds, and Cu is the fractional (non integral) portion of the Courant number $v\frac{\Delta_t}{\Delta_L}$, where v is the velocity in the along channel direction.

SELFE has some flexibility in choice of turbulence closure models. For the model runs in this thesis the *k-kl* (kinetic energy and kinetic energy times length scale) generic length scale (GLS) closure model proposed by Umlauf and Burchard (2003) was used, with the Kantha and Clayson (1994) stability function. The surface mixing length

associated with GLS was set to 0.8 m for the entire grid. Maximum viscosity and diffusion was set to 1 in the ocean, and 0.01 inside the estuary. Minimum viscosity and diffusion was set to 10^{-6} through most of the domain, with the exception of the artificial mixing pools (described in section 2), where it was set equal to the maximum estuarine viscosity/diffusion of 0.01.

Although a version of SELFE with improved temperature simulation has recently been implemented, the version of SELFE used for this study (version 3m) is not considered accurate for temperature. Model accuracy is, therefore, judged only by comparison to elevation, velocity and salinity data. The model time step was set to 30 seconds, with output every 900 seconds.

2. An exploration of new concepts in estuarine modeling systems, with application to Coos Bay

2.1. Introduction

Ocean ecosystems are under increasing stress from a combination of anthropogenic sources, natural variability and global climate change. There are numerous agencies and institutions attempting to understand the effects of these factors, but from a national perspective these efforts suffer from redundancy, scarcity, inaccessibility, and untimeliness of raw data and analysis (Malone, 2003). Recently, a handful of efforts to integrate these groups on a national scale have emerged, including the Integrated Ocean Observing System (IOOS) (Malone, 2003). IOOS seeks to integrate and fund existing and new ocean observing systems so that redundancies are reduced, coverage and access are increased, and data and useful analysis are quickly available. IOOS is envisioned as having three broad components: a monitoring subsystem, a communications network, and a modeling and applications subsystem.

The Columbia River Ecosystem forecasting system (CORIE) provides monitoring, communications and modeling and analysis for the Columbia River estuary and plume (Baptista, 2006). The CORIE estuarine modeling system (EMS) has been developed over a ten year period by experts in the areas of physical oceanography, numerical modeling and sensor deployment and maintenance. EMS is centered on a numerical model of estuarine circulation which produces climate-scale simulation databases and generates forecasts. EMS also provides assessment and analysis tools, has access to a network of observations for quality control, and includes an information technology system. **Figure 2.1** describes the basic components of an EMS. CORIE is representative of the investments in personnel and infrastructure that are required to build, calibrate, validate, maintain and make use of a high skill EMS. With the experience and technological development at CORIE, advances in computer technology and the increasing availability of critical data, however, many of the once formidable

barriers to the development of new EMSs have been greatly reduced. As a greater number of estuaries are covered by an EMS it becomes feasible to combine them into larger scale modeling systems such as a National Estuarine Modeling System (NEMS). This vision is still in its early stages, however, and the means for spreading EMSs are not clear. The Rapid Deployment Forecasting System (RDFS) concept provides one method to stimulate the creation of new EMSs.

As illustrated in **Figure 2.2**, RDFS are early stage EMS. RDFS consists of the knowledge and basic infrastructure needed to quickly deploy a model-based forecasting system. These RDFS can immediately begin generating 3D forecasts of estuarine and near-shore circulation. Individual RDFS can then be leveraged into the missing EMS components (e.g. simulation databases, other simulations and assessment and analysis tools) in part by generating local support and acquiring local experience and resources. It is clear that an existing observation network would be an enormous benefit to this process, but otherwise the exact nature and priority of the components and processes that go into a successful evolution from RDFS to high-skill EMS are largely unknown.

Recently the RDFS to EMS process has been investigated by leveraging the foundation of technologies and experience developed at CORIE to rapidly create and deploy model forecasts of estuaries on the Oregon Coast, in Northern California and Tampa Bay, FL. In addition to these forecasts there are a handful of existing forecasting systems. The NOAA Physical Oceanographic Real-Time System (PORTS) is the most prominent, supporting forecasts for a number of highly used and commercially important estuaries such as New York/New Jersey Harbor, Chesapeake Bay and San Francisco Bay (Center for Operational Oceanographic Products and Services). In light of the successes of these forecasting systems and the expansion of data acquisition and availability due to the growth of IOOS and other monitoring/modeling efforts, there is a considerable opportunity to expand the number of EMS and move towards a NEMS. NEMS would fit well in the data analysis component of IOOS, and could in some regards mirror its integrated structure. NEMS would at its most basic level facilitate model data availability and methods sharing. Additionally, with the expansion of EMS systems comes increasing ability to characterize, compare and classify estuarine behavior.

Implicit in the RDFS concept is assisted development by non-modeling experts in a potentially observation limited environment. The implications of these limitations are investigated in this Coos Bay RDFS pilot. The author, a graduate student with a limited background in physical oceanography and numerical modeling, launched the Coos Bay EMS and brought it through multiple development cycles. From this pilot effort comes a greater understanding of the promise and limitations of RDFS, and some lessons for future applications.

2.2 The Coos Bay EMS pilot: Purpose and Plan

The Coos Bay EMS pilot does not necessarily seek to generate a high quality EMS suitable for management decisions, although such a result would have been welcome. The purpose, rather, is to take a rapidly deployed forecast (deployed by the author using the infrastructure developed by Turner and Baptista, private communication) far enough to provide a basis for understanding the advantages and limitations of RDFS as a system for generating high quality EMS. The assembly of the Coos Bay model and an analysis of the current state are presented in this section with the organizing principle being the implications for the efficacy of RDFS for producing management quality EMS.

Numerical models will require the specification of various parameters which can have a significant affect on the model performance. These parameters include options such as time step, drag, diffusivity and turbulence closure method. Appropriate values for these parameters can be found in model documentation and calibration, and are not discussed further herein. The model used in the Coos Bay EMS, SELFE, is similar to many circulation models in requiring six basic sets of inputs: a 3D grid incorporating bathymetry and major features, atmospheric forcings and boundary conditions, river forcings and boundary conditions, tidal constituents for ocean boundary elevations, values of salinity and temperature at the open ocean boundary, and initial conditions for salinity and temperature. Each of these inputs can be the product of multiple data sets and analyses. The rapid, low-cost assembly of these inputs (as envisioned in an RDFS) will likely result in model errors and uncertainties. The ability to identify model errors and discern their primary source is crucial to the transition from rapid deployment to operational forecasting system.

2.2.1 Grid and Bathymetry

Bathymetry data forms the foundation of a circulation grid, and inaccurate and/or unknown bathymetry can result in significant model error. In an RDFS context it is likely that the initial model deployment will be based on insufficient bathymetry. That this is the case in the Coos Bay EMS will illuminate some of the issues that may result. Because the Coos Bay channel is frequently dredged, recent (2004) channel bathymetry from the U.S. Army Corps of Engineers (USACE) was obtained. Bathymetry data outside the channel is less reliable. Surveys from the National Geophysical Data Center (NGDC) form the basis of the bathymetry outside the channel. NGDC surveys are from a variety of sources, and in this region none of them are recent. For example, the two NGDC surveys that cover portions of the eastern half of the estuary are from 1861 and 1890, making it unlikely that the areas they cover have not undergone significant changes. In addition to bathymetry, digital orthophotos from the Oregon Geospatial Enterprise Office were used to ensure that major features, such as the jetties and the dyke near North Bend, were represented.

The reference grid (**Figure 2.3**) is composed of 14634 triangular elements defined by 8435 nodes. Open ocean element sides are on the order of 5 km, and the deepest points are ~1200 m from mean sea level (MSL). Inside the estuary, element side lengths reduce to ~75 m inside the channel near the mouth, 30-80 m in the South Slough, and 100-200 m elsewhere. Grid features of interest include the main channel, tidal flats and peripheral bays, the South Slough, and the mixing pools.

The Coos Bay channel extends ~24.5 km from the mouth to the turning basin inside Isthmus Slough and is maintained at roughly 300 m across. Channel bathymetry determines the speed of tidal waves and other important circulation characteristics such as vertical circulation structure and stratification. Thus, accurate channel representation is crucial to an accurate EMS. In Coos Bay the areas outside the channel consist primarily of tidal flats and small peripheral bays. Because the bathymetry for the flats is so uncertain many parts of the tidal flats were set to a uniform elevation of 0 MSL. The decision to represent the tidal flats with a constant elevation appears to have had significant negative consequences for the representation of circulation, and represents the

type of choice that might be made in the context of rapid deployment with limited data, and in this case provides a cautionary tale.

The South Slough is geometrically complex with ~12% of the surface area and ~5% of the volume of the main estuary, and numerous inlets and small tributaries. Due to this relatively small size and complexity, designing a South Slough grid that works with the rest of the estuary is a challenge. Additionally, some features, such as the narrow natural channel extending from the mouth of the South Slough to Winchester Creek, are smaller than the available bathymetry resolution.

Early model runs severely under-estimated salinity intrusion in the landward half of the main estuary. One possible explanation relates to specification of salinity boundary conditions at the river heads. Without observational data it is impossible to know what salinity boundary conditions to apply at model river boundaries inside the head of tide. Imposing a salinity value of 0 at such a boundary shortens the area available for mixing. An extension of the rivers increased the model size from 8435 nodes to 11867 nodes without greatly improving the salt intrusion. This also increased computation time from less than 1/3 real-time to over 1/2 real time, severely slowing the calibration cycle. An alternative solution involves the creation of "mixing pools" – deep pools with high diffusivity that simulate the mixing that occurs beyond the model boundary – upstream from the area of concern. The mixing pools solution greatly improved mixing and salinity intrusion while limiting computational and data storage costs. Mixing pools were applied to the five rivers and streams in the main estuary (Isthmus Slough, Coos River, Willanch Creek, Kentuck Creek and Palouse/Larson Creek), but because salinity was not under-represented in the South Slough no mixing pools were placed there. While mixing pools significantly improved model performance, it may have masked the true error rather than compensated for it.

2.2.2 Atmospheric and Ocean Boundary Conditions

Wind effects can be very important as a direct cause of mixing in the estuary and as a driver of plume characteristics and upwelling vs. downwelling conditions outside the estuary. The extent of the effects will be based primarily on wind speeds, estuary surface area and regional topography. Local meteorological data can provide one source of wind inputs. Regional, national and global atmospheric models provide another. These

models can have spatial scales greater than those of the estuary, meaning local variations in wind effects can be lost. For the Coos Bay calibration runs wind and atmospheric pressure data come from the National Center for Atmospheric Research (NCAR) and National Centers for Environmental Protection's (NCEP) North American Regional Reanalysis (NARR) project (Mesinger et. al., 2006). NARR uses the ETA regional climate model (Black, 1994) with a 32 km resolution, 45 vertical levels and 3 hour time steps with data assimilation. While the 32 km horizontal resolution is generally adequate for estimating wind over the open ocean, 32 km is larger than the modeled region of the estuary in any direction. Thus there is a high degree of uncertainty regarding the accuracy of wind inputs directly over the estuary. For the Coos Bay RDFS it was hypothesized that NARR would be accurate enough to provide an indication of the model response to wind over the open ocean, and that directly over the estuary the effect of wind would be less important than other processes. Model results, however, show that even in a small estuary such as Coos Bay the wind can have significant effects.

The values of the eight tidal constituents (O1, K1, Q1, P1, K2, N2, M2 and S2) used to compute elevation boundary conditions were calculated using the tidal model by Mike Foreman (1977). Ocean initial conditions for salinity and temperature for the 2003 run are provided by the Navy Coastal Ocean Model (NCOM) from the Navy Research Lab (Martin, 2000). Initial conditions for the 1982 run were set to a uniform 34 psu and 10 ^{o}C, then ramped up for four weeks.

2.2.3 River Flow Data

Coos Bay receives ~66% of its fresh water from the Coos River, with the rest coming from approximately 20 much smaller rivers and streams. Historical flow data for Coos River tributary the West Fork of the Millicoma (WFM) comes from a U.S. Geological Survey (USGS) monitoring station from 1954 to 1981. The Coos Watershed Association provided flow data for water years 2003-2005, with some gaps, from the three main Coos River tributaries plus the relatively tiny Marlow Creek. Few of Coos Bay's other tributaries have available historical flow records. Data from Winchester Creek (1991 – 1996) and Pony Creek (1971 – 2004) are available from the Oregon Water Resources Department. There are no real-time gauges for any Coos Bay tributaries. A climatology of the total Coos Bay freshwater input based on the USGS WFM data is

shown in **Figure 2.4**. Flows are generally very weak (order of 1 m^3/s) in the summer and early fall, gradually increasing to fairly strong flows in the winter and spring (order of 100 m^3/s).

A visual examination of stream and watershed GIS images was used to aggregate the tributaries into the 7 rivers in **Figure 2.5**. Coos River freshwater discharge inputs for the 1982 run come from a climatology based on the USGS WFM data. A simple ratio of flows from the EFM, SFC, and Marlow Creek to the WFM was computed using 2003-2004 CWA data. Creating a climatology for the smaller tributaries is complicated by the relatively brief time span of the Winchester and Pony Creek records. The Coos River watershed is entirely inland and much larger and more varied than the watersheds of the other Coos Bay tributaries. Therefore, climatology from Winchester Creek is used to approximate the flow from the small watersheds. The uncertainties in this method are many, but in light of the many other possible errors associated with rapidly deployed forecasts are reasonable in the RDFS context. The 2003 run uses the CWA data for the Coos River tributaries, scaled to the total watershed area. The other tributaries use the same climatology described for the 1982 run. **Figure 2.6** shows model inputs for both Coos Bay runs.

2.2.4 Calibration and Validation Data

Data available for model calibration and validation are summarized in **Table 2.1**. Station locations for the primary calibration data can be seen in **Figure 2.7.** The data represents a mix that many RDFS initiatives will face: data of uncertain quality, limited temporal and/or spatial range, and highly discontinuous data.

Data from the 1982 NOAA survey (NOAA82 hereafter) forms the backbone of the calibration/validation effort. It provides temperature and salinity data. Pressure data (convertible to depth) showed evidence of a tidal signal, but was otherwise not in any obvious datum. Richard Patchen (personal communication, NOAA) confirmed that it was in kg-force/cm^2 (1 kg-force/cm^2 ~ 1 m depth) and that the apparent error was likely due to the unreliability of the Aandarra pressure sensors used for the survey. Otherwise, the data generally appears to be of decent quality, but without accurate pressure data the location of the instruments in the water column could not be determined precisely. Uncertainty persists due to salinity data at two stations (noa07 and noa11) between the

mouth and North Bend that show small (<0.5 psu) salinity inversions that persist for multiple days. Those stations with simultaneous salinity data at multiple depths (noa07, noa11, noa03 and noa09) showed little vertical stratification, suggesting that in this period vertical station location does not have a major impact. Instrument water column location was derived from a number in the header of each file indicating height above the bottom. All stations except noa01 have data ~1.5 m (5 ft) from the bottom, and some have data between 4.6 and 9.1 m from the bottom (generally mid-water column). Stations are labeled noa01 to noa11, with a "b" suffix indicating a near bottom station (e.g. noa11b) and an "m" suffix indicating a mid-column station. The data collection periods can be seen in **Figure 2.8**.

SSNERR maintains four water quality monitoring stations in the South Slough (details in **Table 2.1,** locations in **Figure 2.7**). Salinity and depth observations from January 1 – April 27, 2003 were used for comparison to the model. Depth data for each station was converted to elevation by subtracting the mean depth for all of 2003. Other calibration and validation data include a NOAA tide gauge at Charleston, depth, salinity and temperature data from a 10 day EPA survey in August 2005, and salinity and temperature data from Oregon Department of Environmental Quality (DEQ) LASAR database.

2.3 Coos Bay Model Skill Assessment

2.3.1 Methodology

Skill assessment for salinity and elevation is performed visually using time-series and scatter plots, and quantitatively using root mean square error and the index of agreement (IOA) (Willmott, 1981)

$$IOA = 1 - \frac{\sum |X_m - X_o|^2}{\sum \left(|X_m - \overline{X_o}| + |X_o - \overline{X_o}| \right)^2} \qquad \{2.2\}$$

where X_m is model data, X_o is observed data and overbar indicates a time average. The IOA captures the correspondence of the deviation of predicted and observed results from the mean observed value (X_o). IOA ranges from 0 to 1, with 1 indicating exact correspondence and 0 indicating no correspondence. **Figure 2.9a** and **b** illustrate the

metric by comparing a sine wave (representing observations) to sine waves of varying amplitudes, phases, frequencies and offsets (representing model results). When coupled with root mean square error, time-series and scatter plots, IOA can give a good indication of the type and extent of model error. IOA also provides a convenient method of comparing model results across data types.

2.3.2 Coos Bay RDFS Results

2.3.2.1 Results Plan

The discussion of model results is designed to summarize those aspects that illuminate implications for the effectiveness of the RDFS concept, rather than give a copious comprehensive summary of the model results. After numerous calibration runs a configuration was deemed of reasonable quality for forming the basis of further calibration runs. Runs from this configuration are labeled the "reference" run. Because the South Slough appears to have a distinct set of issues it is treated in a separate section.

2.3.2.2 Elevation Results

Table 2.2 shows the RMS error and IOA for all stations with elevation data. Model results for the NOAA Charleston Tide gauge (ccho3) for both winter and summer runs closely follow observed data in phase and frequency. **Figure 2.10** shows plots of ccho3 for both the winter and summer runs. Harmonic analysis of the tidal constituents used as model input (**Figure 2.11**) shows that modeled tidal constituents were in good agreement, but include a consistent phase lag. These lags amount to 62 and 55 minutes in the case of M2 for 1982 and 2003, respectively. This lag suggests errors in the grid representation at the mouth of the estuary, which cause the model wave to propagate more slowly than the observed wave. All harmonic analysis was performed using the Matlab package by Pawlowicz et. al. (2002).

An analysis of the low pass filtered ccho3 elevations reveals that the greatest errors occur when the low pass filtered elevation departs significantly from MSL (**Figure 2.12**). In both the 1982 and 2003 runs a low pass filtered plot of model ccho3 elevation tends to stay near MSL, while the data and error lines move above and below MSL (see **Table 2.6** for standard deviation data). Large deviations from estuarine mean values can come from atmospheric forcings (Dyer, 1997, p. 156). Thus, it appears that considerable

model error at ccho3 comes from low quality model atmospheric inputs and/or poor model handling of atmospheric data. **Figure 2.12** also shows actual errors that track the low pass filtered error, but errors are still considerable when low pass filtered errors decrease, suggesting additional sources of model error.

The brief August 2005 runs displayed in **Figure 2.13**, coinciding with an EPA survey, (Cheryl Brown, personal communication) showed observations suggesting ebb dominant conditions (brief strong ebbs and longer, weaker floods). A likely cause for ebb dominance is a combination of a large channel depth to tidal amplitude ratio and large tidal flats. On flood, friction slows the wave over the flats and inlets, while on ebb the wave speeds out the channel (Speer and Aubrey 1985). Although the model showed good agreement with observations at epa01 (between the mouth and North Bend), it significantly underestimated ebb tides at epa0C.

2.3.2.3 Velocity Results

Only the NOAA82 data included velocity observations. IOA and RMS error was calculated for along-channel velocity. Channel direction was calculated as the inclination of the semi-major axis of the tidal ellipse, as determined using Empirical Orthogonal Function analysis (as described in Emery, 1997). Tidal excursion was calculated at each station, and defined as

$$TE = \frac{\sum_{1}^{N} \int_{T} \frac{|u|\,du}{2}}{N} \qquad \{2.3\}$$

where N is the number of M2 periods (12.4 hours), u is along-channel velocity and T is a 12.4 hour tidal period. Results are summarized in **Table 2.4**, with representative stations in **Figure 2.14**. While the model showed medium to high IOA for along-channel velocity (values range from 0.849 to 0.952), almost all of the errors come from velocity magnitude. RMS errors are large relative to velocities. The model underestimates tidal excursions most near the mouth of the estuary (see noa07 in **Table 2.4**), and model tidal excursions become more accurate towards the head. Model velocities are more accurate on stations lower in the water column. Of the stations with measurements at multiple depths (noa03, noa07, noa09, noa11), all but noa09 do better at the near-bottom, and the RMS difference between the noa09 depths is 0.01 m/s. Care must be taken in

interpreting this result, however, because with the exception of noa11 none of the different depth measurements are temporally contiguous.

Velocity errors near the mouth of the estuary were initially hypothesized to be due to representation of the channel (regarding bathymetry and/or grid design) or a stray node (introduced accidentally just before starting the reference runs) near noa07. Efforts to correct velocity and salinity errors through improved channel resolution and a change in the transport algorithm produced three calibration runs. **Table 2.7** shows the basic characteristics of three calibration runs, and **Figure 2.15** shows selected velocity results. Removing the stray node resulted in only minor velocity improvements at noa07 (the station closest to the stray node), and no improvement further up the estuary. In general the calibration runs showed that none of these changes made significant difference in velocities.

Model analysis of elevation in the 2005 run revealed possible ebb dominance. From this perspective it became clear that observed ebb velocities during the NOAA82 run also show signs of ebb dominance (ebb velocities that are stronger but briefer than flood velocities) that the model does not capture (**Figure 2.14**, especially stations noa07, noa02 and noa09).

2.3.2.3 Salinity Results

Results of salinity model/data comparisons for both runs are summarized in **Table 2.5**. **Figure 2.16** shows salinity time series for some representative stations in the summer run, and **Figure 2.17** shows salinity scatter plots by region. RMS error for the NOAA82 data is around 0.5 psu near the mouth and increases to around 2.0 psu toward the head. IOA, however, shows no obvious correlation to distance up the estuary, with one of the four highest IOA values occurring near the mouth at the noa07m (IOA = 0.805), one occurring in the middle of the estuary near North Bend at noa02b (0.789), and the final two occurring at noa09m and noa09b near the city of Coos Bay (0.780 and 0.868). **Figure 2.17** shows that, with the exception of the two stations nearest the mouth (noa01 and noa07), the model tends to under-predict salinity, while **Figure 2.16** shows increasing errors with time. This effect is especially apparent at the stations near North Bend: noa02, noa06, noa03 and noa08. By noa09b mean model salinity tracks mean observed salinity fairly well, which explains the relatively high IOA of 0.868.

It was noted in section 2.2.4 that there is some uncertainty regarding the vertical position of the stations. The effect of vertical position on model-data comparisons was investigated by plotting observations against model data at 2 m intervals. Vertical position makes little difference in model velocities, but can have a significant affect on salinity even during this well mixed period (**Figure 2.18**). However the noa09 figure suggests that model representation of the salinity signal's amplitude is most accurate near the estimated 6.8 m depth.

When comparing IOA from the mouth to the head, an interesting event that occurs in the data should be noted. Observed salinity at stations near the mouth experienced a freshening event beginning around September 25 and lasting around 5 days. The effect was strongest at noa01, weakest at noa11 and not seen beyond that point. Given this from-the-mouth behavior it is likely a freshening from the ocean, perhaps related to a change from upwelling to downwelling conditions which pushed the plume back into the mouth (the regional re-analysis data used as model input shows a significant period of downwelling winds beginning midday on September 23 and growing especially strong late on the 24th).

River inputs accuracy represents significant source of model uncertainty. For both runs the accuracy of the tributaries other than Coos River relies on a 6-year climatology of Winchester Creek, as well as the dubious assumption that all the non-Coos River watersheds behave the same as Winchester's. Sensitivity runs in which freshwater flow was reduced to ½ and ¼ the original amount show that model river flows may be too large (**figure 2.19**). Decreased flow, however, also causes the model salinity signal amplitude to decrease, and therefore increase model error.

Using the upwind numerical solution to transport has showed significant ability to increase transport in CORIE runs. Calibration runs (**Table 2.7**) showed that using the upwind transport solution actually increases salinity above observations, and that the upwind method combined with channel resolution improvements actually reduce salinity to values closer to observations (**Figure 2.20**). Also, the upwind solution's range of salinities experienced in one tidal cycle was significantly smaller than the observed salinity range.

2.3.2.4 South Slough Results

Model-data comparison in the South Slough shows evidence of significant model distortion of the tidal wave (**Figure 2.11**). Elevation IOA for the four SSNERR stations decreases slightly toward the head. Tidal constituents for the South Slough stations show increasing amplitude and phase errors from mouth to head. **Table 2.3** summarizes the results for the K1 and M2 constituents. M2 errors are the most significant, with model amplitude underestimates increasing landward, and phase errors evolving from a model underestimate of 26.6° at cchwq to a model overestimates ~30° at the head. Low pass filtered elevation show similar atmospheric effects as those described in section 2.3.2.2.

South Slough salinity results (**Figure 2.21** and **2.22**) show that the slough experiences a significant neap-spring signal that is not accurately captured by the model. At Charleston (chawq) the model in general shows a far larger salinity range except during the lower high tide in the neap tide centered around 2/9, when it shows almost no tidal salinity signal. By Valino Island (valwq) the model salinity signal has largely lost the amplitude and become quite noisy. Low IOA at these stations (0.664 and 0.554) is the product of both high errors and poor signal agreement. Near the head the model has switched to over predicting salinity, but now maintains more of the tidal signal, which is reflected in higher IOA values of 0.679 (Winchester) and 0.794 (Sengstacken). Harmonic analysis (**Figure 2.23**) shows that the model suffers primarily from amplitude errors, staying largely in phase with the data.

2.3.3 Summary of Coos Bay Results

Achieving a high quality EMS or a detailed assessment of model performance is not the primary purpose of this project, but a partial summary of the current state of the model is appropriate. In the main channel during the late summer 1982 run, velocity results have a high IOA but show significant errors regarding velocity magnitudes and tidal excursion near the mouth and around North Bend. In this well-mixed period, velocity errors can be generally traced to bathymetry or grid issues, perhaps due to a too-wide channel or too little volume in the head of the estuary. Also, there are signs of ebb dominance in the observations, primarily in the North Bend station noa02 velocity data and the epa0C elevation data, that are not captured in the model. Finally, the drag

coefficient was set at 0.0025 m, which may have been too low. Sensitivity runs to drag showed little overall effect on velocities more than a few meters above the channel bottom, but bottom effects were significant. Model to data comparisons showed consistently better agreement at bottom levels than at mid-depth.

Salinity errors appear to be due in part to a combination of similar bathymetry and/or grid issues. Under-representation of velocities appears to affect the range of salinities experienced upstream, especially in the calibration runs with lower river flows. Lower (than velocity) IOA values suggest there are further error sources, or that bathymetry/grid errors may affect salinity differently. Thus, the consequences of the decision to largely set tidal flat and inlet depth to MSL are probably considerable. The artificial flatness could produce less mixing than a sloped bathymetry, and elevations that are artificially high result in less time spent and volume exposed to high bottom friction induced turbulence. Also, intertidal storage in marshes, tidal flats and inlets can be significant sources of salt retention (Blanton, 2001). The failed calibration attempt to maintain salinity intrusion without mixing pools (by extending the Coos River), along with the failure of the model to capture the ebb-dominant velocities, suggest that the deep salt intrusion in Coos Bay is in part due to the effects of the many inlets and/or the extensive tidal flats and marshes. Grid representation issues appear to be compounded by some limitations of model implementation, such as the effects of SELFE's handling of wetting and drying: when one node goes dry the entire element is considered dry. This restriction may degrade flow accuracy over the tidal flats. Further, this makes it difficult to represent narrow channels without artificially widening them or incurring significant computational costs by increasing resolution (necessitating a smaller time step). Not widening channels or increasing their resolution can cause artificial drying, as seen in epa02 elevations in **Figure 2.13**. Other error sources may include inaccurate (too high) river flow estimates and choices of numerical solutions.

Salinity and elevation errors in the South Slough also appear to be due to in part to bathymetry/grid issues. Additionally, the model salinity intrudes too far up the estuary, which is likely due to the long river run-ups. River run-ups are set to elevations below MLLW to ensure that no part of the river dries up. The actual rivers, however, rise well above sea level at these points. Thus these river run-ups create too much

opportunity for salinity intrusion and mixing. Moving the river boundary closer to the mouth, thus decreasing the space available for mixing, could improve the model salinity results in this region.

2.4 Implications for the Rapid Deployment Forecasting System

From its origins as a low-cost, low-accuracy Rapid Deployment Forecast a hydrodynamic model been refined, calibrated and validated into a model of moderate accuracy. Much of the data used in this process was available on-line and for free, and the rest was made available by local stakeholders after a demonstration of the initial Coos Bay RDFS. While this pilot RDFS project has succeeded in generating a EMS with promising routes for improvement, its broader importance lay in the lessons learned about the challenges and opportunities of RDFS as a method for the propagation of near-coast and estuarine models which can provide the seedbed for a future NEMS. The combination of technology development and experience gained through CORIE with the increasing availability and accuracy of raw and model data used as model inputs (in part through the growth of IOOS) makes it straightforward to develop a basic low to medium quality circulation model. The steps from a rapidly deployed model to a high quality model suitable for management purposes are more complex and ambiguous. The challenges can be organized into two broad categories: lack of input and/or calibration/validation data, and the complexities and ambiguities associated with model calibration.

The experience of the Coos Bay RDFS suggests that of the four major model inputs (tidal constituents, river inputs, atmospheric data and grid/bathymetry), grid/bathymetry followed by atmospheric data are the most critical for making substantial calibration progress, while accurate river inputs are crucial for a high skill EMS. Tidal constituents for calculating elevations at the ocean boundary are well known and easily calculated using existing models. Reasonable ocean boundary conditions can be obtained from the Naval Coastal Ocean Model. Basic climatology based on nearby gauged rivers, historical records or analysis of watershed area and rainfall can produce reasonable river flow estimates for calibration purposes, but because river flow can have a large affect on estuarine circulation, a quality EMS requires major tributaries to be permanently gauged or (at worst) be very well studied. Calibration runs with varying river flows can then be

used to reasonably assess the degree to which model error can be explained by errors in river input. While a management quality forecasting system will generally require the gauging of all major tributaries, a significant amount of model calibration can occur without river flow observations.

Atmospheric data, primarily winds, are important for many systems. Atmospheric models such as ETA, COAMPS (Hodur, 1997) and MM5 (Grell et. al., 1995) and other atmospheric models can provide wind data of sufficient accuracy to make significant calibration progress. Estuaries with large surface areas and/or strong winds may require local atmospheric observations. The Coos Bay model did not capture the 1982 freshening event around 9/25/82 or the deviations from MSL of the mean tidal elevation at Charleston. Both of these phenomena are probably caused by wind and ocean interaction outside the estuary. Even without capturing these events, however, the model still has ccho3 elevation IOA values above 0.99 for both the 2005 and 1982 reference runs. An important consideration is the resolution of the atmospheric model's resolution. The re-analysis data used in the Coos Bay RDFS was a very coarse 32 km. A non-comprehensive survey revealed that ETA, COAMPS and MM5 forecasts are available at resolutions as high as 4 km. The effects of atmospheric forcings were not explored deeply for this study, but it is clear that calibration efforts towards a management-quality EMS must consider both the accuracy of wind inputs and the model's handling of them.

Accurate bathymetric data and a grid design that reflects it are crucial to model accuracy. The more complex the estuary bathymetry the more crucial grid and bathymetry become. Any estuary with a dredged channel should have accurate bathymetry data available for the channel, and grid resolution should be sufficient to capture the shape of the channel. Areas outside the primary channel can also be very important. The Coos Bay model results suggest that the grid does not capture the actual bathymetry in these areas. This model deficiency is not surprising considering the coarse approximations that characterized the grid development in these little-surveyed regions. Generally, accurate bathymetric data throughout an estuary is essential for a high quality model, and calibration will require significant grid development and refinement. Lacking accurate bathymetry data in the traditionally neglected bays and flats, the path to

providing a reasonable estimate that captures essential aspects of the estuary's behavior are not straightforward. There is significant evidence of the importance of tidal flats and inlets in Coos Bay, as can be seen in **Figure 2.13**. In the absence of accurate data or when dealing with a model that does not handle shallow, complex areas well it may be necessary to use tricks such as mixing pools to approximate their effects. In such cases care should be taken when interpreting model results. In circumstances such as Coos Bay the EMS would likely benefit from a sensitivity analysis to major variations in tidal flat and inlet representation.

In addition to model inputs, it is vital that numerous continuous observations of elevation, salinity, velocity and temperature exist for purposes of calibration and validation. Monitoring stations should span meaningful spatial and temporal conditions. The Coos Bay RDFS calibration effort suffers most noticeably from a lack of medium to high flow observations in the main channel. Given the length of the channel, the numerous peripheral bays and the scattering of tributaries, it would be useful to have a minimum of three stations located in the channel located roughly near NOAA82 stations noa07, noa03 and noa09. Without long term observations it is not reasonable to expect to develop a high quality EMS.

Finally, the ability to proceed from the collection of model inputs and creation of an initial model to a high quality EMS requires significant knowledge of physical oceanography, the general characteristics of numerical modeling and of the particular model used. Although part of the purpose of this project was to investigate the ability of a non-expert in any of these areas to generate a quality model, this project did benefit greatly from proximity to the CORIE group. In the short run the propagation of forecasting systems beyond the CORIE group and other expert users would benefit from the cultivation of a users group (which already exists in the case of most widely used numerical models), a well-documented and extensive knowledge base, and the part-time assistance of CMOP staff to aid the non-expert user. This knowledge base could begin with links to discussions of the basics of estuarine physics and error sources found in numerical modeling, and grow based on the user group, experiences at CORIE and other user feedback. In the long run the development of an expert system to automatically identify possible error sources and suggest solutions could be an enormously interesting

and beneficial project. Software that eases the process of viewing model results and comparing to observations has already been developed at CORIE. Making this software available to the general user would also greatly facilitate the growth of high-quality estuarine forecasting systems.

Chapter 2 Figures and Tables

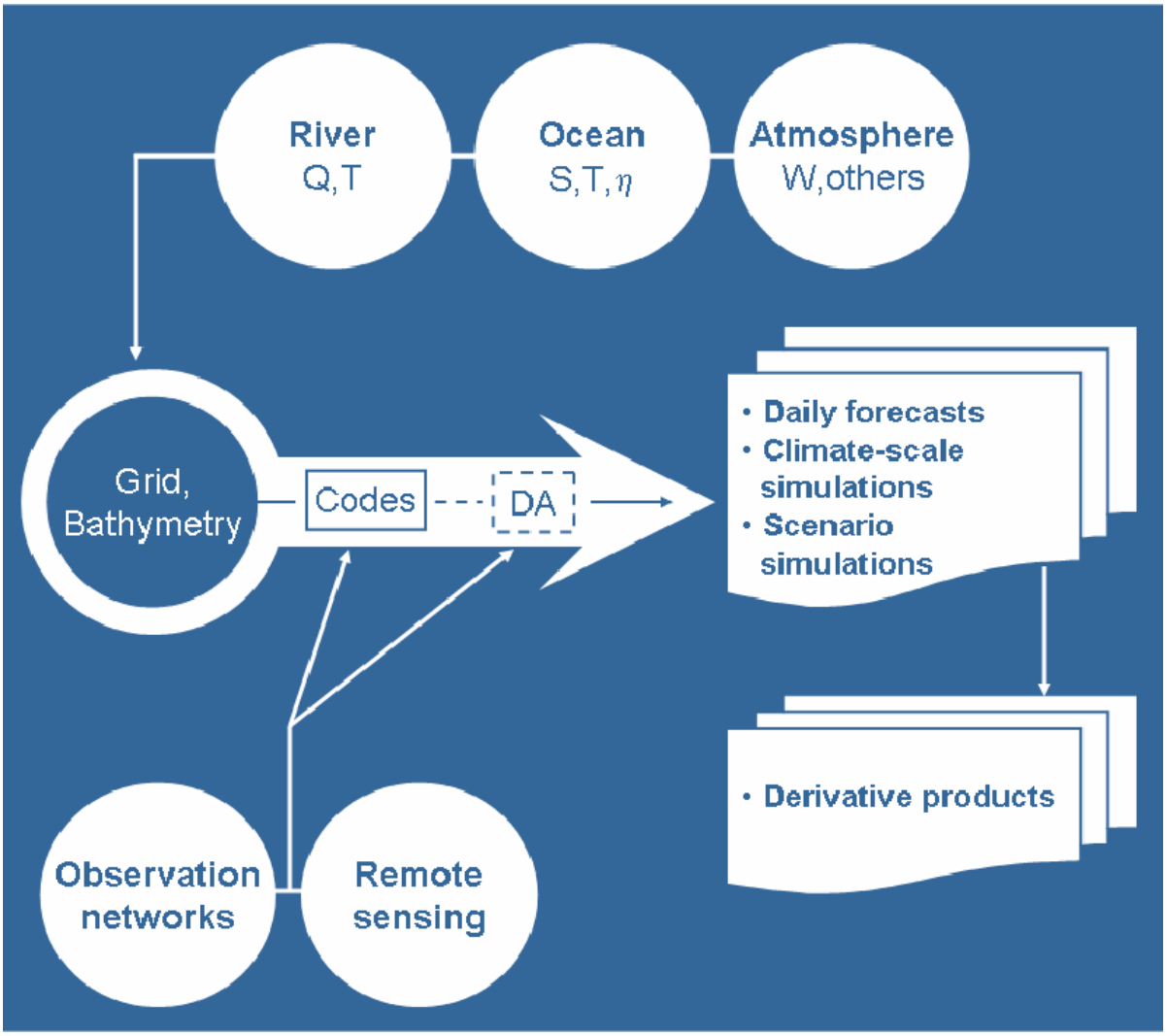

Figure 2.1: Components of an Environmental Modeling System (EMS). The EMS is centered on a 3D grid and numerical model ("Codes"). The model accepts boundary conditions in the form of river flows (Q) and temperature (T), ocean salinity (S), temperature and elevation (η), and winds (W) and atmospheric pressure. Observation networks and remote sensing provide quality control. The model produces data results, which are analyzed (data analysis, "DA") and form the foundation for daily forecasts, climate scale simulations and hypothetical simulations. From these basic products various derivative products are possible, one of which is the Model-based Estuarine Characterization and Classification System described in chapter 2.

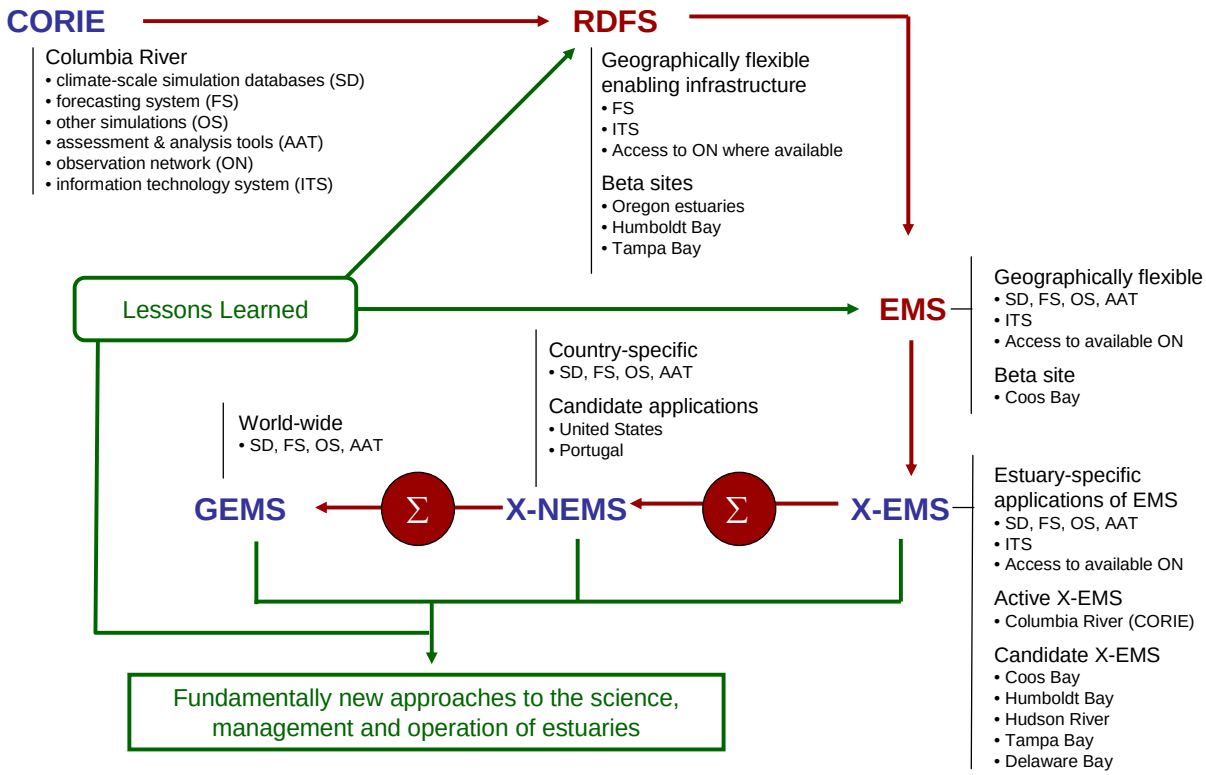

Figure 2.2: The estuarine modeling systems vision. The Rapid Deployment Forecasting System (RDFS) concept, derived from the experiences at CORIE, provides a foundational concept bringing local stakeholders, experienced institutions and data owners together to create new estuarine modeling systems (EMSs). Through the rapid, low cost deployment of reasonable quality, useful forecasting systems, the will and funding to develop existing EMS (X-EMS) into management quality forecasts is generated. Once developed, high skill EMSs can become part of a future national, and even global, EMS that can provide a rich set of data products and analysis. In turn, as the number and sophistication of EMSs grow, knowledge and other resources are generated that enable a more effective RDFS and EMS process.

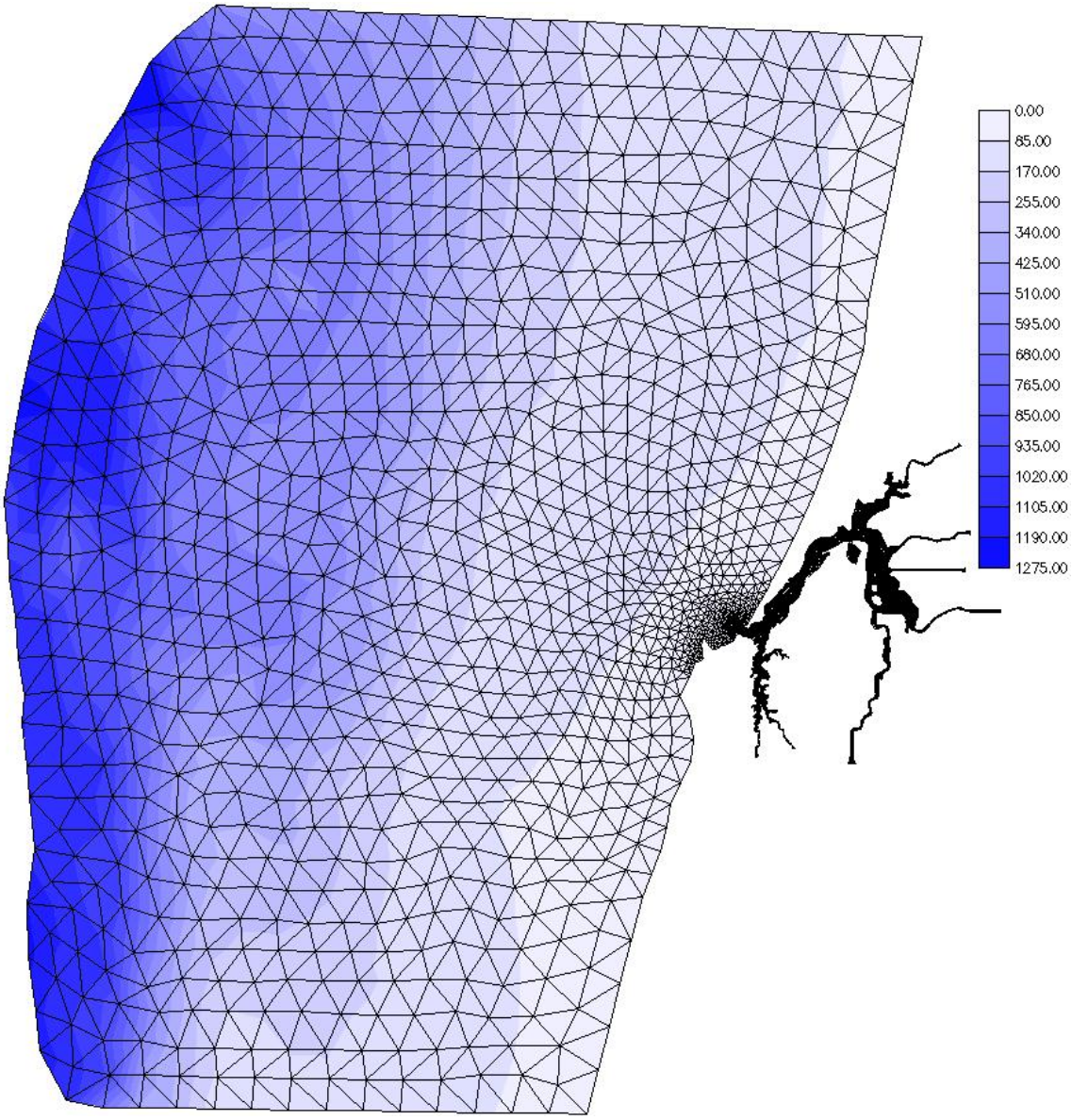

Figure 2.3a: Grid and ocean bathymetry. Depths are in meters. Side lengths are on the order of 5 km in the open ocean.

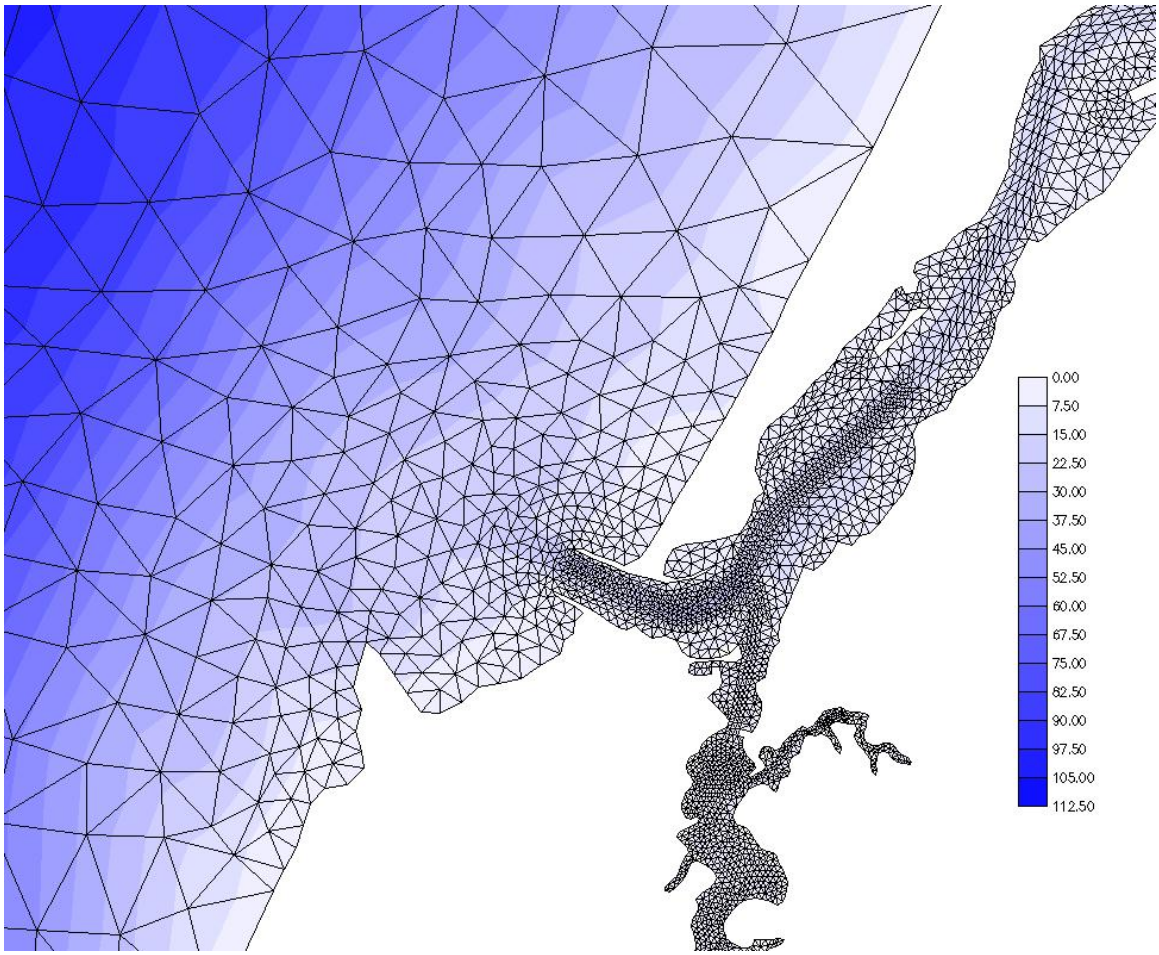

Figure 2.3b: Grid transition from ocean to mouth. Depths are in meters. In the transition from ocean to estuary grid side lengths reduce from ~2.5 km at the eastern (left) boundary of the image to ~75 m inside the mouth.

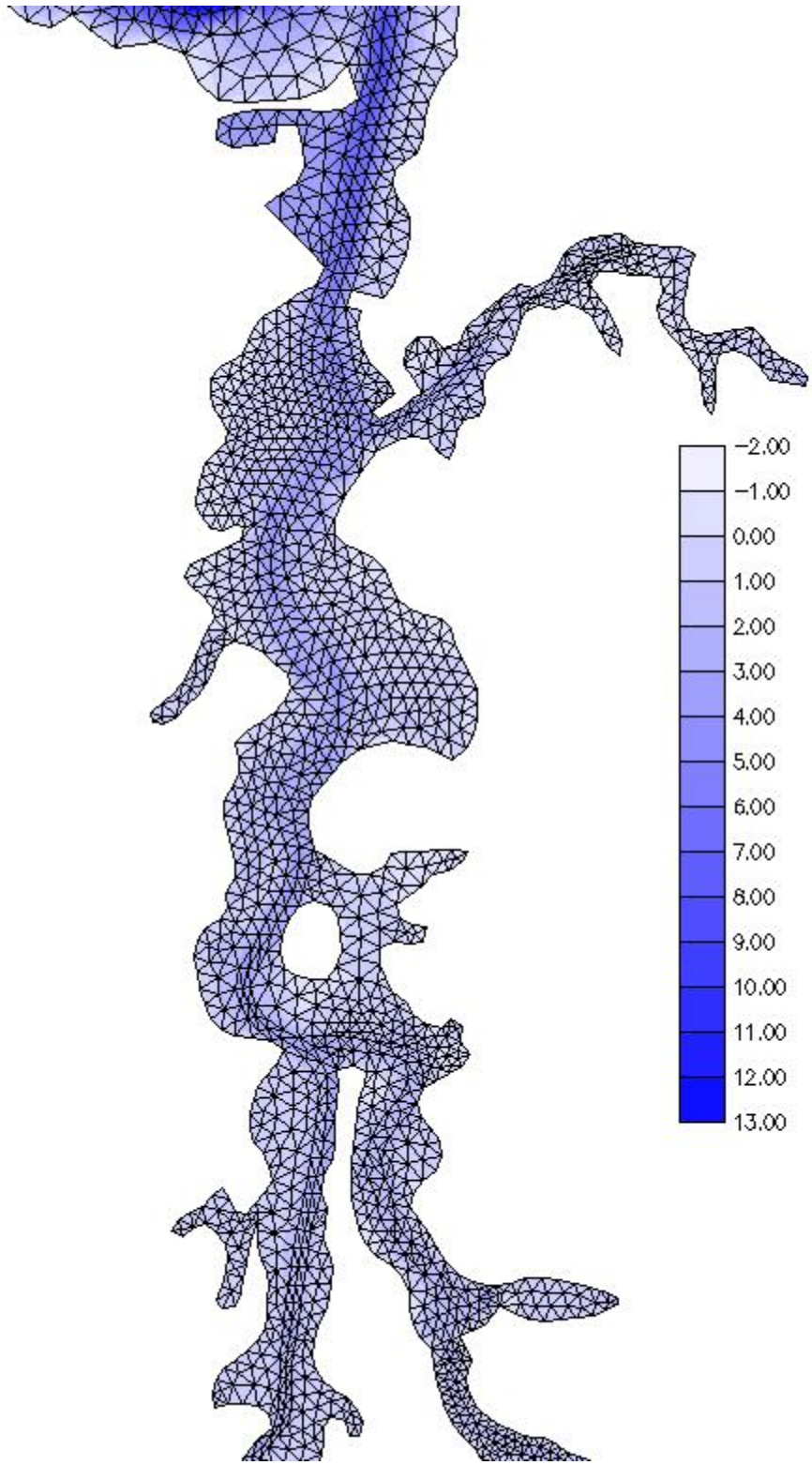

Figure 2.3c: South Slough grid. Depths are in meters and side lengths are between 30-80 km.

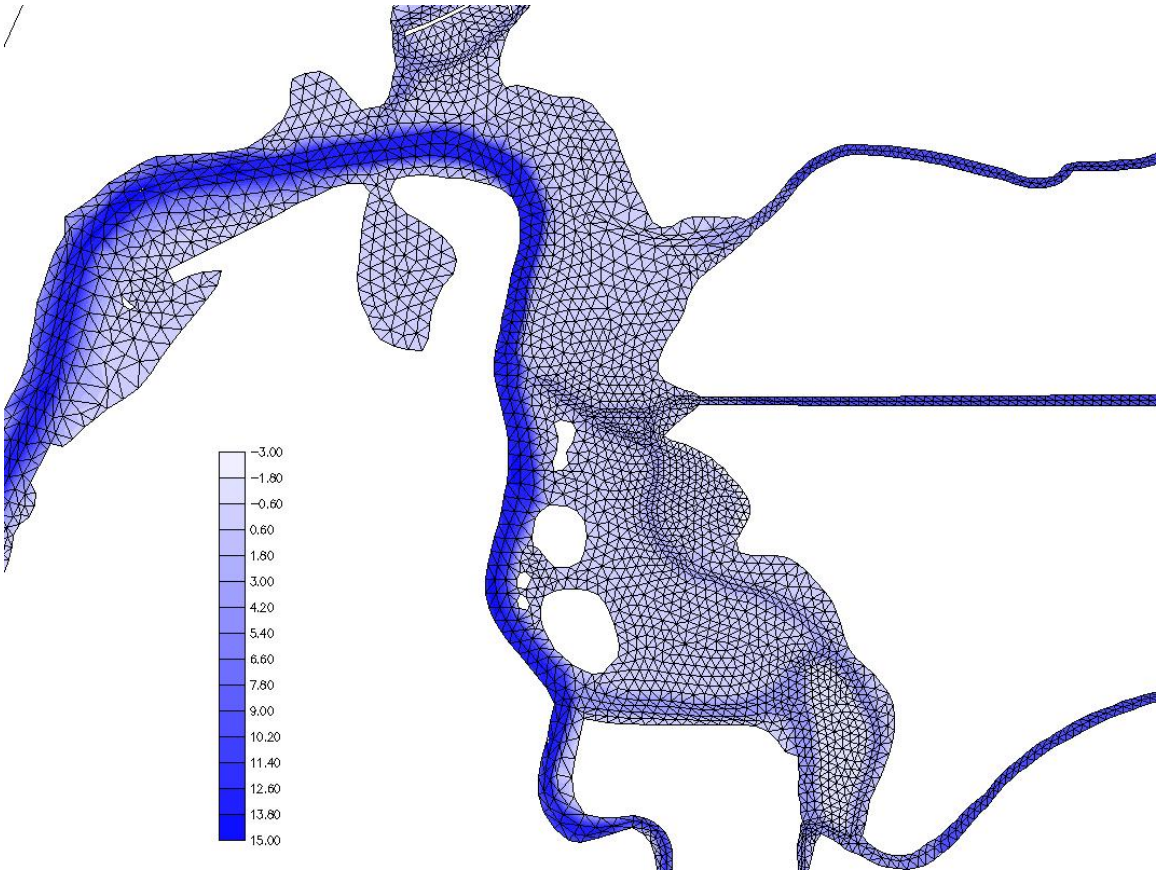

Figure 2.3d: Grid from Empire to Isthmus Slough. Depths are in meters, and side lengths are on the order of 100 m.

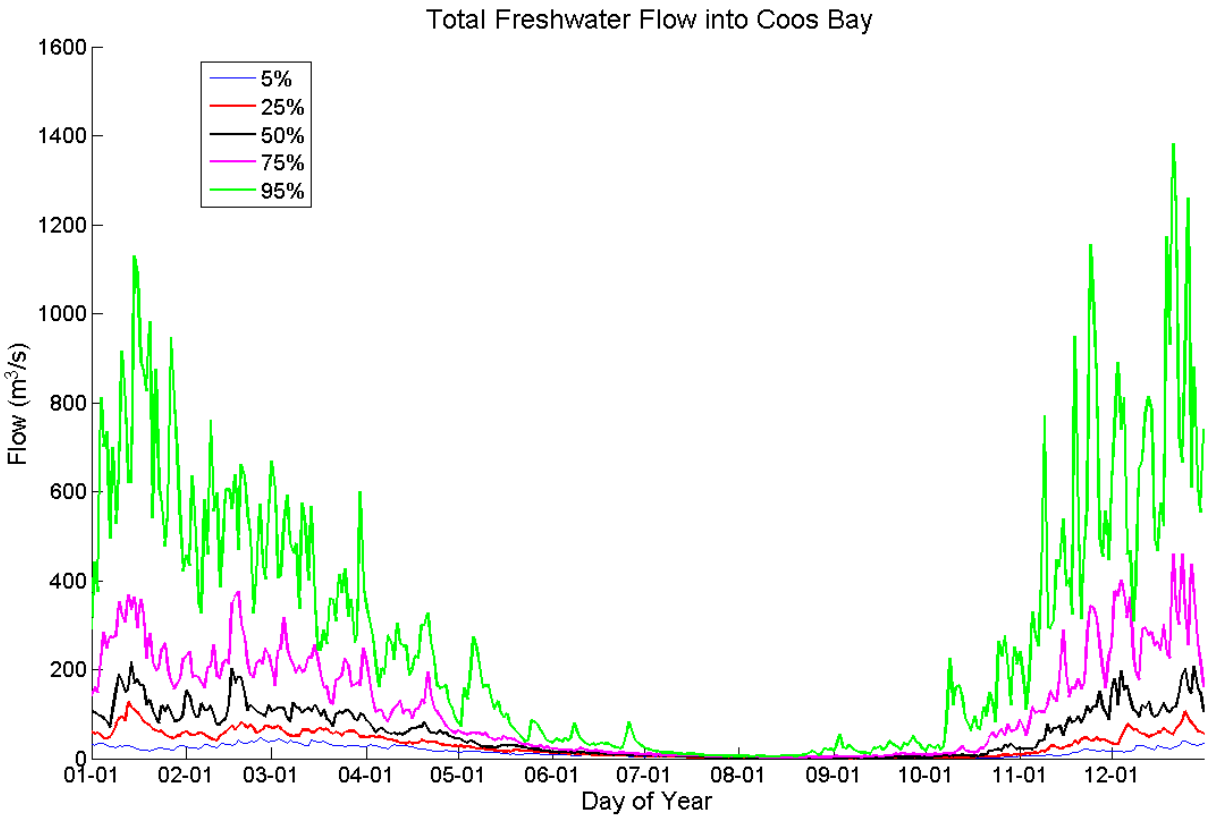

Figure 2.4: Total Coos Bay freshwater input based on 1954-1981 West Fork of the Millicoma data from USGS. These values are a simple scaling of the WFM data by watershed area. The area of the gauged portion of the WFM watershed is approximately 7.5% of the total Coos Bay watershed area.

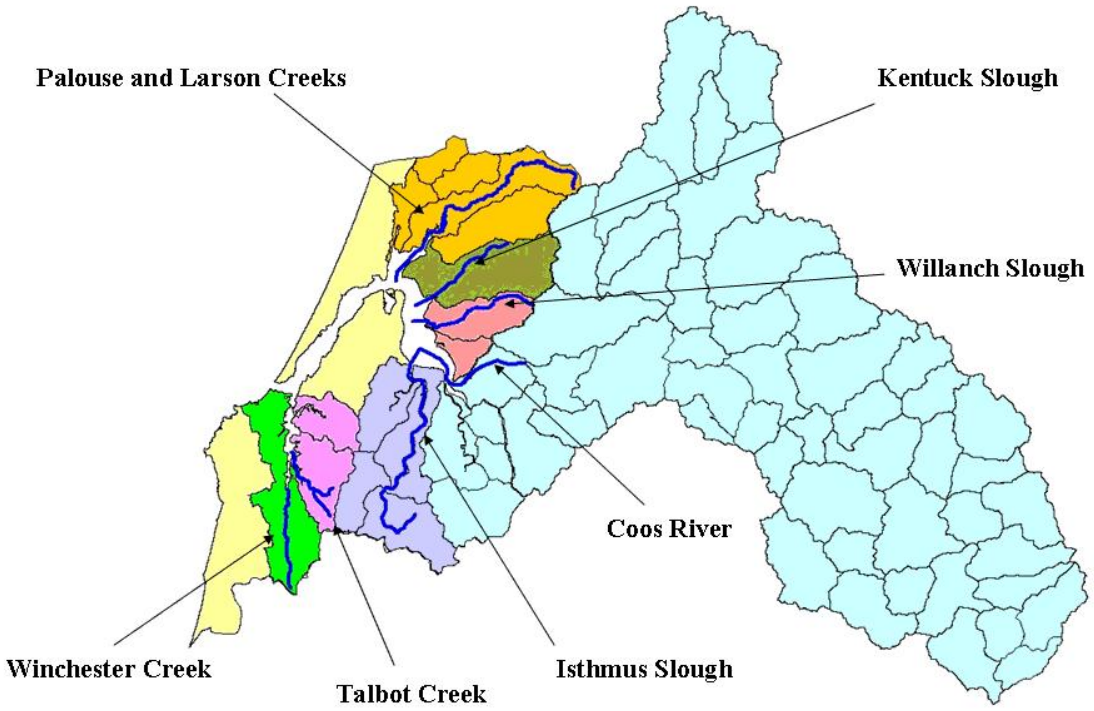

Figure 2.5: Coos Bay tributaries used as model inputs. The large number of tributaries was reduced by aggregating watersheds. Approximately 66% of the freshwater inputs are from the Coos River, which has a drainage basin of ~12,000 km^2.

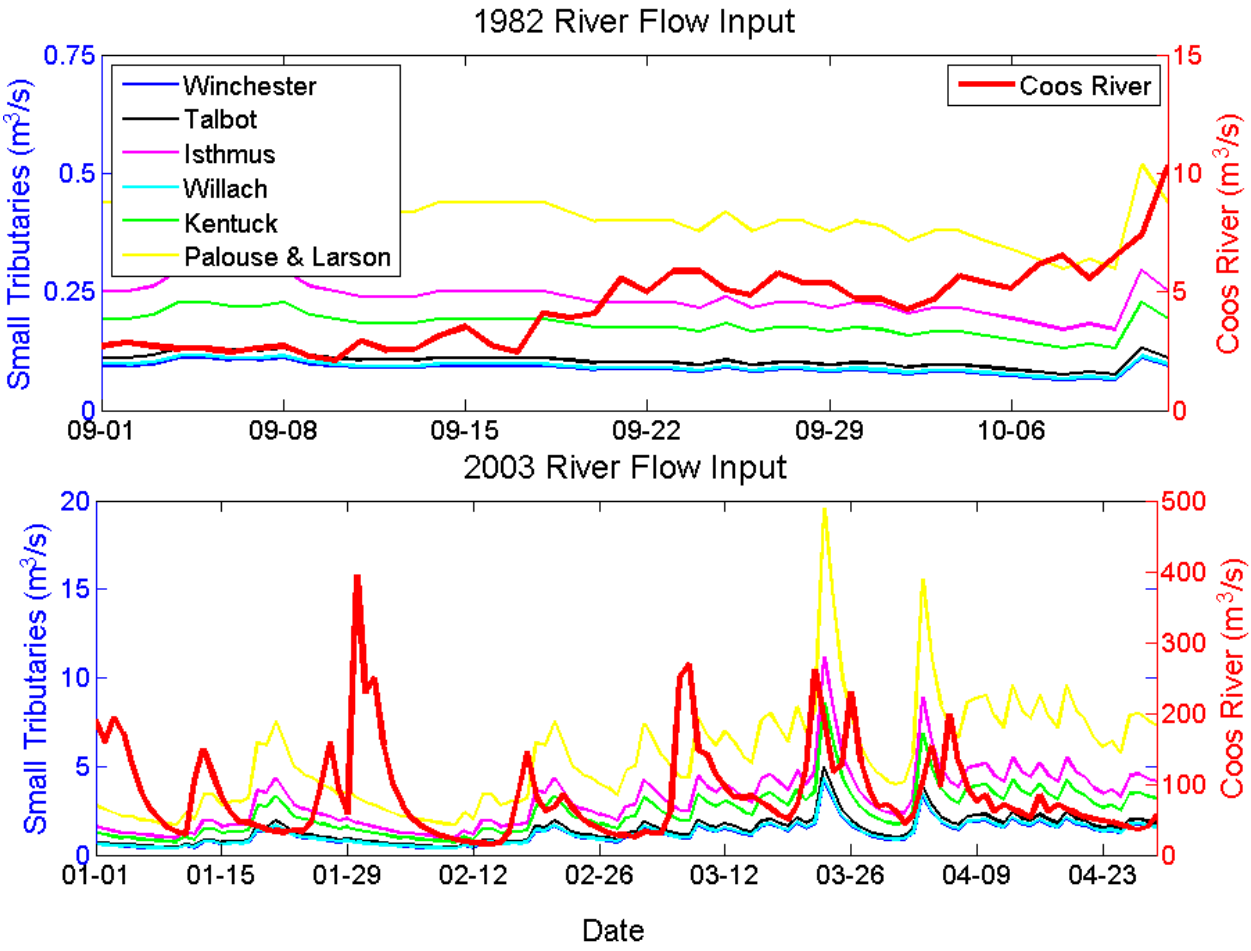

Figure 2.6: 1982 (top) and 2003 (bottom) model freshwater inputs. The Coos River is in red with the scale on the right Y axis. All river inputs are from climatology except the 2003 Coos River, which is from data but is scaled according to the ungauged portion of the watershed.

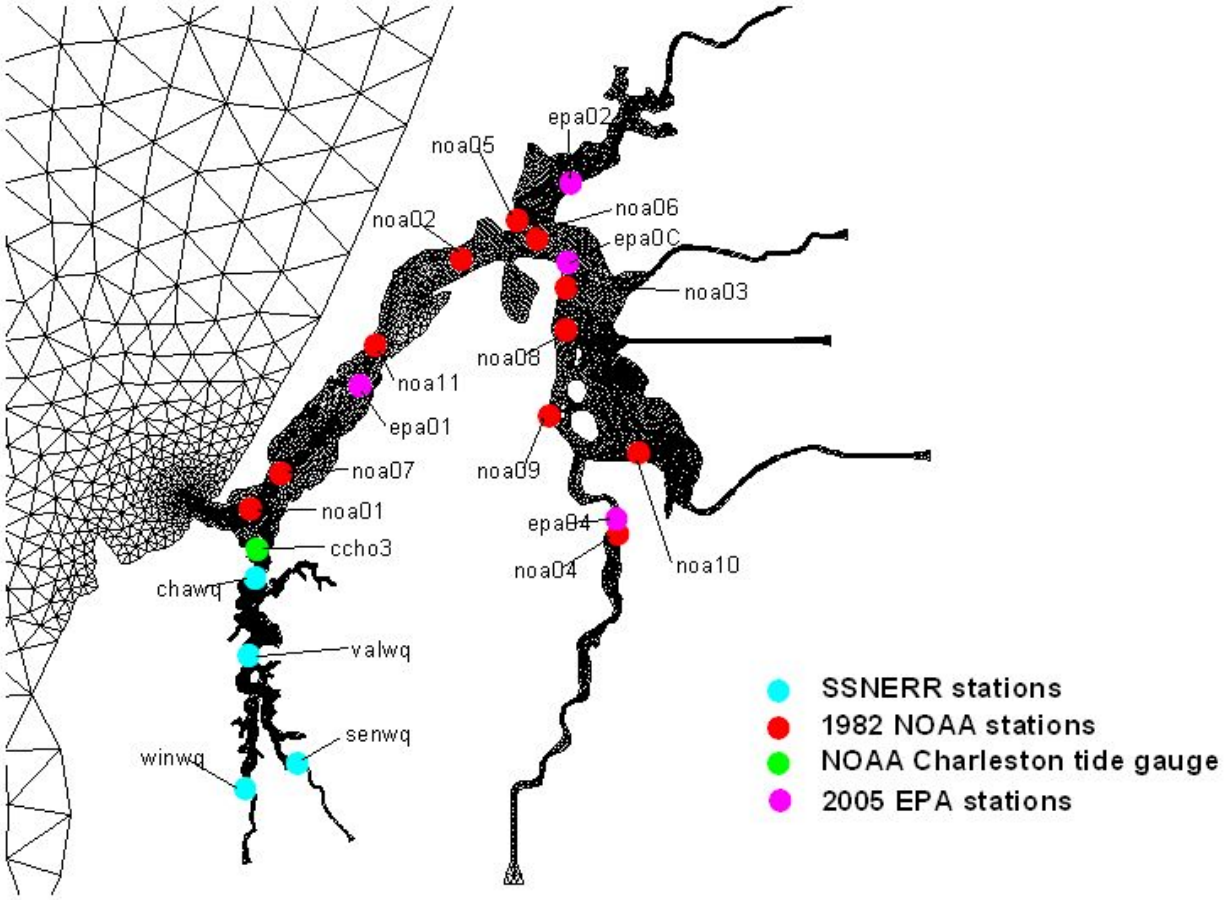

Figure 2.7: Primary calibration/validation sites. **Table 2.1** summarizes data sources, types and time periods.

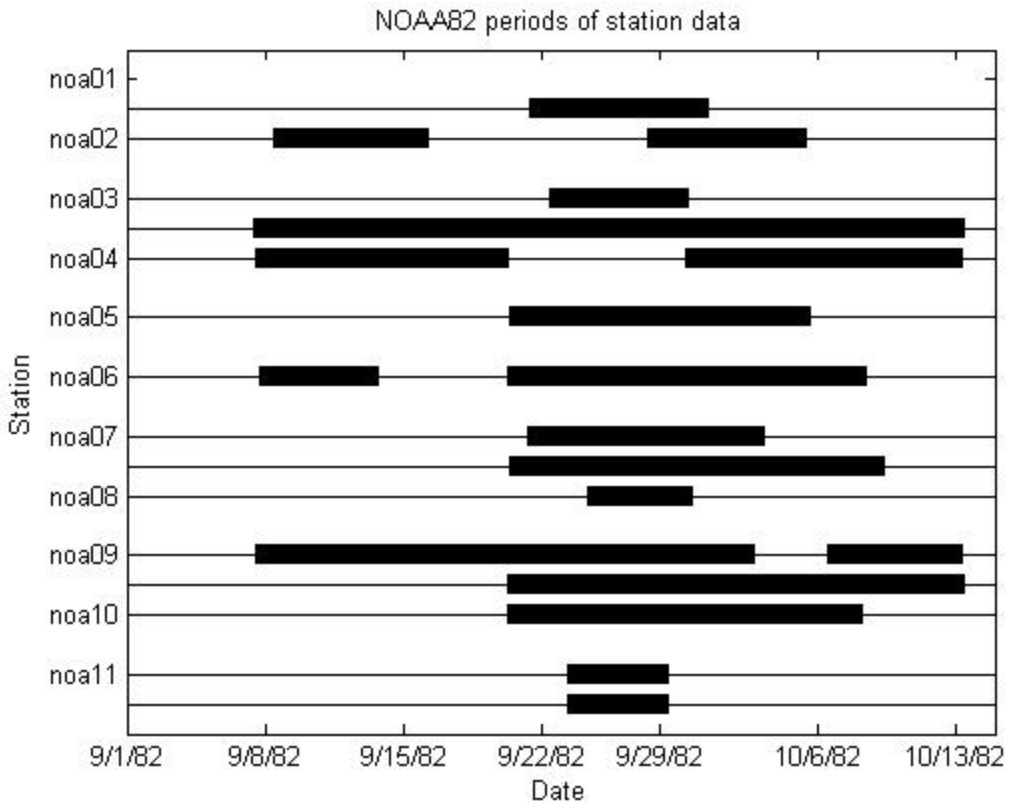

Figure 2.8: Periods of data for NOAA82 stations. The top bar for each station represents bottom data. The bottom bar represents data near the middle of the water column. No bar means no data for that station at that level. All other data sources have data (with a few ~1 day gaps in the South Slough National Estuarine Research Reserve data) from all stations for the length of the total deployment.

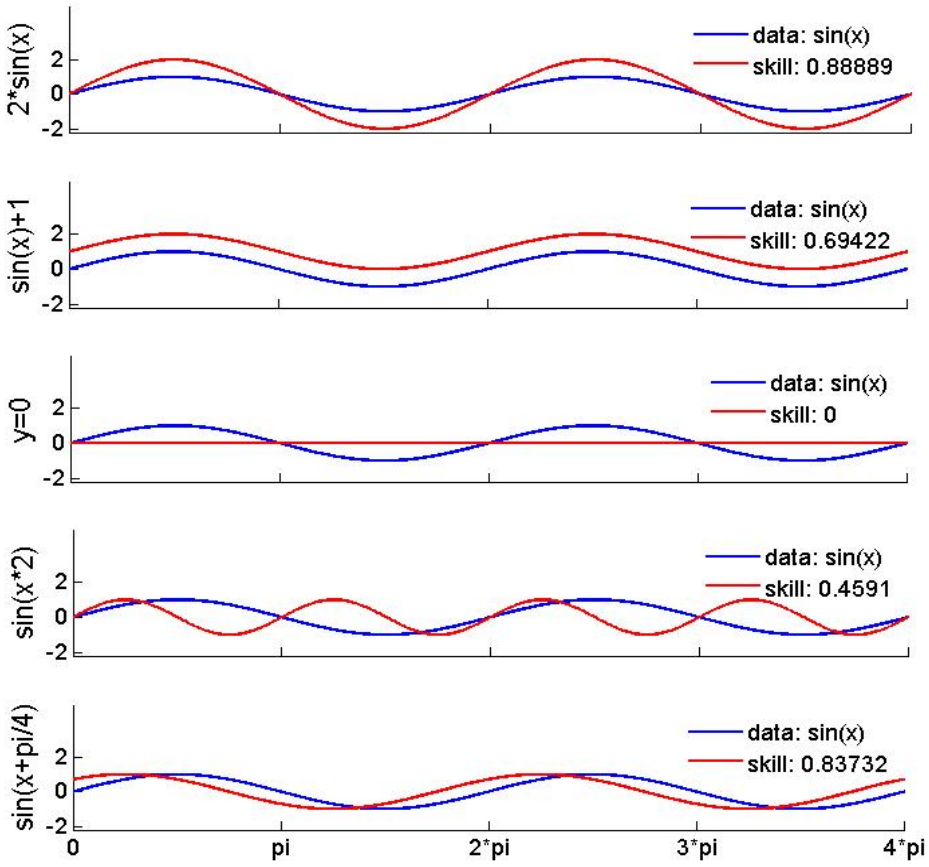

Figure 2.9a: Index of Agreement for different error types against a sine wave.

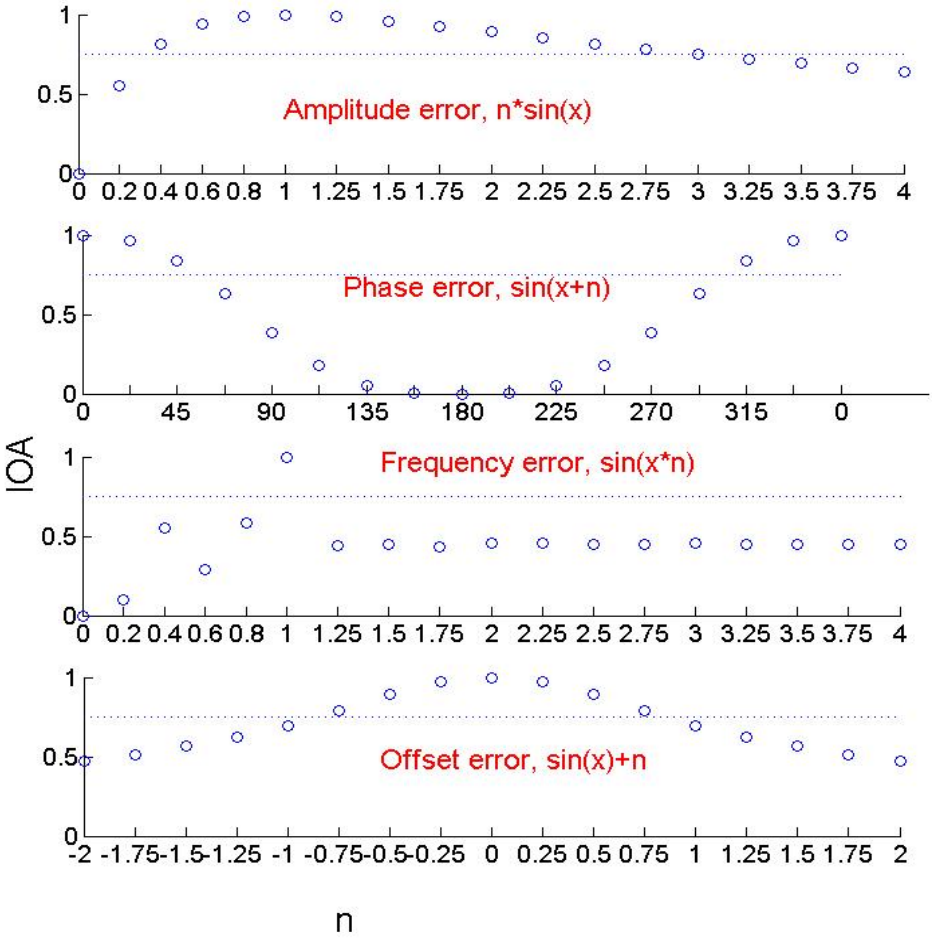

Figure 2.9b: Index of Agreement vs. a range of errors for different error types. Variable *n* is the error factor. The dotted line represents an IOA of 0.75.

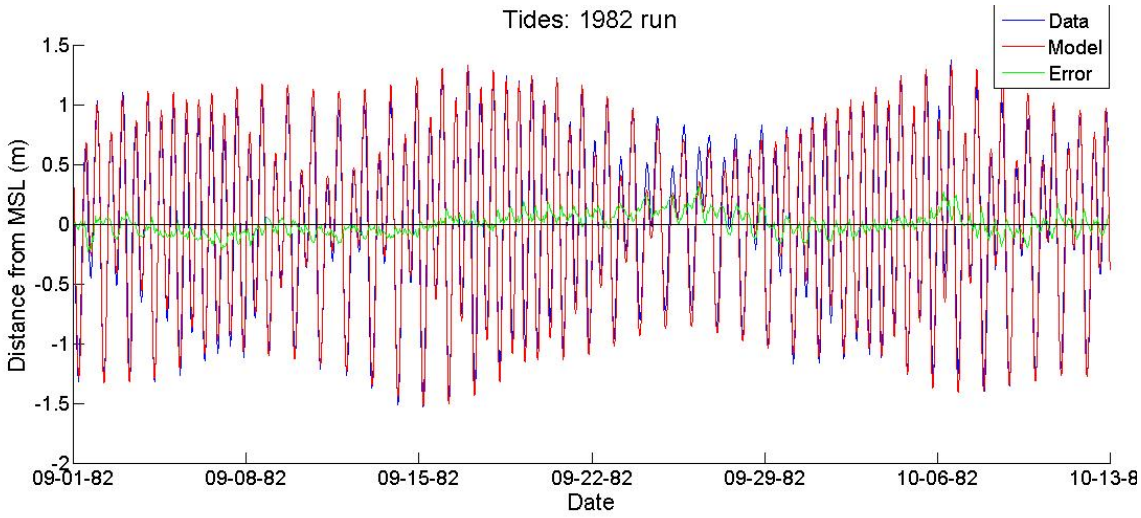

Figure 2.10a: NOAA Charleston tide gauge model-data comparison for 1982 model run

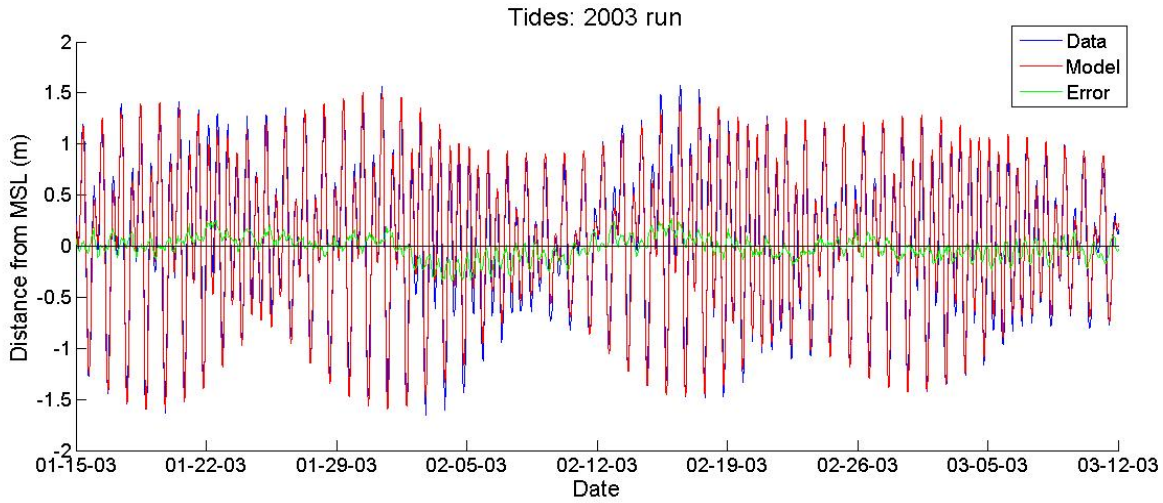

Figure 2.10b: NOAA Charleston tide gauge model-data comparison for 2003 model run

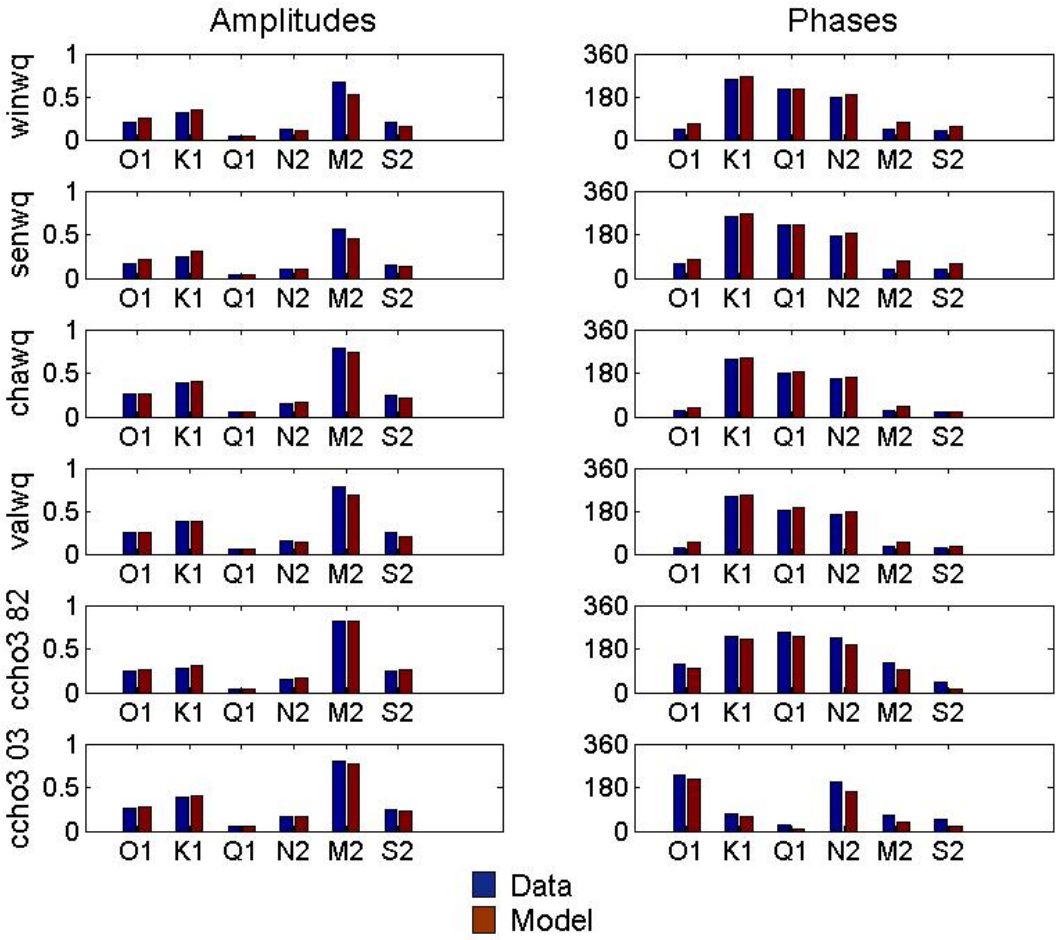

Figure 2.11: Model/data elevation harmonic analysis comparison of major constituents for SSNERR stations and for the NOAA Charleston station during the Summer 1982 Winter-Spring 2003 model runs.

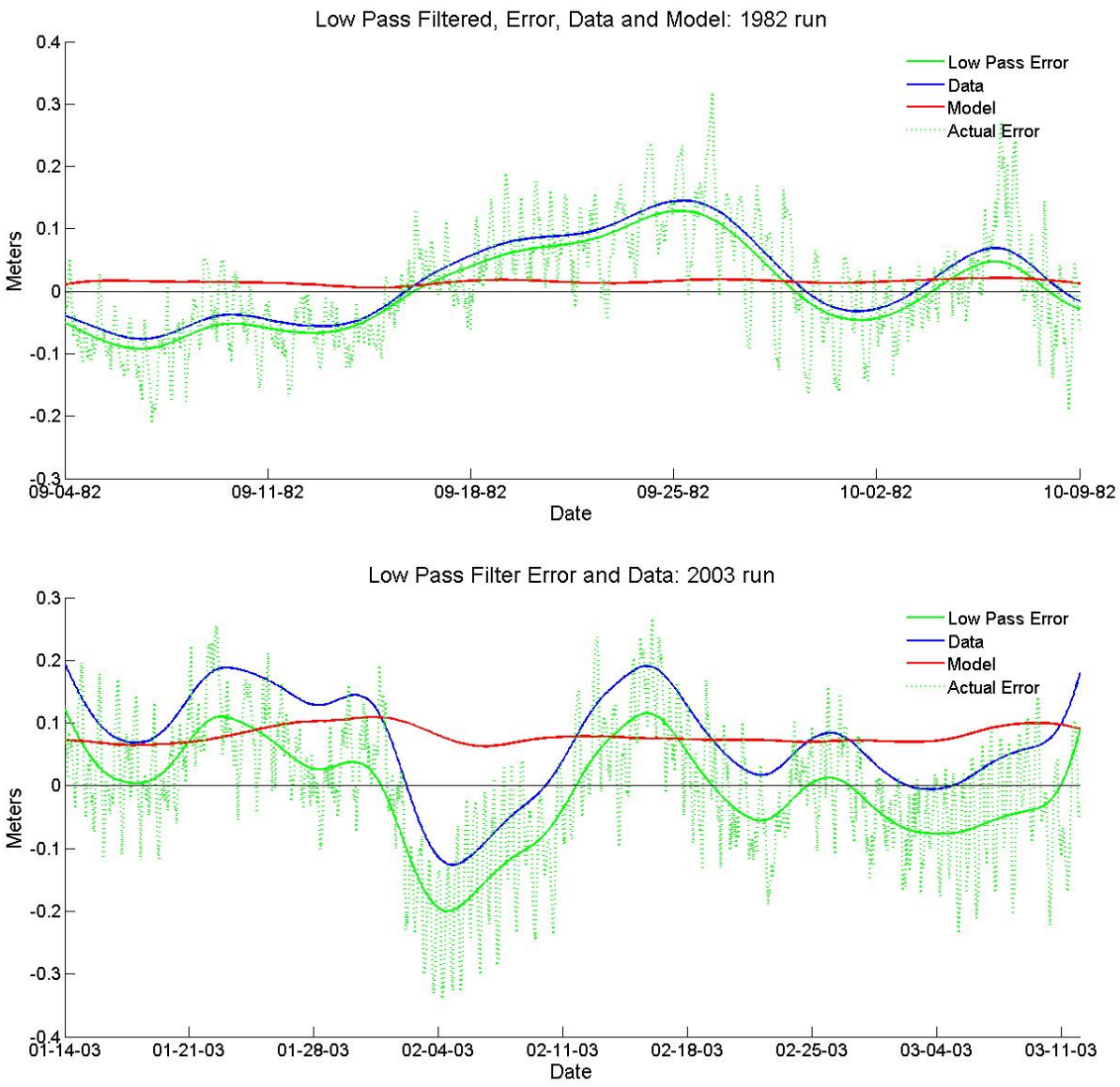

Figure 2.12: Low pass filter (7 day Butterworth filter) on the NOAA Charleston tide gauge data and the model-data error. Low pass filtered model data varies little, observations vary considerably more, and the low pass filtered error tracks the observations. Actual errors do not appear to decrease as the low pass filter errors decrease, suggesting additional error sources.

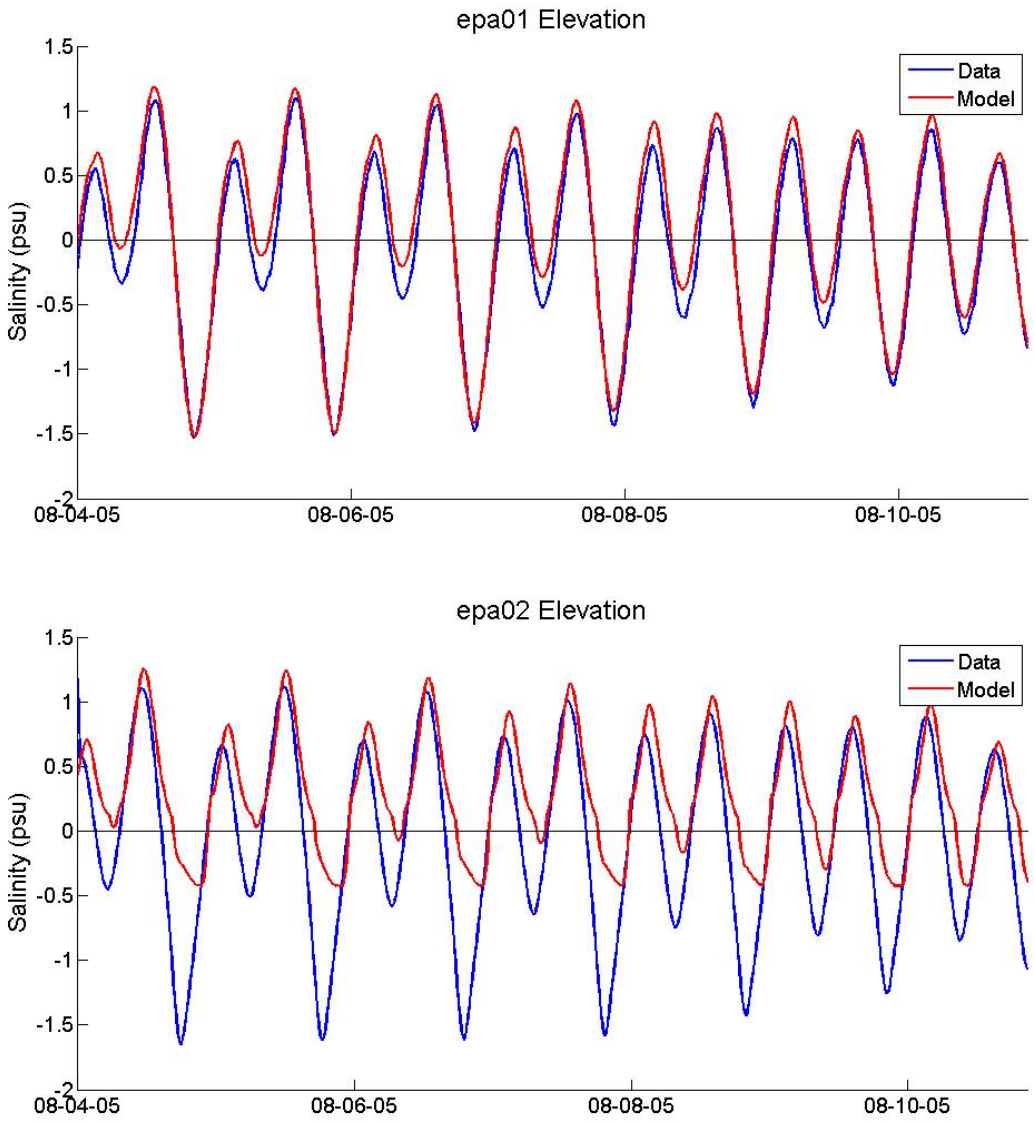

Figure 2.13 a-b: Elevation at station epa01 and epa02. Commentary at **Figure 2.13 c** (next page)

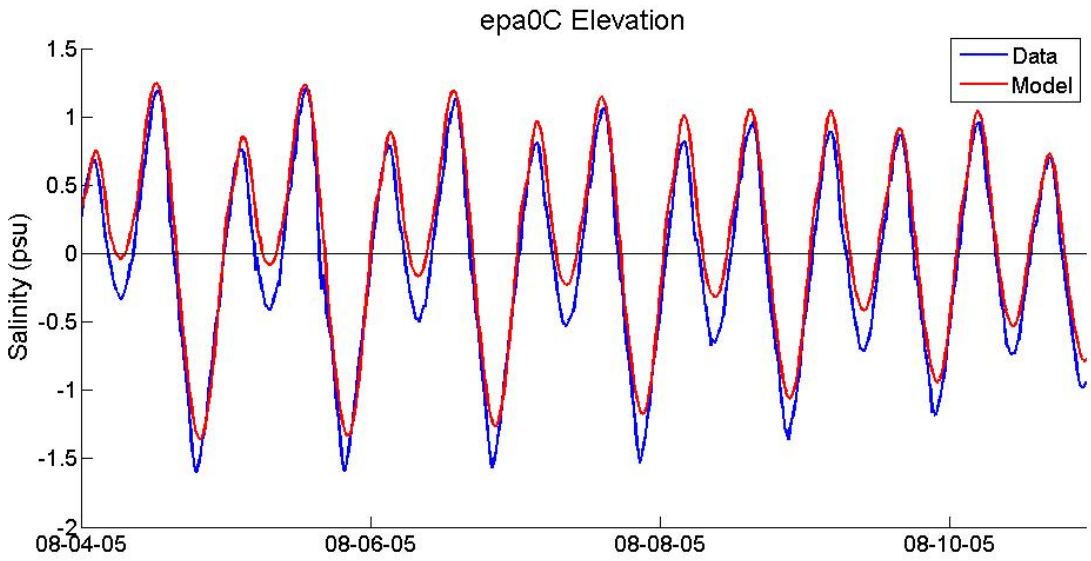

Figure 2.13 c: Elevation at station epa01, epa02 and epa0C for an August 2005 calibration run. The EPA depth data was not normalized to MSL, so elevation data was derived by de-meaning the EPA data and adding the mean elevation of NOAA's Charleston tide gauge over the same period. Bathymetry data for the epa02 region (the tributary formed by the Palouse and Larson rivers near North Bend) was considered very unreliable. Model-data comparison shows that either model bathymetry is too shallow or the channel in this region is not functioning properly numerically due to the SELFE rule that if one node is dry the element is considered dry. Observations at both stations show that ebb tides are significantly deeper than model ebbs.

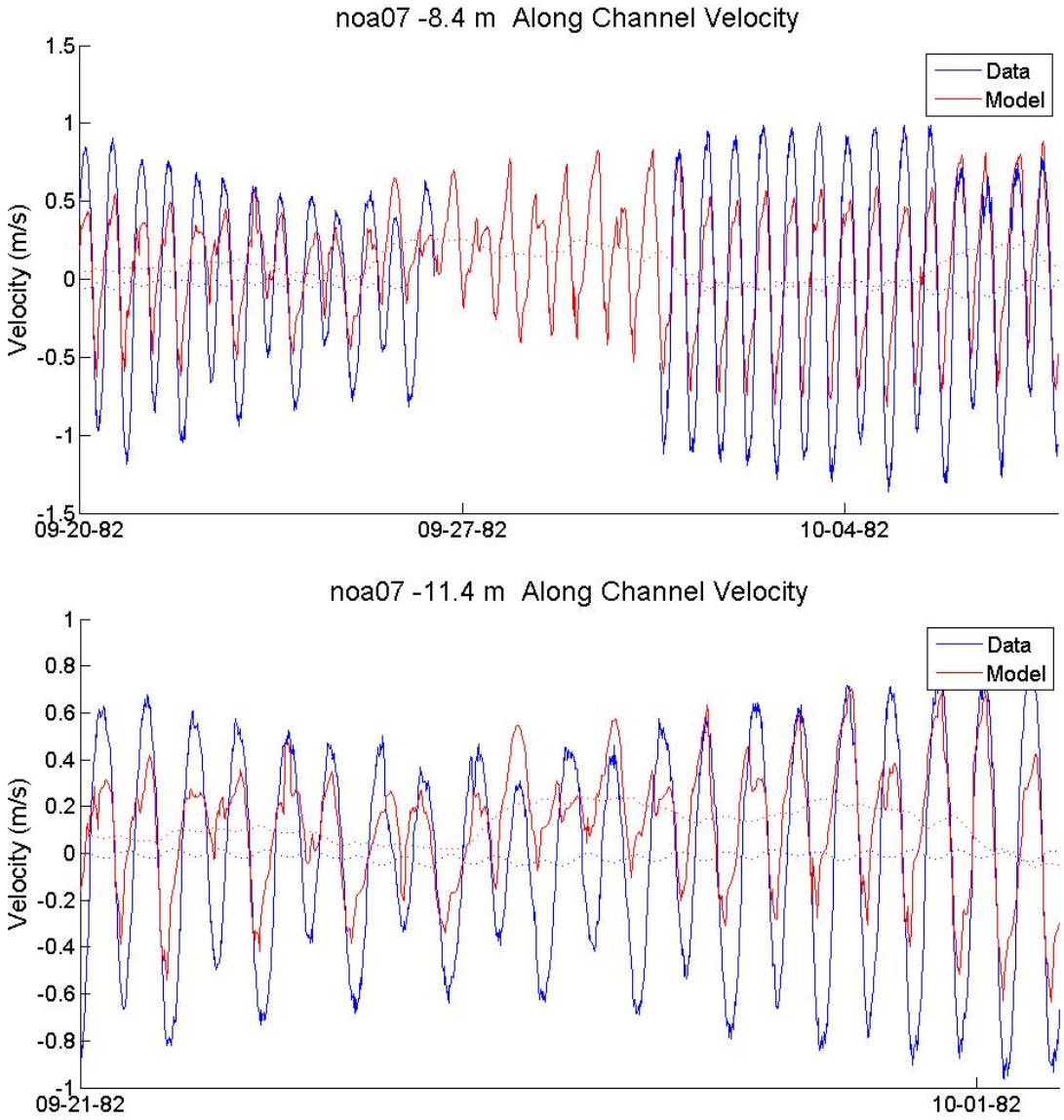

Figure 2.14 a-b: Model-data comparisons of along channel velocity from the NOAA82 data. Images are ordered from mouth to head. Velocity representations are poorest in the mouth, which results in considerable under-representation of tidal excursions (**Table 2.4**).

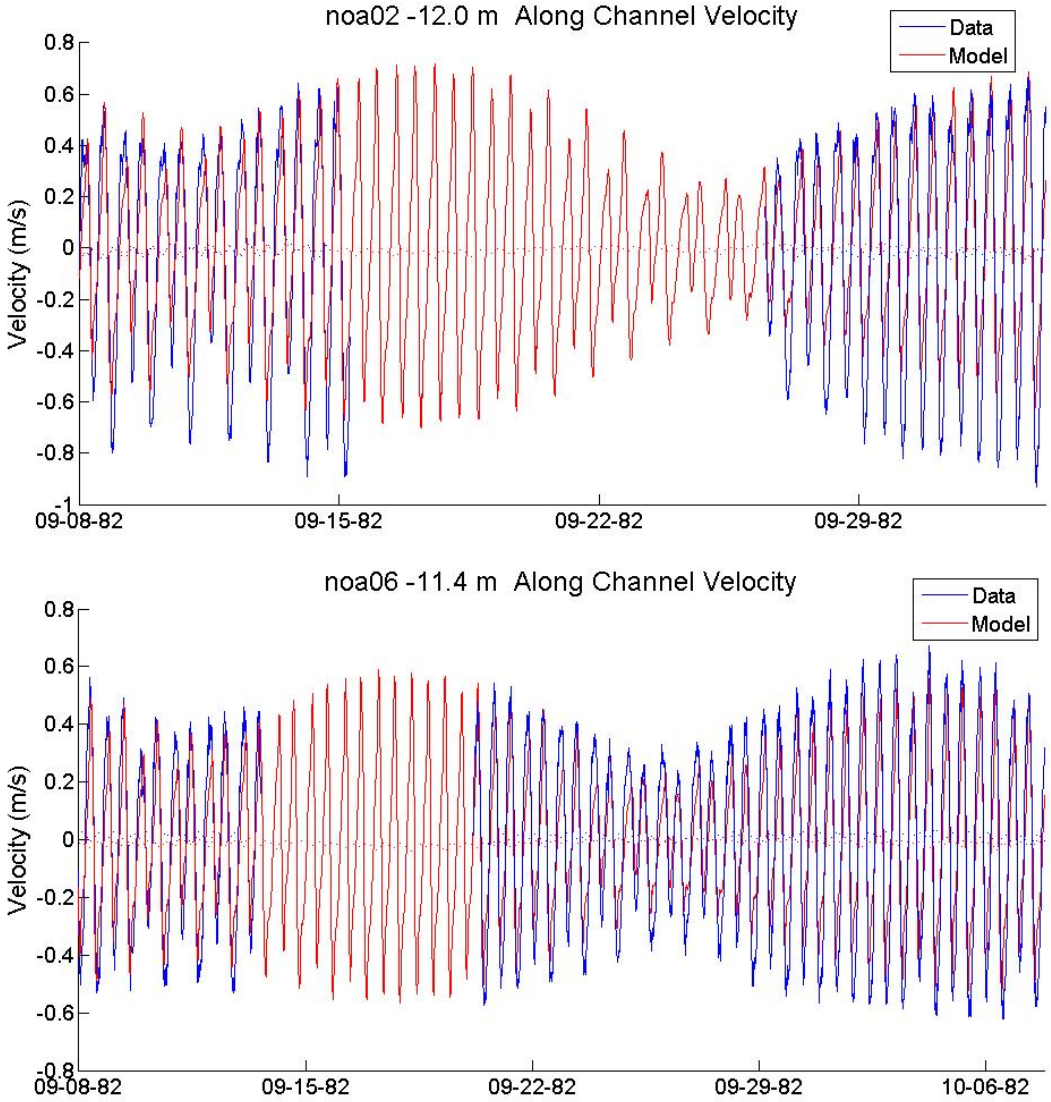

Figure 2.14 c-d: Model-data comparisons of along channel velocity from the NOAA82 data. Images are ordered from mouth to head. Velocity representations are generally improving from the higher errors at the mouth, but tidal excursions remain under represented (**Table 2.4**).

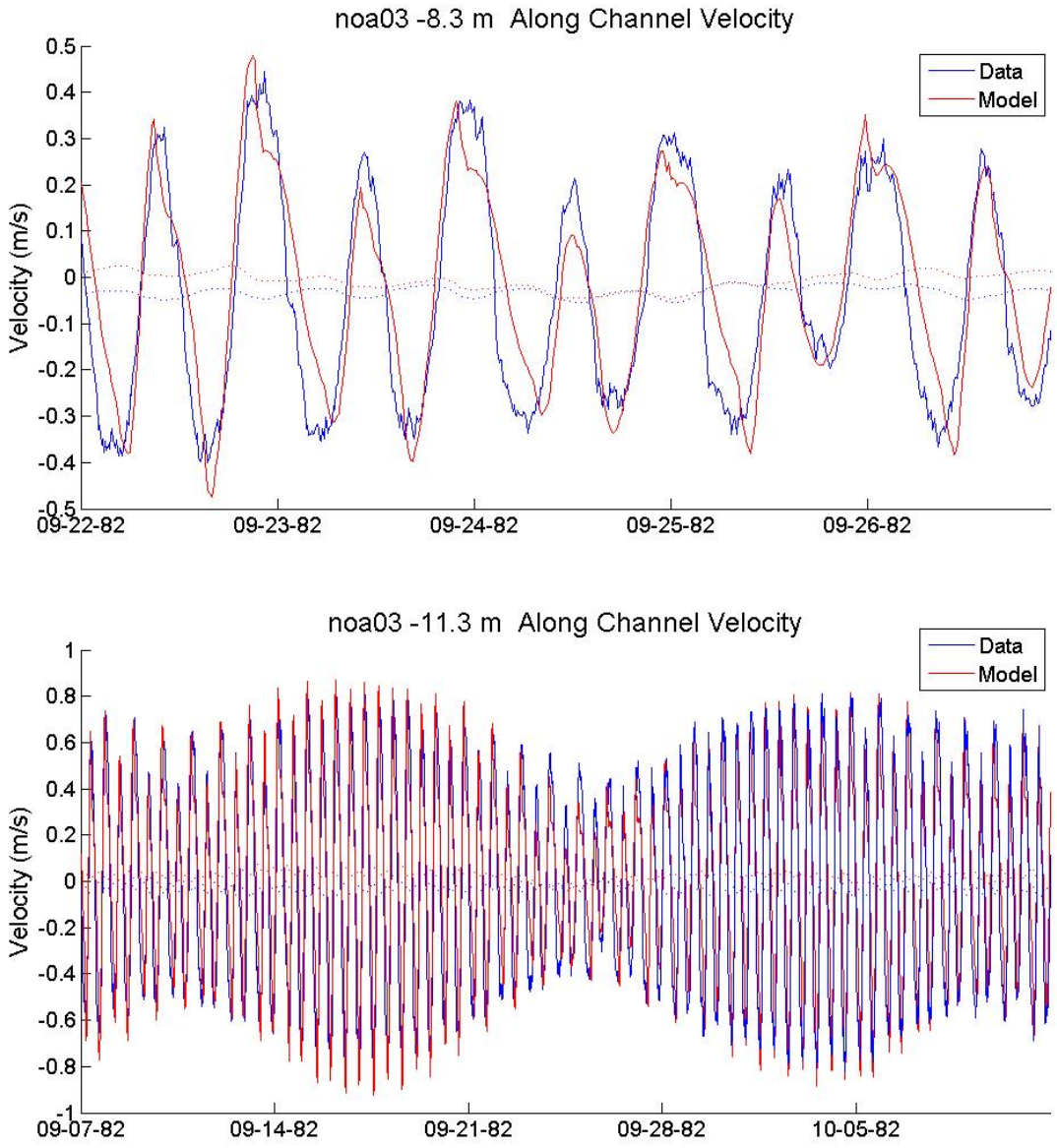

Figure 2.14 e-f: Model-data comparisons of along channel velocity from the NOAA82 data. Images are ordered from mouth to head. Again, velocity representations are generally improving from the higher errors at the mouth, but with continued under-representation of tidal excursions (**Table 2.4**).

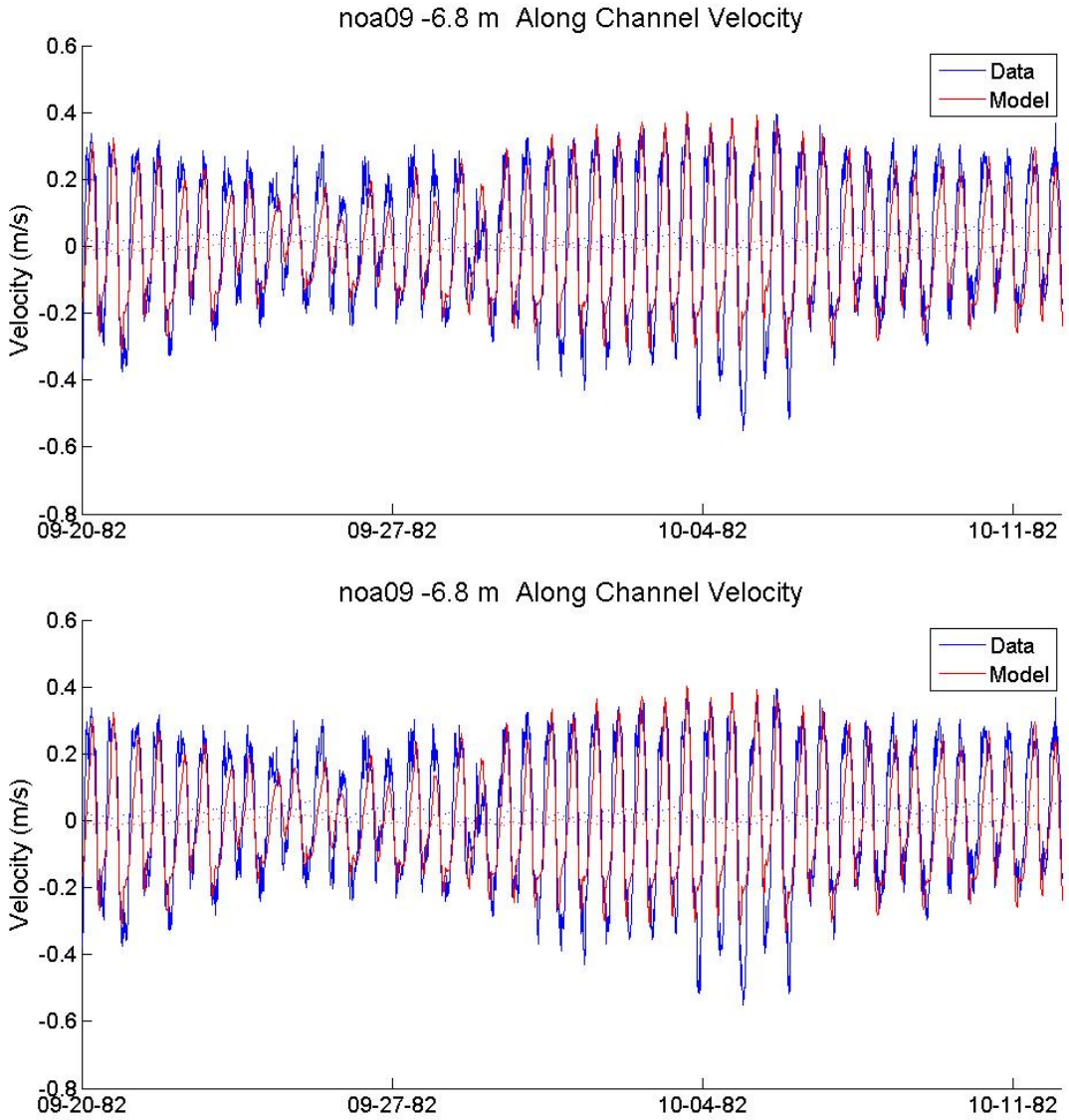

Figure 2.14 g-h: Model-data comparisons of along channel velocity from the NOAA82 data. Images are ordered from mouth to head. While velocities are generally well represented, there is still some difference in the tidal excursion (**Table 2.4**).

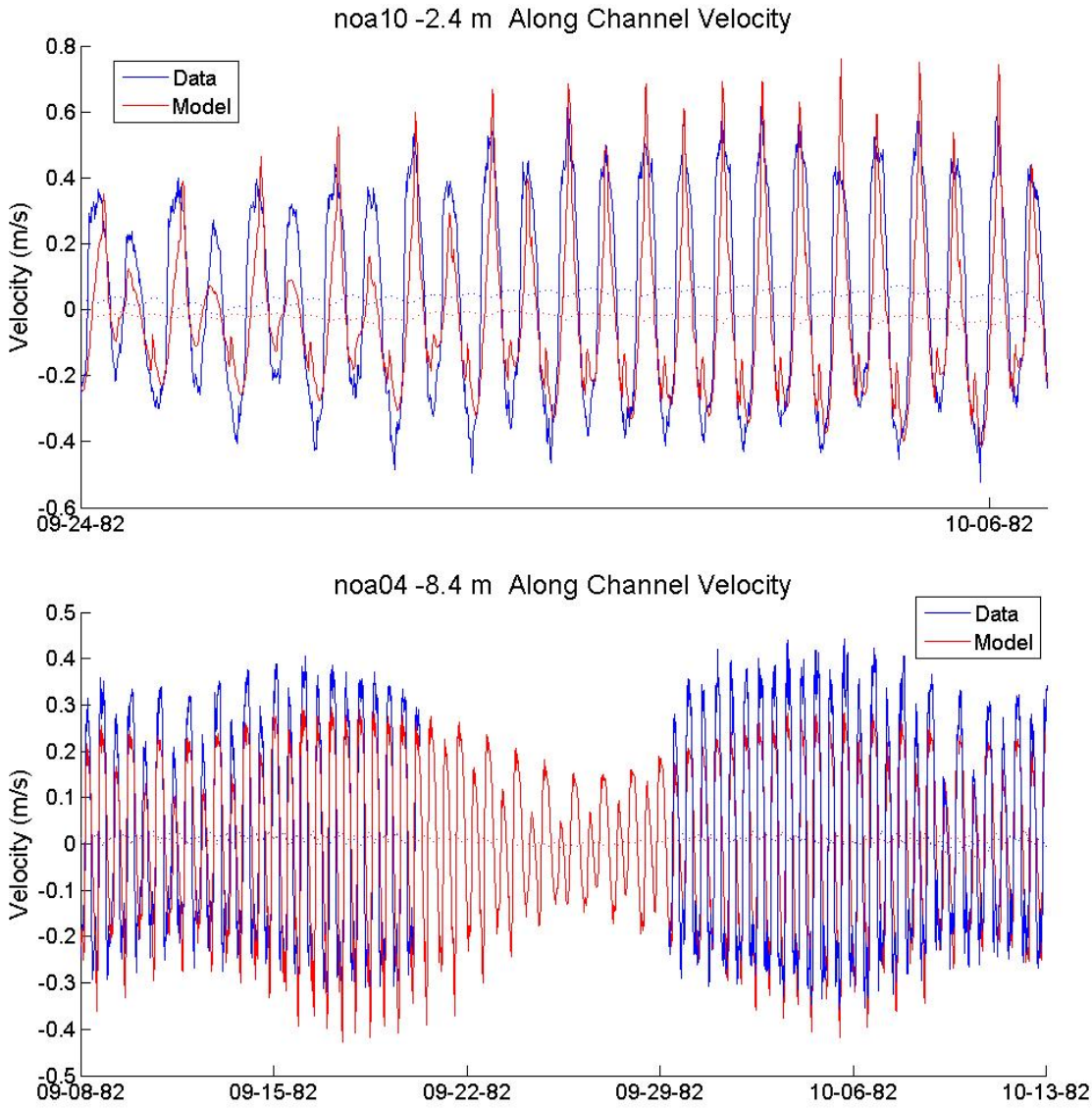

Figure 2.14 h-j: Along-channel velocity plots stations at the head of the estuary.

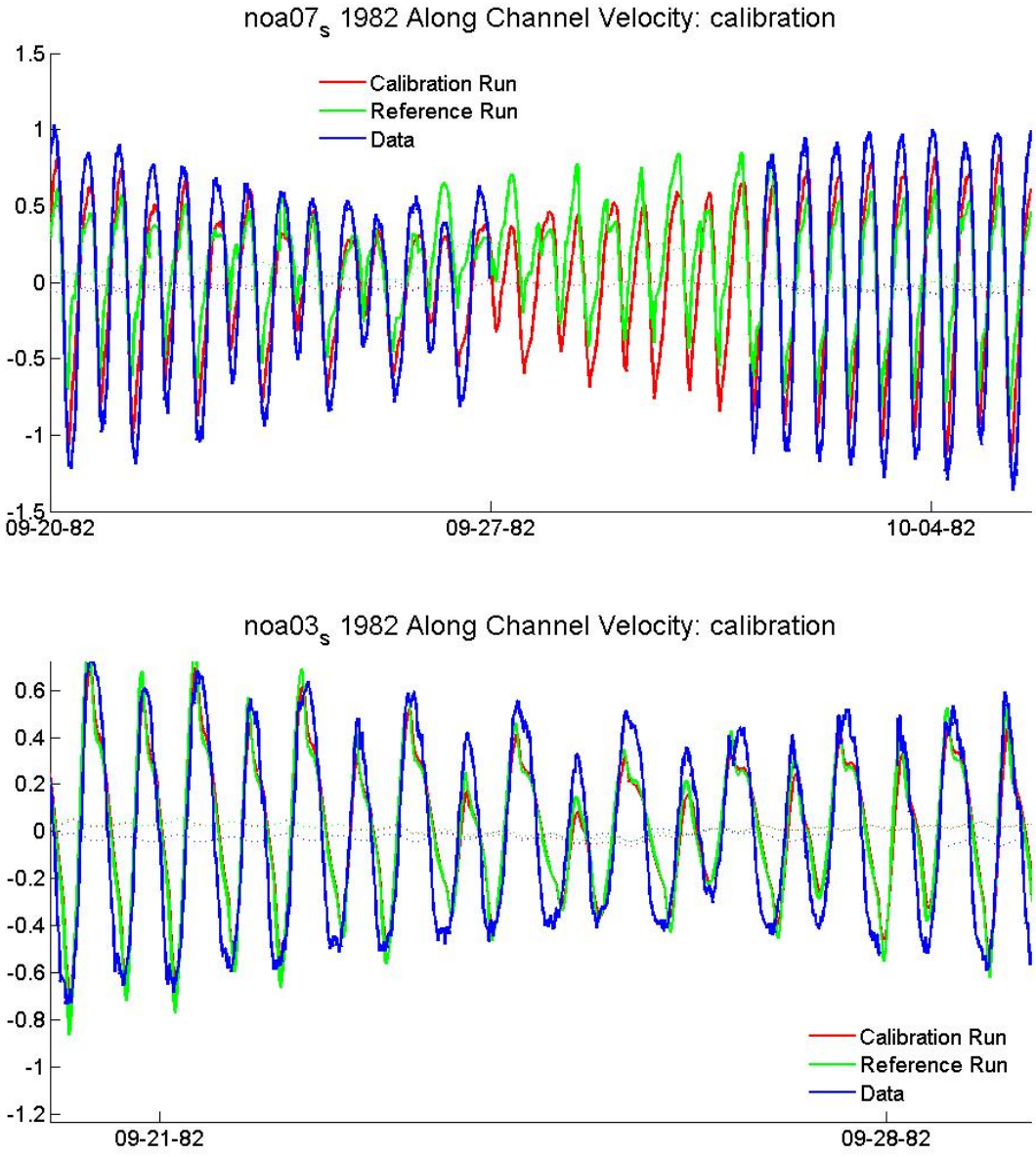

Figure 2.15: Comparison of velocity: reference model, calibration model with the stray node removed and increased grid resolution and data. **a)** station noa07, near the mouth and stray node, shows some improvement. **b)** station noa03, near North Bend, shows little difference.

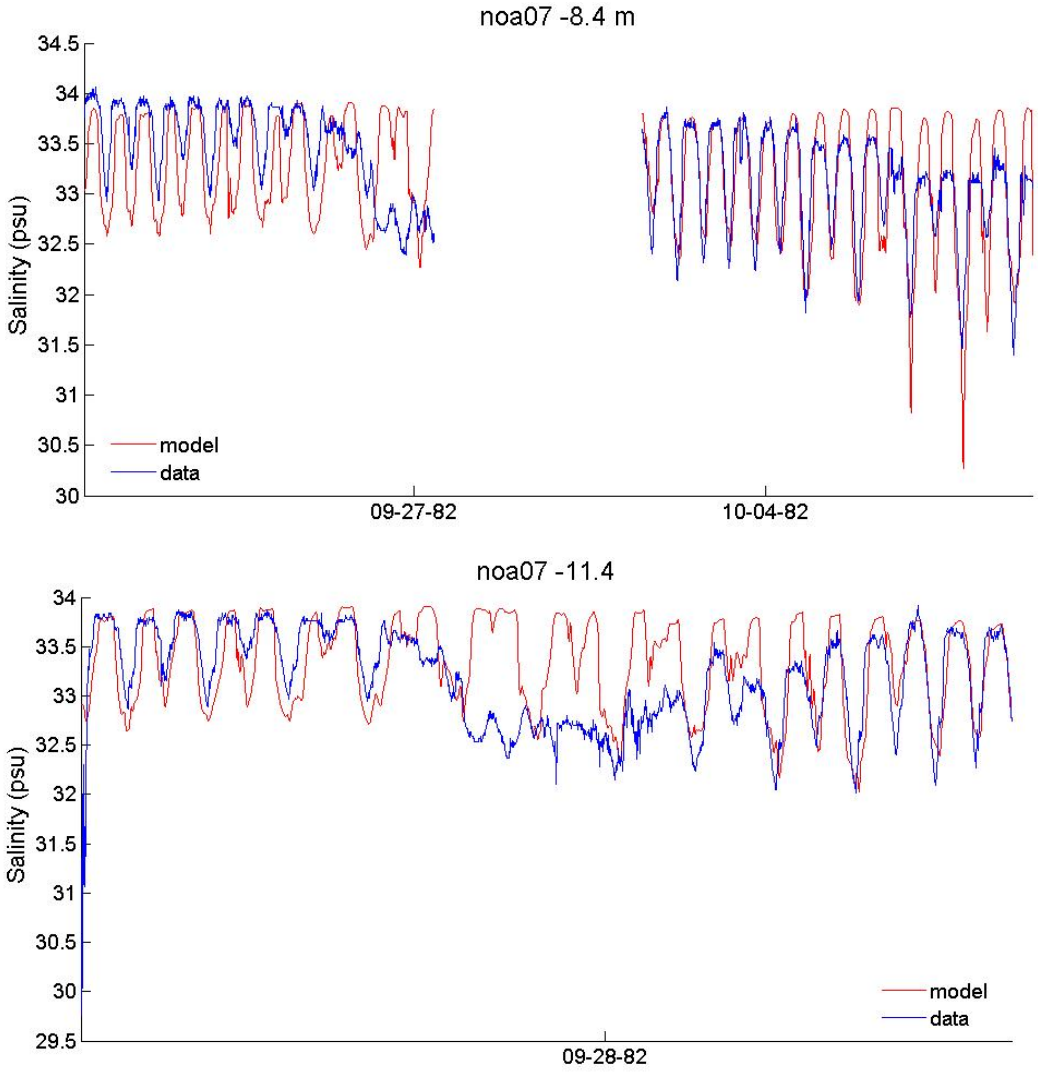

Figure 2.16 a-b: Salinity plots for the summer 1982 run, with images ordered from mouth to head. Model results show that salinity is well represented in the mouth, but that a significant observed ocean based freshening was not captured. This suggests poor model representation of wind effects and/or open ocean conditions.

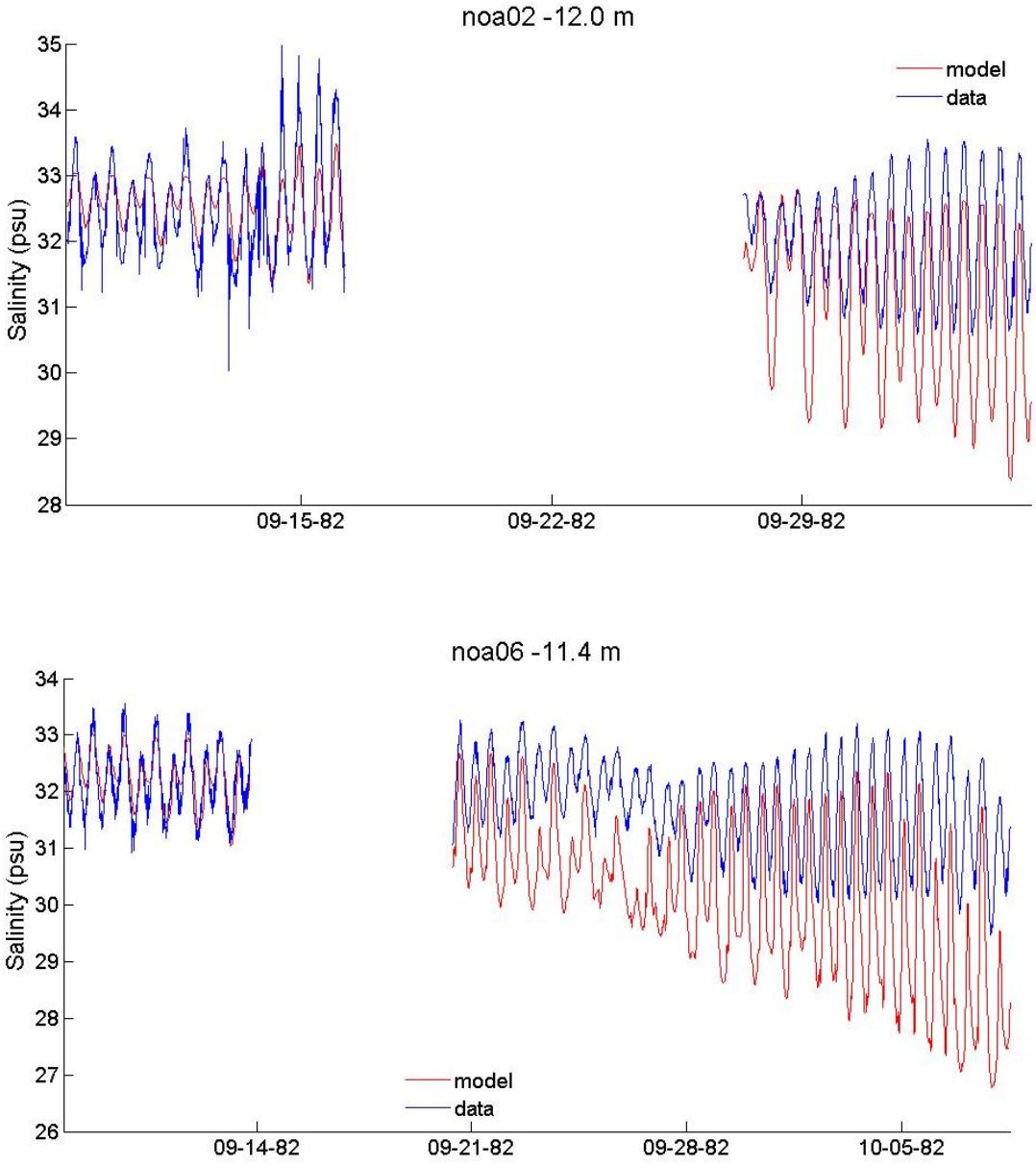

Figure 2.16 c-d: Salinity plots for the summer 1982 run of stations near North Bend. Model and observed salinity fall with increasing river flow, but the model falls considerably faster.

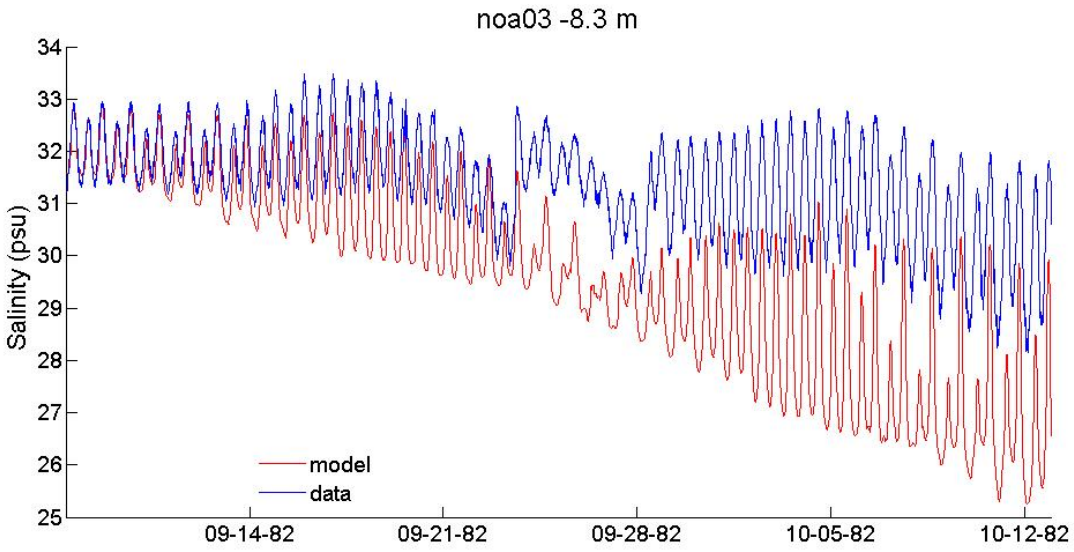

Figure 2.16 e: Salinity plots for the summer 1982 run of another stations near North Bend.

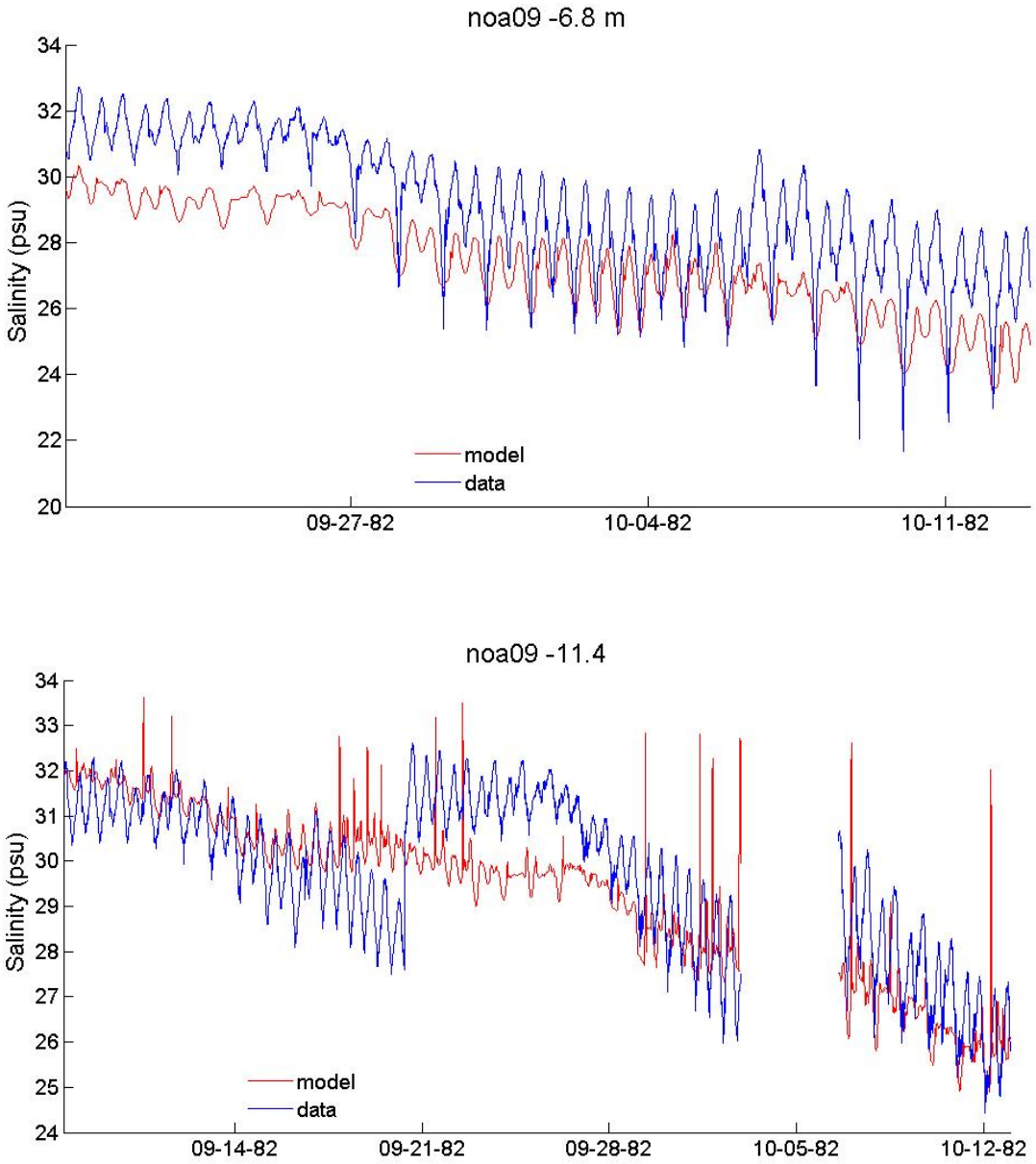

Figure 2.16 f-g: Salinity plots for the summer 1982 run for a station near the city of Coos Bay. The observations at the deeper station show evidence of measurement error, while the model at that depth shows salinity spikes due to a modeling artifact in which elements that go from dry to wet end can be assigned too-high salinity. In general, the data does not experience as large a range of salinities, which may be directly due to tidal excursion under-representation or other model errors relating to salinity intrusion.

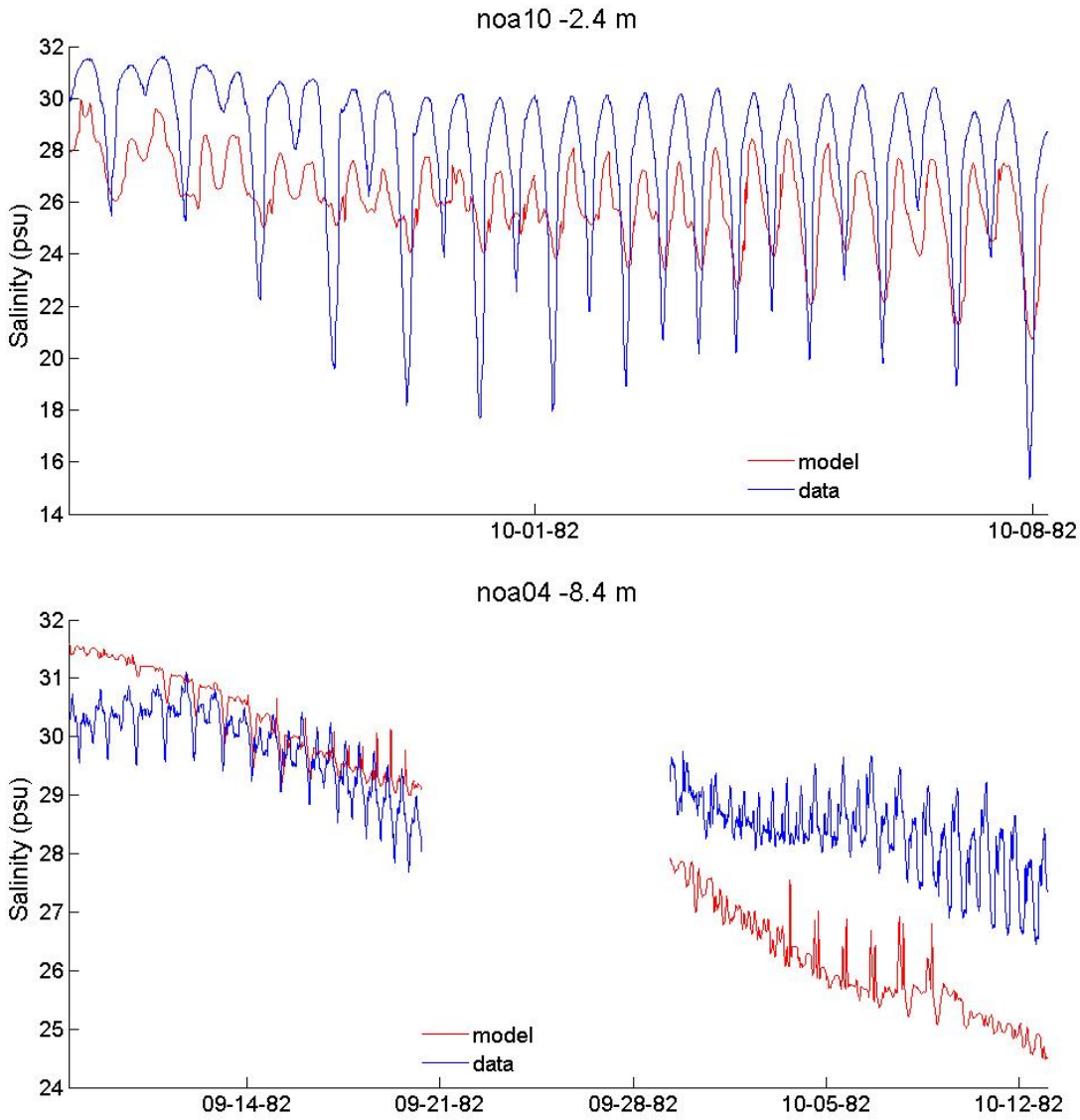

Figure 2.16 h-i: Salinity plots for the summer 1982 run of stations at the head. Again the model under-represents salinity, and the amplitude of the salinity signal.

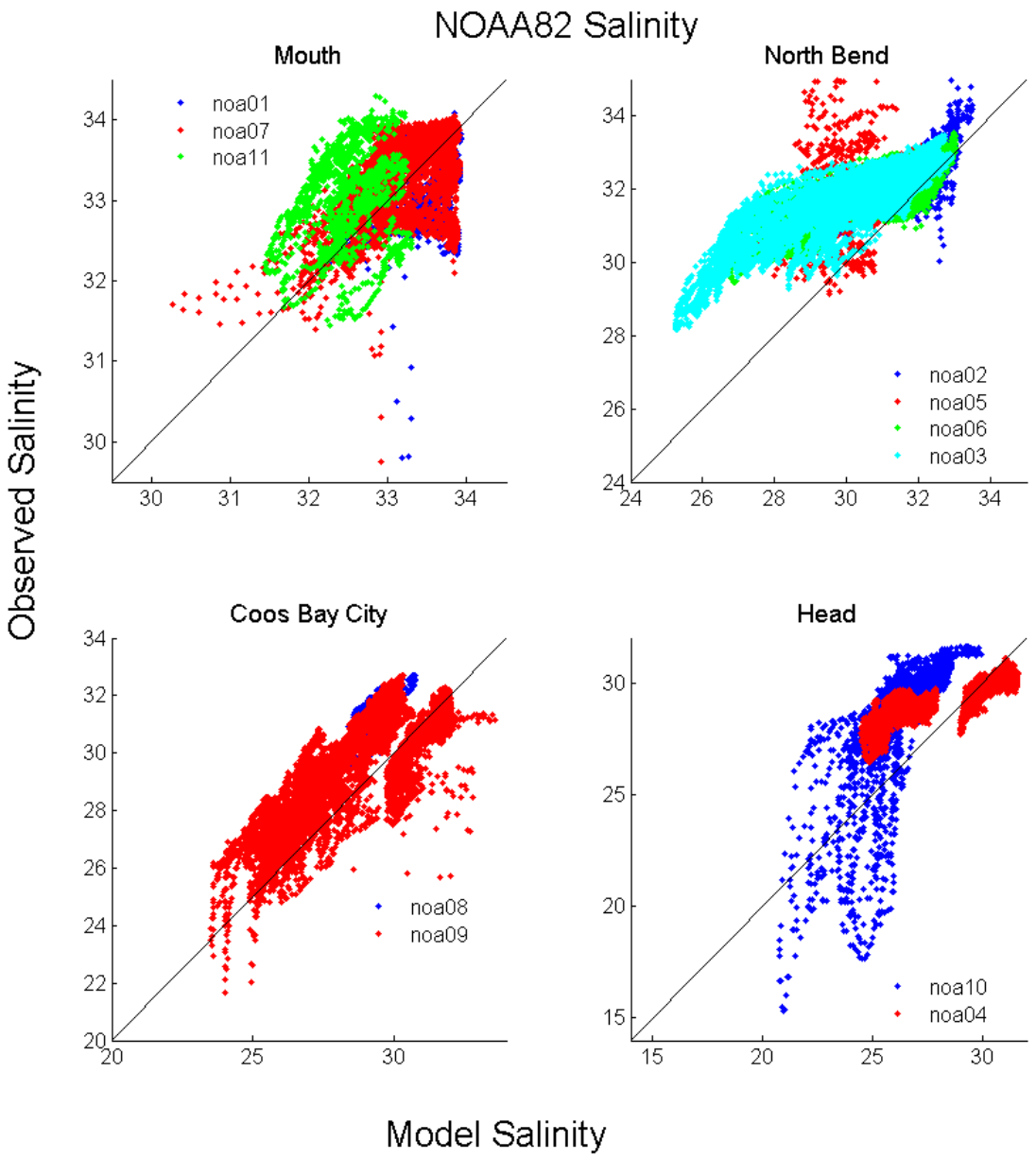

Figure 2.17: Salinity scatter plots for all depths at all NOAA82 stations. Stations are combined by general region. At the stations near the mouth the model does not show a consistent over or underestimate. Near North Bend the model underestimates salinity especially as the model gets fresher. Near the city of Coos Bay the model both over and underestimates, but underestimates are more common. At the two head stations, the model again consistently underestimates salinity, although during the early deployment of noa04 the model is fairly accurate.

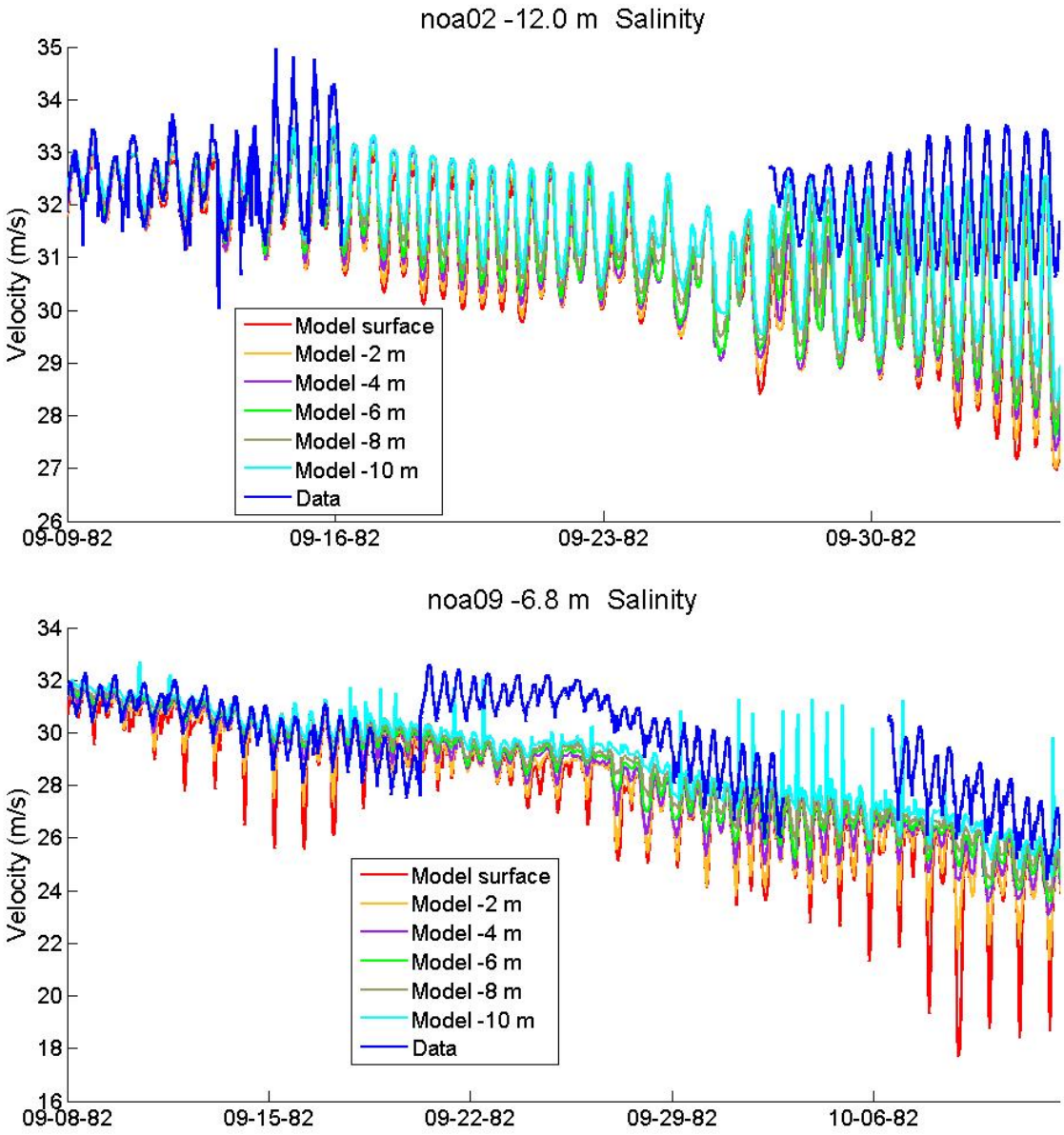

Figure 2.18: Comparisons between observations and the model at various depths. Because of the uncertainty about the location of NOAA82 station deployments in the water column, the effect of comparing different model elevations to observations was investigated. Vertical position has increasing affect on salinity towards the head.

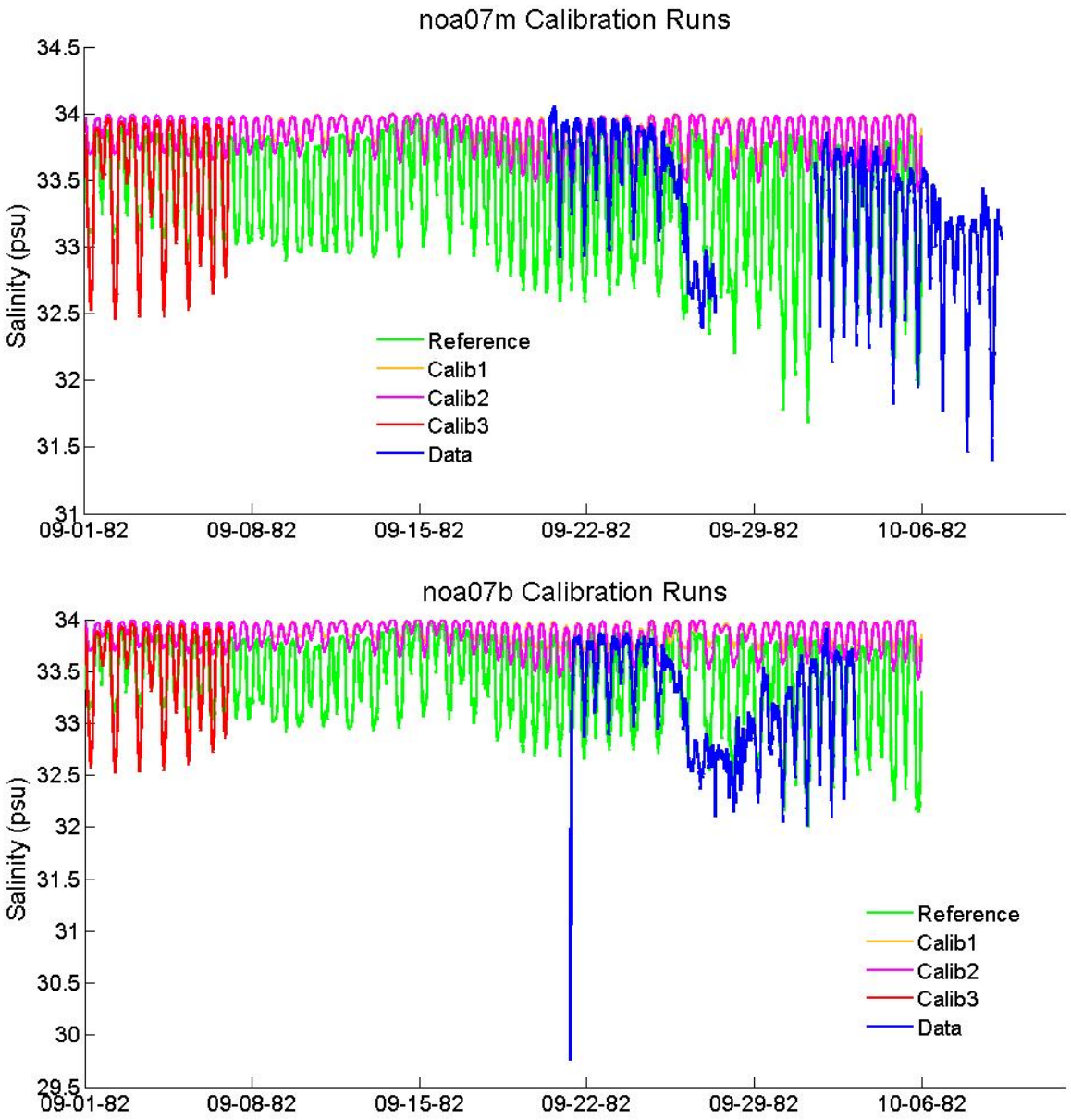

Figure 2.19 a-b: Salinity sensitivity to calibration runs at noa07, with observed data. Run details appear in **Table 2.7**.

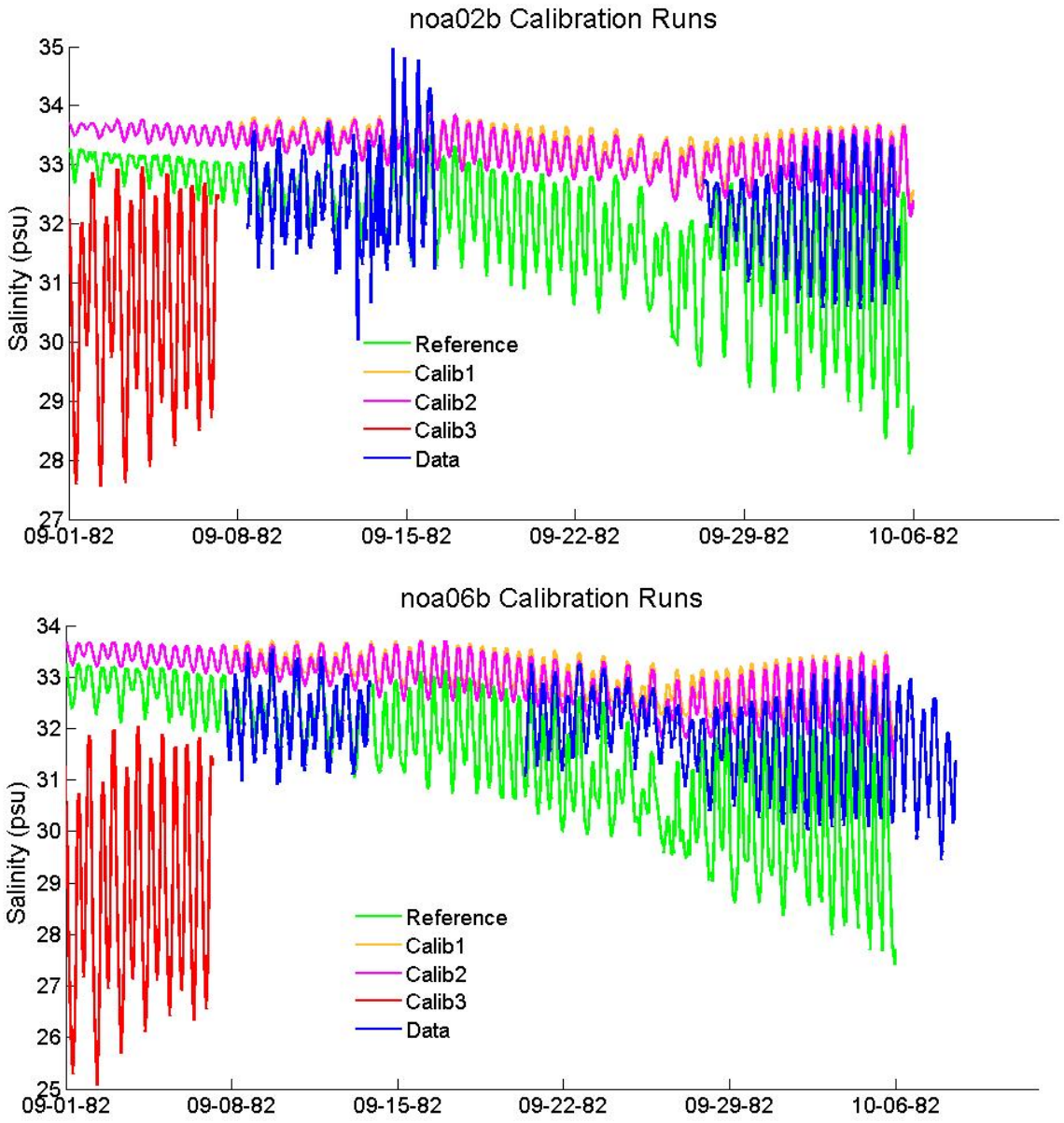

Figure 2.19 c-d: Salinity sensitivity to calibration runs at noa02 and noa06, with observed data. Run details appear in **Table 2.7**.

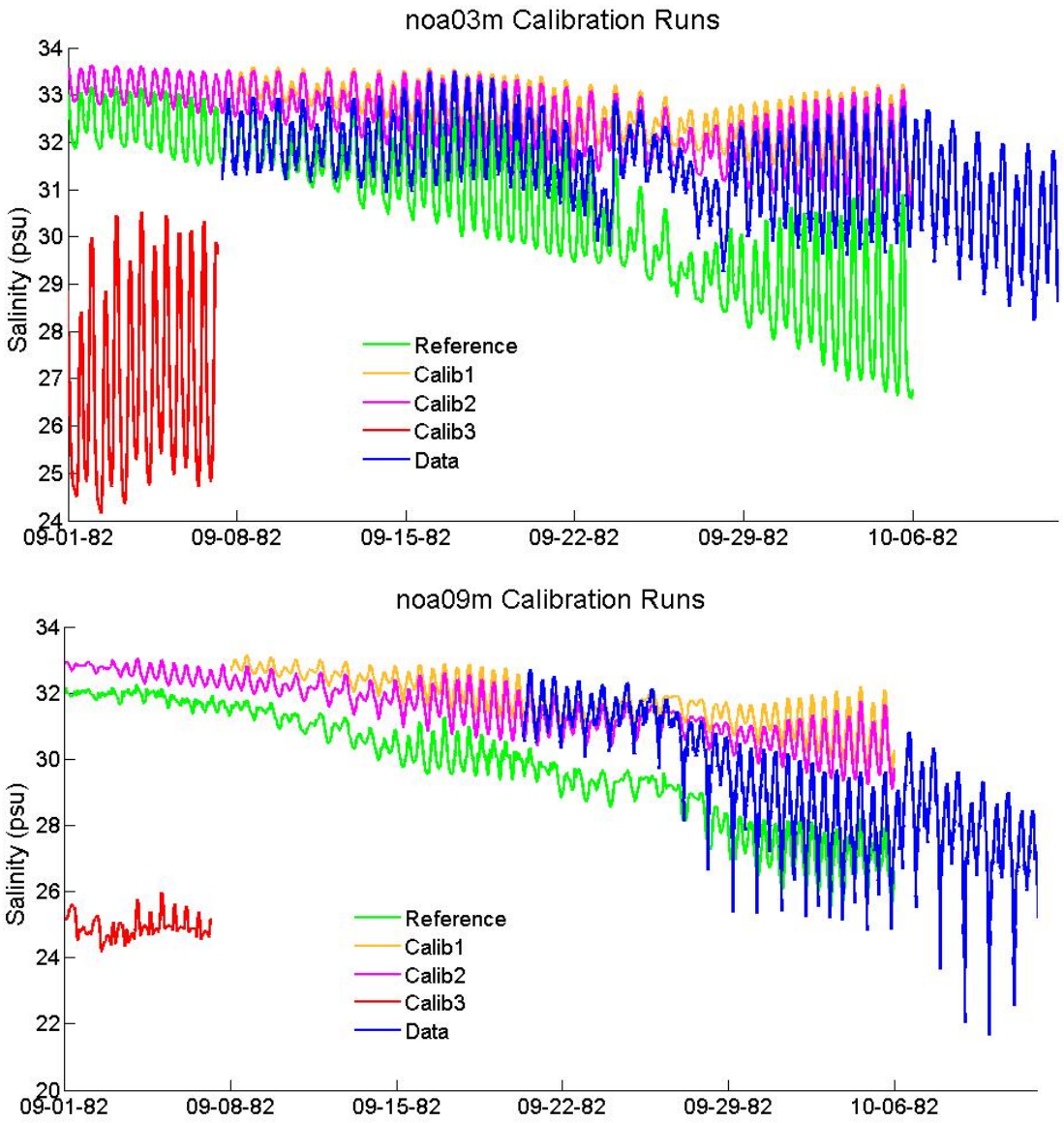

Figure 2.19 e-f: Salinity sensitivity to calibration runs at noa03 and noa09m, with observed data. Run details appear in **Table 2.7**.

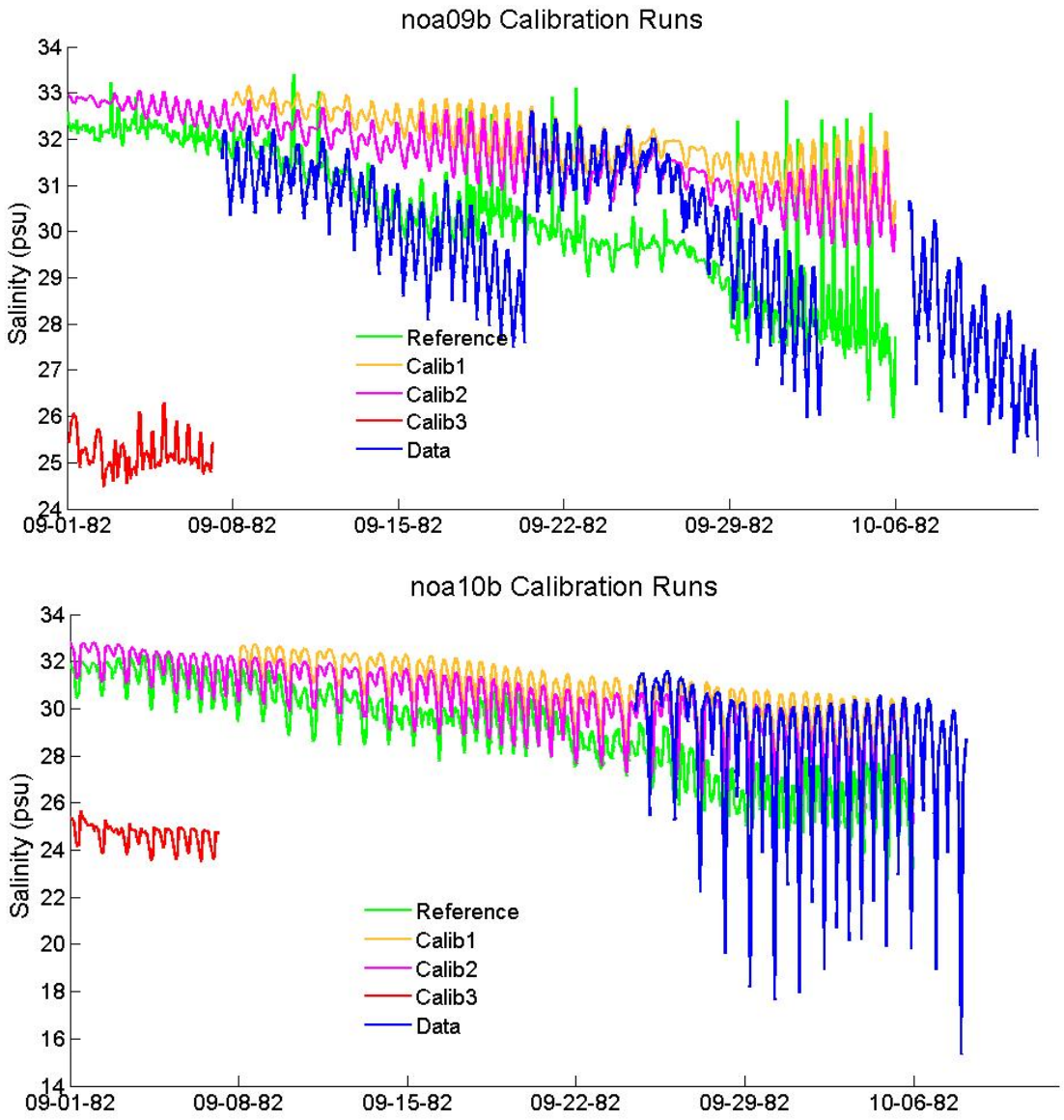

Figure 2.19 g-h: Salinity sensitivity to calibration runs at noa09b and noa10, with observed data. Run details appear in **Table 2.7**.

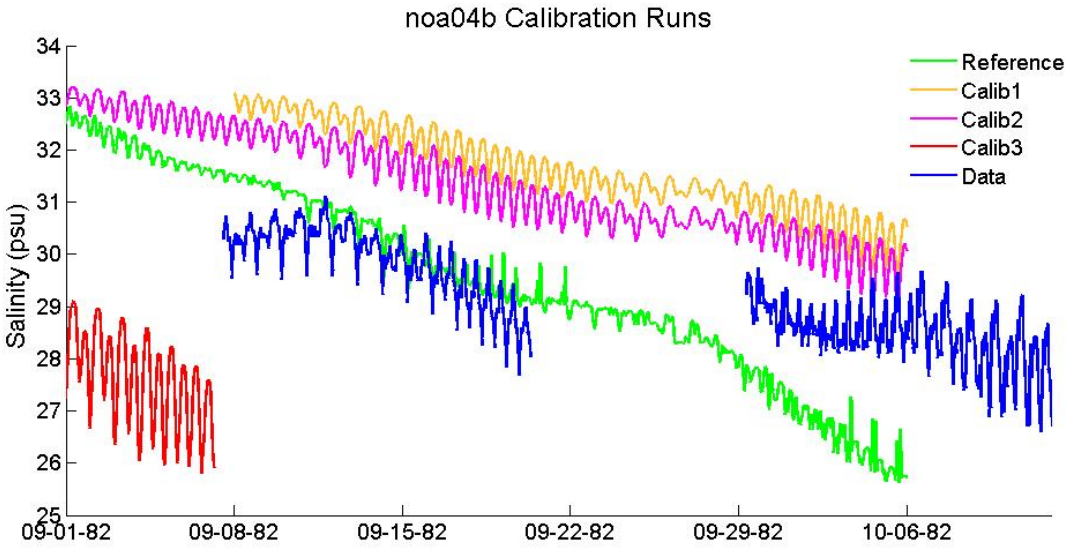

Figure 2.19 i-j: Salinity sensitivity to calibration runs at noa04 with observed data. All calibration runs use the upwind transport algorithm and have the stray node removed. Calib3 was stopped early once it became clear that replacing mixing pools with a long Coos River would greatly decrease salinity intrusion.

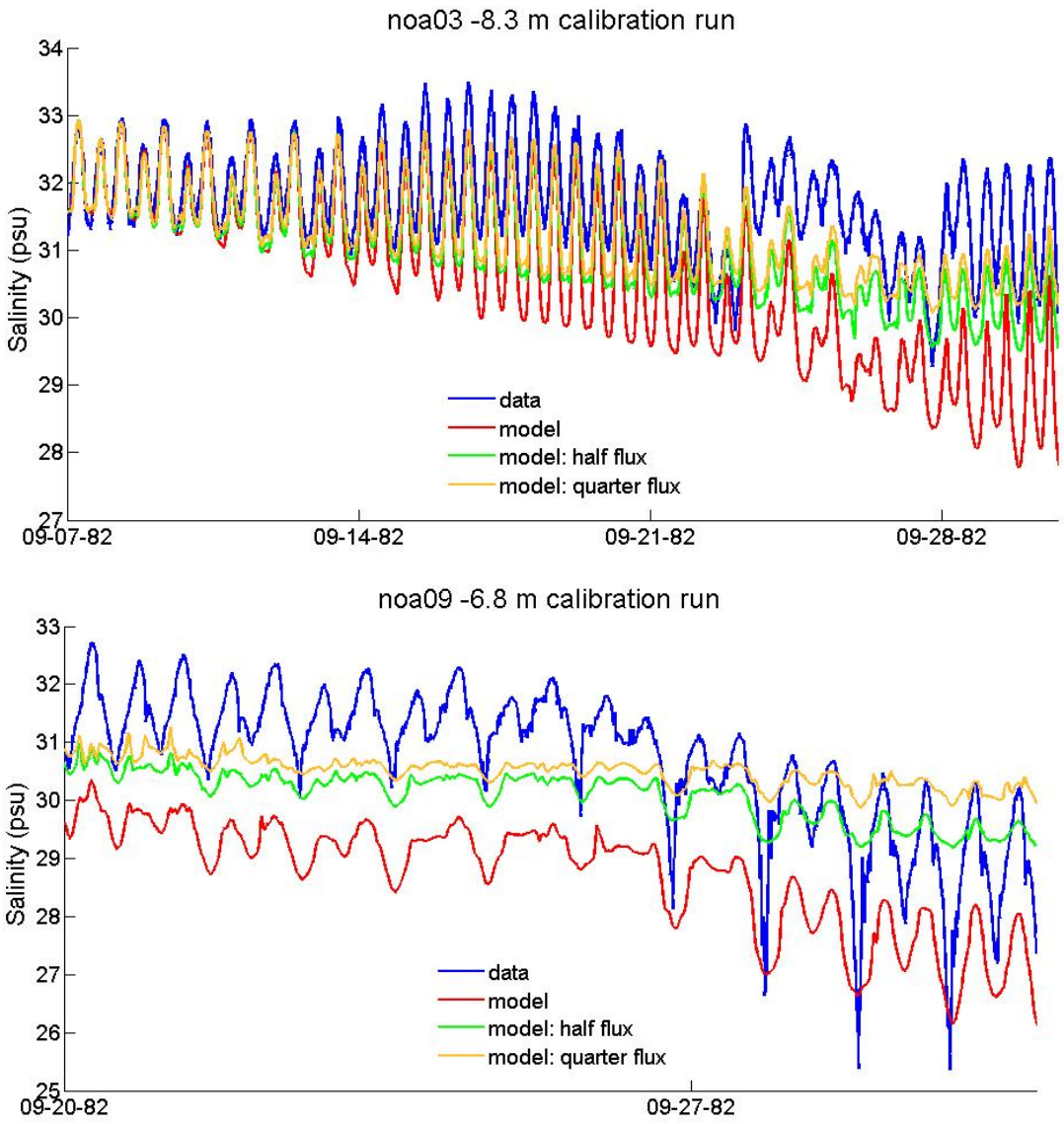

Figure 2.20 a-b: Salinity sensitivity to reductions in freshwater flow for the 1982 run, with observed data. The flux sensitivity analysis shows reduced flows raises the tide salinities, but causes the model to lose much of the tidal range.

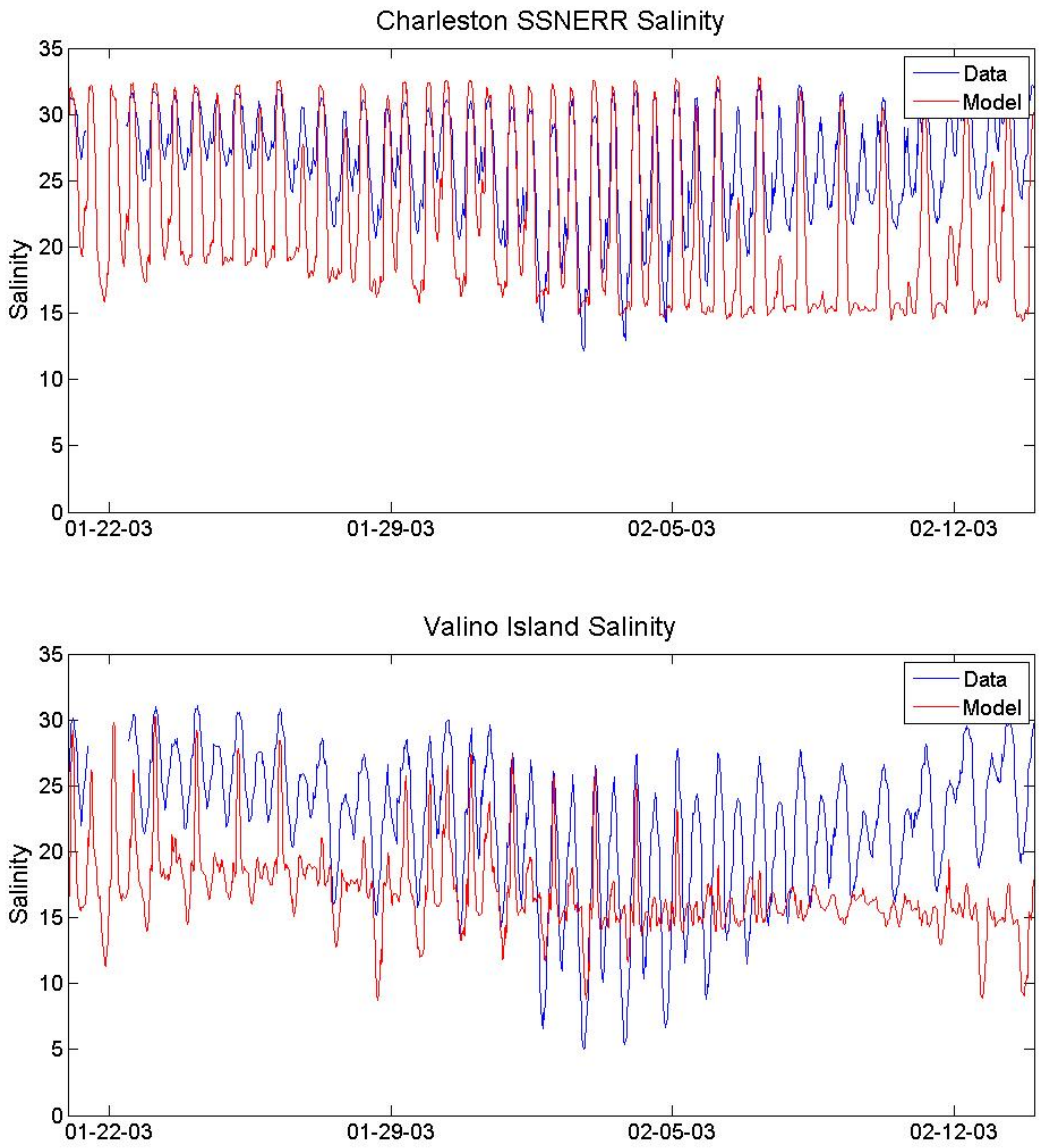

Figure 2.21 a-b: Salinity time series for each depth at the SSNERR stations near the head of South Slough. For visibility the SSNERR stations plot only the first 8 weeks of data. Model errors are considerable in the South Slough.

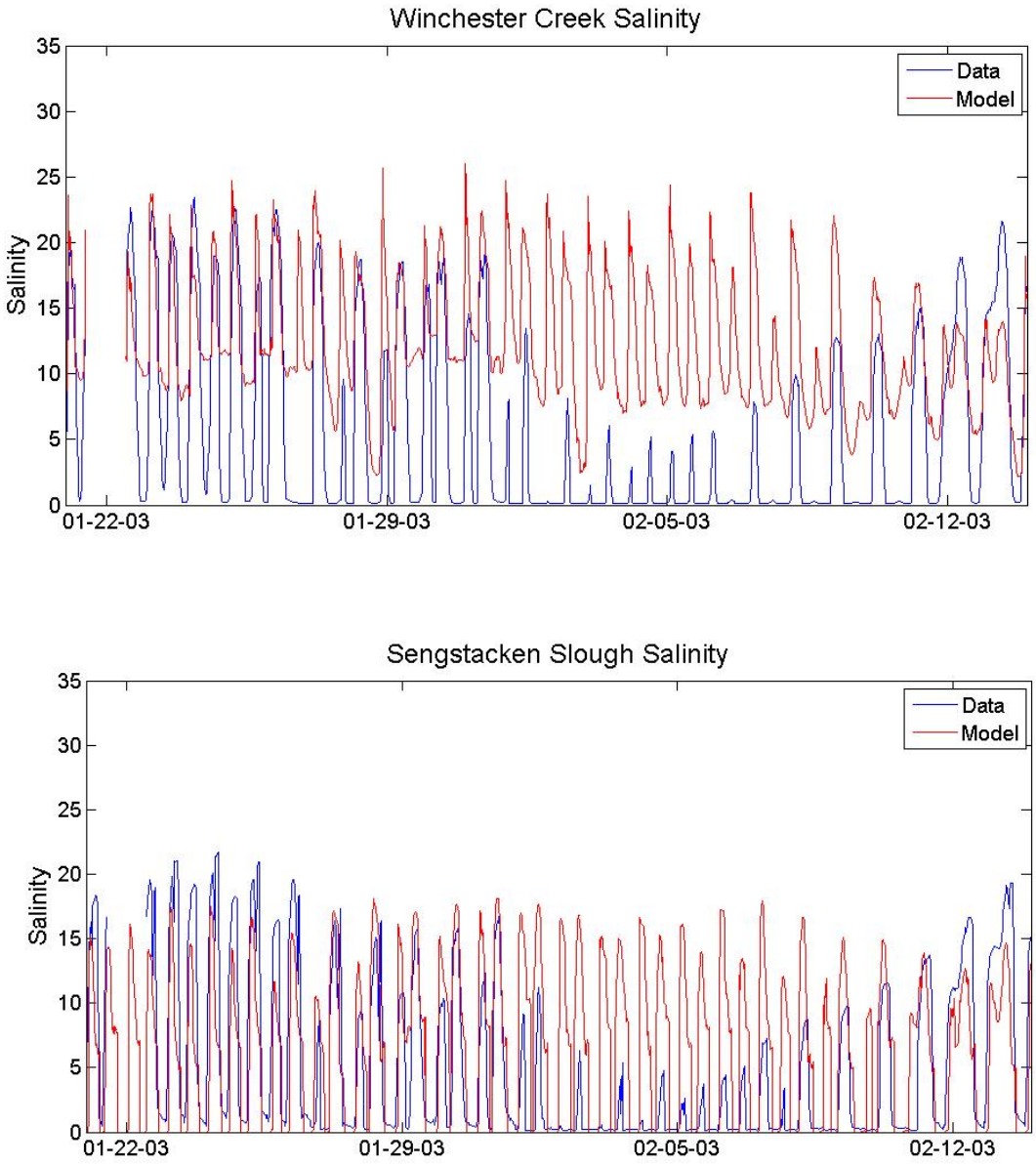

Figure 2.21 c-d: Salinity time series for each depth at the SSNERR stations near the head of South Slough. For visibility the SSNERR stations plot only the first 8 weeks of data.

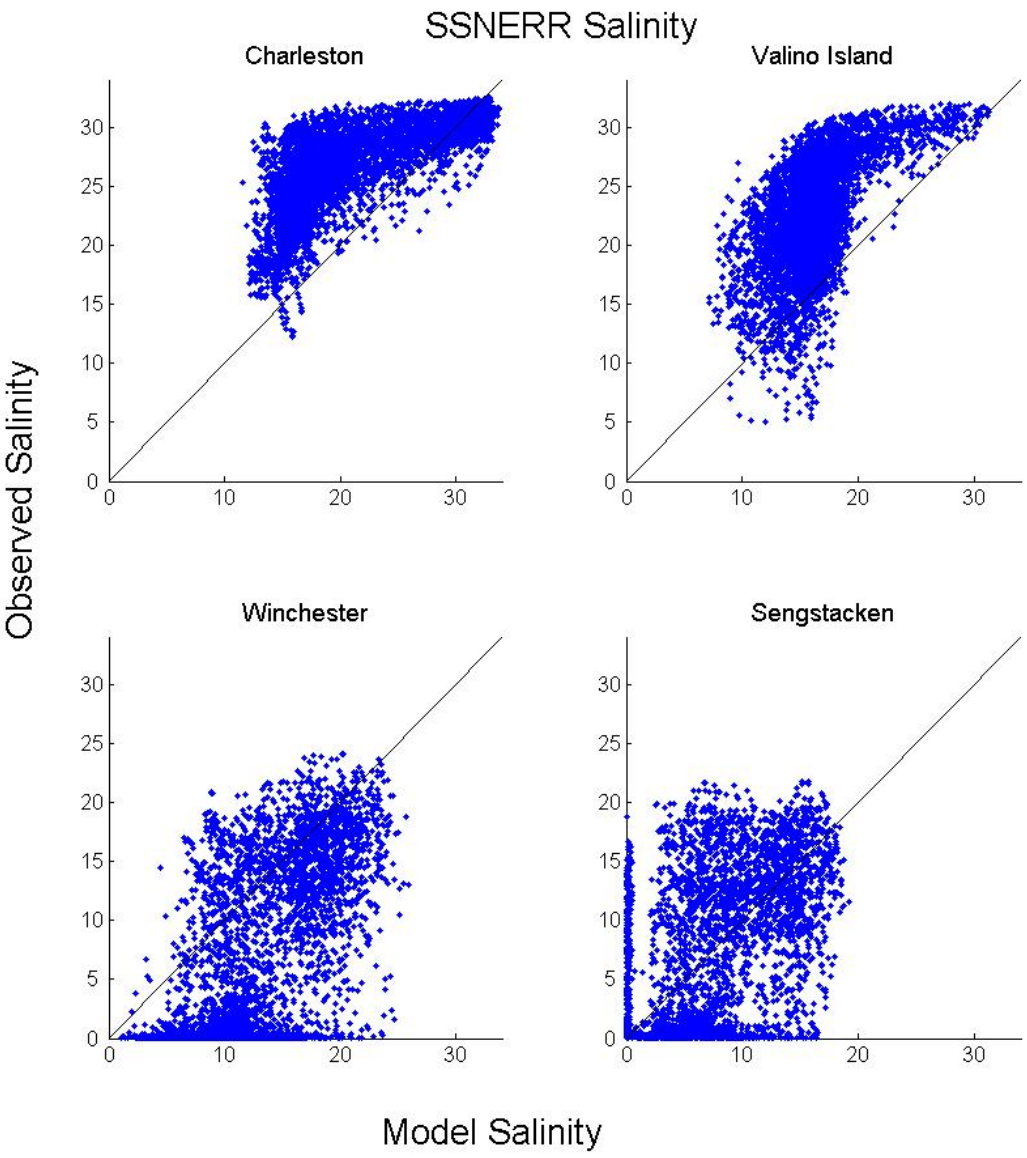

Figure 2.22: Model vs. data scatter plot for SSNERR salinity. The stations plot only the first 8 weeks of data. The data show underestimation of salinity in Charleston and Valino Island. Winchester and Sengstacken model results show significant under and overestimates.

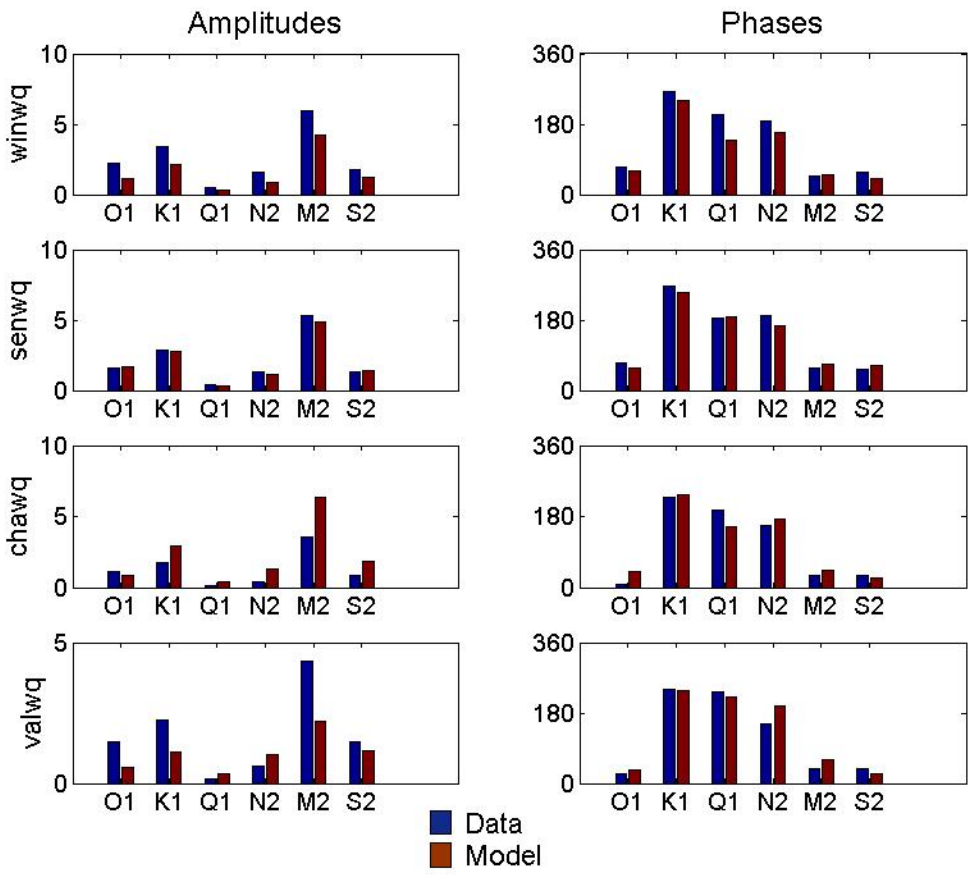

Figure 2.23: Harmonic analysis of salinity for the 2003 SSNERR stations

Tables

Source	Period of Record	Data Description
NOAA	September 8 – October 12, 1982	• Temperature, current and salinity from 11 Aanderaa current meters • Stationed from the mouth to Isthmus Slough • Measurement periods range from ~5 days to over 3 weeks • Measurements generally at near bottom and mid water column
NOAA	1977 – present	• Tide gauge at Charleston
SSNERR	1999 – 2004	• Temperature, salinity (plus other water quality data) from 3-4 (4^{th} added in 2002) YSI 6600 sondes • Stations are all in the South Slough • Measurements are all year, with only a few short gaps • All measurements are 0.5 m from the bottom
EPA	August 3 – 10, 2005	• Depth, temperature and salinity (plus other water quality data) from 4 stations • Temperature and salinity from a 2 day cruise on August 8 and 9
DEQ	1978 – present	• Grab samples of temperature and salinity (plus other water quality data) from throughout the estuary • No time-series data • Data was all collected at 1 m depth at roughly low tide

Table 2.1: Data sources

Station Name	Model Run	RMS error (m)	IOA
ccho3	1982	0.09	0.996
ccho3	2003	0.13	0.991
Chawq	2003	0.31	0.947
Valwq	2003	0.31	0.941
Winwq	2003	0.38	0.880
Senwq	2003	0.40	0.830

Table 2.2 RMS error and index of agreement for all stations with elevation for all runs. Elevation results are accurate for Charleston, and accuracy decreases moving upstream in the South Slough.

Station Name	Tidal Const.	Model Run	Amplitude (m)	Phase (°)	Amp. error (m)	Phase error (°)
ccho3 model	K1	1982	0.316	219.8	0.032	-13.7
data			0.284	233.5		
ccho3 model	M2		0.815	93.7	-0.002	-30.1
data			0.817	123.8		
ccho3 model	K1	2003	0.410	60.2	0.02	-11.6
data			0.390	71.8		
ccho3 model	M2		0.773	39.8	-0.026	-26.6
data			0.799	66.4		
chawq model	K1	2003	0.402	240.3	0.013	5.06
data			0.385	238.6		
chawq model	M2		0.744	40.43	-0.043	13.3
data			0.787	27.1		
valwq model	K1	2003	0.379	247.8	0.001	5.1
data			0.380	242.7		
valwq model	M2		0.683	50.6	-0.104	17.5
data			0.787	33.1		
winwq model	K1	2003	0.348	263.3	0.038	11.2
data			0.310	252.1		
winwq model	M2		0.529	71.7	-0.146	30.4
data			0.675	41.3		
senwq model	K1	2003	0.308	268.2	0.060	11.8
data			0.248	256.4		
senwq model	M2		0.451	74.0	-0.117	34.9
data			0.568	39.1		

Table 2.3 Amplitude, phase and model-data differences for K1 and M2 tidal constituents for all stations with elevation data lasting more than 4 weeks. 2003 stations are listed in their order from estuary mouth to head.

Station	Depth from MSL	RMS Error (m/s)	IOA	Avg Magn data (m/s)	Avg Magn model (m/s)	Data Tidal Excursion (km)	Model Tidal Excursion (km)
noa01m	-8.6	0.29	0.897	0.51	0.29	11.3	6.4
noa07m	-8.4	0.38	0.865	0.59	0.33	13.1	7.5
noa07b	-11.4	0.29	0.873	0.42	0.30	9.5	6.7
noa11m	-8.4	0.19	0.920	0.36	0.24	8.1	5.4
noa11b	-11.4	0.14	0.941	0.27	0.24	5.9	5.4
noa02b	-12.0	0.19	0.946	0.39	0.29	8.7	7.3
noa05b	-2.76	0.15	0.919	0.25	0.23	5.5	5.1
noa06b	-11.4	0.13	0.952	0.30	0.26	6.6	5.4
noa03m	-8.3	0.18	0.955	0.42	0.33	9.9	7.7
noa03b	-11.3	0.12	0.938	0.22	0.22	5.0	4.9
noa08b	-11.3	0.14	0.850	0.18	0.15	4.0	3.3
noa09m	-6.8	0.10	0.920	0.19	0.15	4.2	3.1
noa09b	-11.4	0.11	0.914	0.19	0.15	4.2	3.2
noa10b	-2.4	0.14	0.941	0.28	0.19	6.2	4.2
noa04b	-8.4	0.12	0.939	0.22	0.16	4.8	3.8

Table 2.4 Along channel velocity model-data comparison of RMS error, index of agreement and data and model tidal excursion for all 1982 NOAA stations. Stations are listed from mouth to head.

Station	Depth from MSL (s | b)	Model Run	RMS Error (m)	Index of Agreement
noa01m	-8.6	1982	0.62	0.574
noa07m	-8.4	1982	0.48	0.805
noa07b	-11.4	1982	0.52	0.695
noa11m	-8.4	1982	0.96	0.521
noa11b	-11.4	1982	0.51	0.592
noa02b	-12.0	1982	0.91	0.789
noa05b	-2.76	1982	2.09	0.455 (*messy data*)
noa06b	-11.4	1982	1.66	0.616
noa03m	-8.3	1982	2.18	0.600
noa03b	-11.3	1982	1.74	0.455
noa08b	-11.3	1982	2.02	0.398
noa09m	-6.8	1982	1.90	0.780
noa09b	-11.4	1982	1.24	0.868
noa10b	-2.4	1982	2.88	0.701
noa04b	-8.4	1982	1.80	0.719
Chawq	-2.6	2003	6.5	0.664
Valwq	-1.4	2003	7.5	0.554
Winwq	-1.0	2003	8.2	0.679
Senwq	0.0	2003	5.2	0.794

Table 2.5 Salinity RMS error and Index of Agreement. All stations from the 2003 model run are 0.5 meters above the bottom.

Run	Standard Deviation (cm)	Mean Elevation (cm)
1982 data	7.3	1.39
1982 model	2.1	1.38
2003 data	11.1	7.5
2003 model	2.3	7.8
chawq data	14.0	24.0
chawq model	2.3	7.6
valwq data	14.4	2.7
valwq model	2.9	10.8
winwq data	14.2	6.8
winwq model	5.2	15.8
senwq data	13.7	1.2
senwq model	5.6	21.1

Table 2.6 Standard deviation and mean elevation for the NOAA tide gauge at Charleston, ccho3 and the SSNERR stations. The model shows considerably less variability than the data.

	Resolution / Bathymetry improvements	**Mixing Pools**
Calib1	No	Yes
Calib2	Yes	Yes
Calib3	Yes	No

Table 2.7 Calibration runs for determining source and solutions for velocity and salinity errors. Calib3 was stopped early once it became clear that removing the mixing pools greatly reduced salinity intrusion. All three calibration runs include the removal of a stray node near noa07 and use an upwind (as opposed to Eularian-Lagrangian) numeric solution to transport in the momentum equations. All three runs also include improved resolution and bathymetry representation from the mouth to North Bend.

3. Model-Based Estuarine Characterization and Classification Systems: Concept and Pilot Application

Abstract

The advent of climate-scale simulation databases of circulation creates the opportunity to re-visit and expand fundamental understanding of estuarine processes, including the extended ability to conduct comparisons across estuaries. Here, we describe the vision and conceptual underpinnings for a new model-based estuarine characterization and classification system (MECCS), and explore, through a pilot application, the implementation of such system. The pilot implementation focuses on Coos Bay (a mostly well-mixed estuary), but includes selected contrasts with the Columbia River (a highly stratified estuary). At the core of MECCS is the filtering of simulation databases of 3D baroclinic circulation, using mostly classical definitions of a range of dimensionless numbers and classification parameters. As illustrated in this paper, MECCS offers effective logistical means to hypothesize, to classify and to contrast estuarine behavior.

How model error and uncertainty affect estimates of estuary parameters and associated inferences on estuary characteristics and classification, is an issue of paramount importance, which will ultimately determine the usefulness of MECCS. In a separate paper, the observation-rich Columbia River estuary will provide a controlled environment for exploration of the implications of model error and uncertainty.

3.1 Introduction: The vision for a model-based estuarine characterization and classification system

Much work has been done on estuarine characterization and classification, dating back to the classical works of Pritchard 1952, Pickard 1956, Simmons 1955 and others. Classification has been based on characteristics such as tidal range, tidal propagation, morphology and salinity structure (Dyer, 1997), typically defined through field

observations. A wide range of estuarine quantities, often organized through composite dimensionless numbers, form the basis for most classification systems.

Advances in modeling systems within ocean observatories make it feasible to consider characterizing and classifying estuaries through quality-controlled long-term simulation databases, such as those developed for the Columbia River as a part of the CORIE observatory. However, the power of modeling systems as a basis of estuarine characterization and classification will be far more transformative if it can be extended beyond observation-rich systems such as the Columbia River.

As a null hypothesis, we consider that there is value in using for characterization and classification of estuaries, an estuarine modeling system (EMS) that is progressive in the number and level of simulation skill of the estuaries represented. The vision and an incipient implementation of an EMS exist (Section 2.1), developed under the umbrella of the Integrated Ocean Observing System (IOOS) through an expansion of the CORIE modeling system.

We recently developed on top of EMS a set of constructs that allow numerical model outputs to be filtered towards calculation of diverse estuarine numbers. While they do not yet qualify as robust cyberinfrastructure, these constructs already constitute a potentially useful model-based estuarine characterization and classification system (MECCS). Here, we describe MECCS and explore its value through a pilot application to Coos Bay, a well-mixed Pacific Northwest estuary that has been simulated through EMS with a moderate degree of modeling skill (Section 2.3). For control, we resort selectively to higher skill CORIE simulations of the strongly stratified Columbia River estuary.

3.1.2 Characterizing flushing times in estuaries

Flushing times (and/or residence times, a closely related concept) play an important role in determining biological and geochemical conditions of estuaries, and in evaluating the time required to remove water-borne pollutants from estuaries. In particular, the U.S. Environmental Protection Agency (EPA 2001) identifies flushing rate as a critical factor influencing estuarine susceptibility to nutrient over-enrichment; Dettmann (2001), for instance, uses various flushing rate estimates to evaluate the susceptibility of estuaries to de-nitrification.

Flushing times are generally defined as the amount of time necessary to replace a volume of water in the estuary. Various methods for estimating flushing times exist (e.g., see review in Dyer 1997), with various degrees of sophistication. Some of these methods are based on simple unidirectional concepts, while others account for return flow (e.g. Sanford et. al., 1992 and Luketina, 1998) and tidal excursion (Williams, 1986), and some introduce Lagrangian perspectives (Oliveira and Baptista, 1997). As noted by Monsen et. al. (2002) and others, each method is based on a set of assumptions that make them appropriate under specific conditions.

The evaluation of flushing times from modeling efforts is certainly not new, with underlying circulation models ranging from simplified 1D models (e.g. Monsen et. al., 2002, Wang et. al., 2004, Sanford et. al., 1992) to sophisticated 3D models (Banas and HIckey, 2005, Edinger et. al., 1998). The combination of EMS and MECCS offers the opportunity for quick, easy access to alternative flushing time estimates (Section 3.2), all reliant for a given estuary on an identical underlying simulation database.

3.1.3 Characterizing baroclinic circulation and density stratification

Circulation characteristics are an important factor determining the appropriate flushing time calculation, making the automatic calculation of stratification and circulation parameters a useful complement to flushing time calculations. The flow ratio (R_F) provides an example of one of the simpler stratification classification parameters. First calculated by Simmons (1955), flow ratios have been used by researchers in a variety of fields to provide a general sense of the stratification (e.g. Lane and Prandle, 2006 and Borrego et. al., 2002). Some of the more complex classification parameters relating to stratification and circulation include the fraction of saltwater (F_{SW}) and the interfacial Froude number (F_i). Together F_i and F_{SW} can provide insight into the time averaged estuarine circulation and salinity structure and their relationship to the tidal forces, wind and river flow.

In the classic paper by Hansen and Rattray (1966) three processes control the salt balance in a 1D theoretical model: river flow, gravitational circulation and horizontal diffusion. River flow provides fresh water and a net seaward flow, pushing salt out of the estuary. Baroclinic gravitational circulation and horizontal diffusion add salt. Horizontal

diffusion is, in this case, a catch-all for salt flux through non-baroclinic circulation, including tidal dispersion. The interaction between the three processes is non-linear. Increased river flow may lead to a net decrease in salt water in the estuary, but the amount of that decrease can be mitigated by an increase in baroclinic circulation. Increased tidal amplitudes may bring more salt into the estuary and increase tidal dispersion, but attendant higher velocities can cause sheer that breaks down stratification and decreases baroclinic salinity intrusion. From their analysis Hansen and Rattray created a classification scheme based on salinity stratification and a measure of the strength of baroclinic circulation. One of their Figures is reproduced in **Figure 3.1**, with Coos Bay values included. This Figure illustrates an important aspect of MECCS: the ability to use the volume of data created by EMS to classify an estuary at different points and times.

This chapter does not seek to delve deeply into these complexities in estuarine dynamics. Rather, it seeks to examine the feasibility of using automatically generated classification numbers to gain insight into the general interaction between these processes.

3.2 Methods

3.2.1 From EMS to MECCS

Implementation of an Estuarine Modeling System generates a dense, fully 3D set of physical data, with outputs at regular intervals (e.g. 15 minutes for CORIE and the Coos Bay EMS). Assuming a model of reasonable accuracy (a fundamental issue), a long term database of estuarine circulation provides a potential wealth of information. However, deriving meaning from this copious data can be difficult and time consuming. A MECCS provides a set of tools that can distill essential characteristics and relationships from EMS data. The basic components of a MECCS include classification and characterization parameter definitions, computer programs to extract and organize EMS data for calculating these parameters, and programs to display results in ways that can reveal important characteristics and/or relationships. These characteristics and relationships can focus on individual EMS, or be used to compare across EMS.

An essential trait of MECCS is its adaptability. Current parameters are based on classic numbers such as flushing times and a Froude number. As MECCS produces results and generates feedback from EMS users, the list of parameters calculated and their range of spatial and temporal scales can be readily expanded. **Figure 3.2** demonstrates the basic relationship between EMS, MECCS and the end users. MECCS receives data from EMS and parameter definitions from the literature and users. Parameters can then be plotted with the goal of illuminating relationships that provide useful information to end users. EMS/MECCS users can then recommend new parameters or potential relationships, thereby expanding the utility of EMS and providing further insight into estuarine characteristics and relationships important to research, industry and management.

3.2.2 Parameter Definitions and Descriptions

The classification numbers calculated in this pilot MECCS are summarized in the following reference Table, and are described in detail below. All parameters except the freshwater flushing time were defined in MacCready (2006). Freshwater flushing time is described in Dyer (1997, p. 166).

Name	Definition	Description	Eq #
Tidal Exchange	$T_E = \frac{\overline{V}}{P}$	An estimate of the number of tidal periods for tidal motions to replace the volume of the estuary or region.	{3.1}
Filling Time	$T_F = \frac{\overline{V}}{\overline{R}T}$	An estimate of the number of tidal periods for fresh riverine water to fill the volume of the estuary or region	{3.2}
Freshwater Flushing Time	$T_R = \frac{\overline{V_f}}{\overline{R}}$	An estimate of the amount of time to replace an estuary's volume of freshwater.	{3.3}
Flow Ratio	$R_F = \frac{\overline{R}T}{P}$	A rough comparison of the relative strength of tidal (mixing) and river (buoyant, or stratifying) forces using the surrogates P and RT. Simmons (1955) interpretation of R_F values: $R_F > 1$ highly stratified $R_F \sim 0.25$ partially mixed $R_F < 0.1$ well mixed	{3.4}

Fraction of Saltwater	$F_{SW} = \frac{\overline{V_{SW}}}{\overline{V}}$	The percentage of an estuary or region's volume that is from the ocean.	{3.5}
Stratification Internal Wave Speed	$c = \sqrt{\frac{\Delta\rho}{\rho_0} gH}$	The speed of a wave traveling at the interface between stratified fluids of different density: a reduced version of the surface gravity wave produced by tides. It is also the square root of the potential energy deficit between waters of equal volume with $\Delta\rho$ density difference over distance H.	{3.6}
Interfacial Froude Number	$F_i = \frac{u_m}{c}$	An estimate of the relative strength of tidal (mixing) vs. buoyant (stratifying) processes at a point. Generally: $F_i > 1$ mixing dominant $F_i < 1$ buoyancy dominant	{3.7}
Tidal Excursion	$TE = \frac{\sum_{1}^{N} \int_{T} \frac{\lvert u \rvert du}{2}}{N}$	An estimate of the along-channel distance a mass of water travels in a tidal period.	{3.8}

Variable Definitions

R	river flow (m^3/s)
T	tidal period, defined here as 2 M2 tidal periods: 12.4 hrs
P	tidal prism (m^3): volume difference between high high and low low tides in one T.
V	estuary volume (m^3)
V_f	volume of freshwater (m^3), defined here as V-V_{SW}
V_{SW}	volume of saltwater (m^3), defined in {3.10}
g	acceleration due to gravity (9.8 m/s^2)
$\Delta\rho$	bottom to top density difference (g/m^3)
ρ_0	reference density: set to fresh water density of 1000 g/m^3
H	depth from mean sea level (m)
u	along-channel velocity (m/s)
u_m	root mean square tidal current (m/s)
N	number of tidal cycles sampled.

overbar indicates a time average

The above parameters include numerous volume calculations. The model spatial domain is discretized horizontally into an unstructured grid of triangles, and (inside the estuary) into sigma coordinates in the vertical. The volume of a region, then, is calculated as

$$V = \sum_{i=1}^{n} A_i \frac{\sum_{j=1}^{3} \eta_{ij} - b_{ij}}{3} \quad \{3.9\}$$

where n is the number of elements inside a given region, A_i is the area of element i, and η_{ij} and b_{ij} are the surface elevation and bottom depth of node j of element i. Two classification numbers use the volume of saltwater (V_{SW}), defined as

$$V_{SW} = \int_V \frac{S}{S_{ocn}} dV \,, \quad \{3.10\}$$

where S is salinity, and S_{ocn} is the salinity of seawater (herein defaulted to 34 psu). The discretization of {3.10} is

$$V_{SW} = \sum_{i=1}^{n} A_i \frac{\sum_{j=1}^{3} \left(\sum_{k=1}^{m} \frac{S_{ijk1} + S_{ijk2}}{2} dz_{ijk} \right)}{3 S_{ocn}} \quad \{3.11\}$$

where n is the number of nodes, A_i is the area of element i defined by 3 nodes j, m is the number of vertical segments at each node, dz_{ijk} is the length of segment k at node j of element i, and S_{ijk1} and S_{ijk2} are the salinity values at the two endpoints of segment k. Finally, u_m is calculated at a point as the root mean square of the depth averaged velocity during a given period (generally one tidal day, or 24.8 hrs).

3.2.2.1 Tidal Exchange and Filling Time

Tidal exchange (T_E) {3.1} and filling time (T_F) {3.2} relate the volume of the estuary to the two primary sources of new water into the estuary or region. Both numbers can be interpreted in terms of estuarine flushing, with tidal exchange estimating tidal flushing and filling time estimating river flushing. Both are fairly coarse estimates. For example the tidal exchange is an underestimate because some of the water leaving on an ebb tide will re-enter the estuary on the succeeding flood (return flow, not calculated in this study), and the water actually exchanged will be dependent on estuary length and circulation. Mean volume and river flow for both parameters are calculated over a 24.8 hr period (two M2 tidal cycles), and the tidal prism is the difference between the highest and lowest volumes over the period.

3.2.2.2 Freshwater Flushing Time

The freshwater flushing time (T_R) {3.3}, also known as the residence time, calculates the amount of time to replace an estuary's volume of freshwater. It has been calculated in numerous ways, including in a manner similar to T_E (Dyer, 1997, p. 166). Here it has been calculated using an adaptation of the fraction of fresh water method described in Dyer (1997, p 166). R and V_f are averaged over 24.8 hours.

3.2.2.3 Flow Ratio

Simmons (1955) described the flow ratio {3.4}, the simplest of the circulation related classification numbers. He found that flow ratios above 1.0 indicate a highly stratified estuary, ratios around 0.25 indicate a partially mixed estuary, and ratios below 0.1 indicate a well-mixed estuary. The transition between classifications is ambiguous. Also, the term well-mixed may be misleading, as few if any estuaries do not show some vertical stratification during some point in the ebb-flood tidal cycle (Jay and Smith, 1990b). Even a well-mixed estuary can show signs of the baroclinc circulation generally associated with partially mixed and stratified estuaries. Finally, a longer (more than a few tidal excursions) or more bathymetrically complex estuary may have different mixing characteristics at different points. R_F's usefulness lies in its ability to provide a general prediction of estuary behavior over the range of expected tides and river forcings. It should only be considered a rough indicator of estuarine behavior.

3.2.2.4 Fraction of Saltwater

The fraction of saltwater (F_{SW}) {3.5} takes advantage of the fully 3D model data set. F_{SW} over an entire estuary indicates the amount of salt intrusion, and the F_{SW} of sub-estuary regions can show its extent. A comparison of F_{SW} to the drivers of estuarine salt flux (from Hansen and Rattray, 1965: river flow, gravitational circulation and diffusion) can provide insight into the interplay between these processes under modeled forcings. For example, F_{SW} has been used in a model study by MacCready (1999) to assess estuarine response to changes in tidal or river forcings.

3.2.2.5 Stratification Internal Wave Speed and Interfacial Froude Number

The interfacial froude number (F_i) {3.7} is based on the stratification internal wave speed (c) {3.6}. Velocity of the internal wave, c, can be seen in two, complementary, ways: as the speed of a wave traveling between stratified fluids of density difference $\Delta\rho$, or as the square root of a measure of the potential energy that must be overcome to mix volumes of water with density difference $\Delta\rho$. As used here, c is a bulk parameter that does not explicitly reflect either a true internal wave or the (square root of the) exact potential energy deficit that needs to be overcome to mix the estuary. Instead, c is a rough measure of the resistance by stratification to momentum transfer through mixing.

The interfacial Froude number (F_i) is the ratio of the root mean square velocity u_m to c. F_i can be seen as a ratio of kinetic energy (associated with turbulence) to potential energy (associated with buoyancy). MacCready (in press) shows that the vertical eddy diffusivity, which can be used to determine the turbulent vertical salt flux, is inversely proportional to his layer Richardson number (his equation 3.8), which is analogous to $\frac{1}{\sqrt{F_i}}$. When Fi < 1 turbulent forces are weak relative to buoyant forces, and flows tend to remain stratified. When Fi > 1 turbulence is strong relative to buoyancy, and kinetic energy is converted to potential energy through mixing. When $F_i >> 1$ there will be no real internal waves because their existence would cause enough mixing to break down the stratification that supports them (Jay and Smith 1990b). The components u_m, $\Delta\rho$ and H are time averages over one or more tidal cycles. Over the course of the ebb and flood tides the instantaneous versions of these parameters can change significantly, and the instantaneous F_i can move above and below the critical value of 1. The F_i value presented here does not reflect these processes and should be treated only as an indicator of the time averaged mixing state at a point.

3.2.2.6 Tidal Excursion

The tidal excursion (TE) {3.8} is the along-channel distance a mass of water travels in a tidal period. The best way to calculate the model tidal excursion would be in a Lagrangian method through particle tracking experiments. Comparing such results with

real-world observations, however, requires costly experiments, and at this stage we are seeking a simple *TE* estimate. Here *TE* is defined in a Eularian sense {3.8}. This definition of *TE* was used extensively in the analysis of the Coos Bay Model in Chapter 2 (equation {2.3}). *TE* is also useful for understanding the effects of headlands and inlets on tidal dispersion (Geyer, 1992), and can be used to divide the estuary into along-channel sections for monitoring purposes or for the development of other models such as the flushing rate box model described in Williams (1986).

3.3 Characterizing Coos Bay

3.3.1 Introduction

Coos Bay is a mesotidal coastal plain estuary on the southern Oregon coast. It consists of a 24.5 km channel dredged to ~11.5 m depth (from MLLW) and 300 m wide, and is rimmed by a number of small tributaries and inlets as well as considerable tidal flats (~1/2 its surface area). Its primary source of fresh water is the Coos River, which flows into the eastern end of the estuary and is characterized by extremely low (~2 m^3/s) summer flows with few spikes, and winter flow which has both much greater flow (~50-400 m^3/s) and variability. The Coos Bay MECCS results presented here are based primarily on the pilot Coos Bay EMS presented in section 2. As has been noted, MECCS results must be viewed in the context of model errors. The current state of the Coos Bay EMS suggests that it is accurate enough to provide interesting MECCS results, but has enough inaccuracies and uncertainties that results relating to the baroclinic circulation and the South Slough especially should be viewed with some suspicion. Index of Agreement (IOA) (Willmot, 1982), which ranges from 0 (no agreement) to 1 (perfect agreement), was introduced as a synthesis of model skill. By that measure South Slough IOA results for elevation were good at the mouth (0.947), but fell to only decent at the head (0.88 and 0.83). South Slough salinity was quite bad, but actually improved from the mouth (0.66) and middle (0.55) to the head (0.68 and 0.79). In the channel only summer observations were available, and indicated a model that represented velocity frequency and phase well but with errors in velocity amplitude and tidal excursion which decreased from mouth to the head. IOA values were generally above 0.9. Summer salinities were fairly good as well (IOA values ~0.75 for long deployment stations from mouth to head), staying in phase and frequency throughout the run, but with model underestimates increasing towards the head as river flow increased.

Coos Bay results for each classification parameter are discussed individually and, where useful, in combination with other parameters. Additional examples from a Columbia River Estuary (Zhang, 2004) model are included to illuminate some parameter uses and provide a control. The classification numbers described in section two are

defined over the volumes or at the points shown in **Figure 3.3**. All points have been placed at the deepest point in the channel (along the thalweg). The primary regions used for the flushing time calculations in Coos Bay are the entire estuary without the artificial mixing pools and the South Slough, while the entire estuary and mouth are used for the Columbia River. Time averages are 24.8 hour periods unless noted otherwise. This period is used rather than the 12.4 hr M2 period in order to eliminate the effects of the diurnal asymmetry. The Coos Bay model runs include a period of very low flow (summer 1982 run) as well as a period of high to medium flows (winter 2003 run). Classification numbers were calculated for the periods from 9/1/1982 to 10/12/1982 and from 2/6/2003 to 3/27/2003. The reference model from section 2 is used for all classification numbers.

3.3.2 Flushing Time Parameters

Tidal exchange (T_E) and filling time (T_F) values are based on estuary volume and (respectively) tidal prism and river flow. In Coos Bay river flow does not significantly affect T_E, and **Figure 3.4a** shows the expected inverse relationship between T_E and the tidal prism for the estuary (no mixing pools) and for the South Slough. **Figure 3.4b** compares T_E to the tidal prism and tidal amplitude. More interestingly, it shows the range of tidal exchange values for each of the two regions. It should be noted that these values reflect the prism as defined by diurnal high and low water levels. Thus, when there is a large diurnal asymmetry the actual number of tidal periods for tidal exchange will be larger. T_E can be seen as a low-end estimate of the time for the flushing of effluent from Coos Bay. The filling time compares estuary volume to river flow. **Figure 3.5** shows plots of T_F vs. river flow for the entire estuary (no mixing pools) and for the South Slough. In the Coos Bay model the river flow has little significant affect on estuary volume, and T_F has a very clear inverse relationship to flow. Where the tidal exchange represents a low-end estimate for the flushing of effluent from Coos Bay, T_F represents a high-end estimate.

Intermediate between tidal exchange and filling time in Coos Bay, the freshwater flushing time (T_R) provides an estimate for effluent flushing that attempts to account for the relative concentrations of oceanic and fresh water, and assumes that the effluent originates in the fresh water. **Figure 3.6a** shows T_R results for the estuary and the South

Slough vs. river flow for both the summer 1982 and winter 2003 model runs. Also included are results from the Columbia River Estuary model. Despite the partial dependence of the volume of saltwater on tidal amplitude, the Coos Bay freshwater flushing time shows no significant correlation with tidal amplitude (**Figure 3.6c**). This is unsurprising for the summer period, when the fraction of saltwater (F_{SW}) is dependent almost exclusively on river flow (section 3.3.2). A noticeable T_R to tidal amplitude correlation would be expected during the winter period, however, when tidal amplitude has a significant affect on F_{SW}. It may be the case that the model run was too short to capture this relationship, or the river flow spikes overwhelm it. The Columbia River summer (lower flow, but with a well defined salt wedge) period (**Figure 3.6d**) does show significant T_R to tidal amplitude correlation. Generally a strong inverse relationship to river flow is apparent in both summer and winter seasons for each region. The exception is the entire Coos Bay region during the summer. In all cases, however, there are distinct low flow and medium-high flow T_R response patterns.

3.3.2 Circulation Related Parameters

An initial, coarse, picture of Coos Bay mixing and circulation can be gleaned from the flow ratio (R_F). **Table 3.1** presents typical R_F values for the entire model at low, medium and high net flows during spring and neap tides. From the analysis of Simmons (1955), these numbers indicate that the estuary is dominated by tidal forces and will always be well to partially mixed. While this assessment is generally accurate, the estuary is significantly longer than the tidal excursions throughout the main channel (**Table 2.4**), which suggests the possibility for the estuary to contain a range of mixing regimes. The other classification numbers show this to be true, and enable a richer characterization under the range of modeled flows and tides.

During the six week summer 1982 run the net river flow began at ~4 m^3/s and increased steadily to ~10 m^3/s (**Figure 2.6**). High F_{SW} values at the start of the run show an estuary that is nearly saturated with ocean water, as expected at the end of a typically dry August with net flows around 2 m^3/s. On 9/1/82 F_{SW} in the mouth region is 0.97, falling to about 0.92 in the head region. As the flow rises, F_{SW} in the middle and head regions fall almost linearly from 0.96 to 0.83 and 0.92 to 0.72, respectively. **Figure 3.7a** shows the summer F_{SW} results and its correlation to river flow and tidal amplitude, and

Table 3.2 contains the correlation coefficients. For all regions except the South Slough, river flow has a strong negative correlation with F_{SW}. Under this flow regime spring vs. neap changes in tidal velocities have no significant affect (F_{SW} correlations with tidal amplitude < 0.10) on the overall saltwater concentration in all regions but the South Slough.

The South Slough is a relatively shallow region (maximum depth south of the Charleston bridge is ~4m) with a low (frequent) tidal exchange (range between 0.7-1.3 vs. 1.6-3 tidal periods for the main estuary, **Figure 3.4**). T_E values near 1 suggest that much of its volume is mixed with outside water on each tidal cycle. The summer South Slough F_{SW} correlated weakly with river flow and strongly with tidal amplitude (**Figure 3.7a**). This result is expected given the combination of a very small T_E and very large T_F. Its total watershed area is ~4% the size of the Coos River watershed, and the modeled river flow is smaller relative to the slough volume than the entire Coos Bay relative to its total inflow (**Figure 3.5**).

The winter 2003 run includes periods of medium (~20-100 m^3/s) to high (~275 m^3/s) water flow. The periods of high flow are characterized by flow spikes, followed by a gradual tapering to medium flow levels. F_{SW} ranges from 0.41 to 0.63 at the mouth, and falls to between 0.10 to 0.29 and 0.06 to 0.19 at the North Bend and head regions (respectively). Unlike the tidally dominated low flow summer 1982 run, winter 2003 F_{SW} responds noticeably to both tidal range and river flow variations. While the estuary may be broadly characterized as partially mixed, the mouth region shows characteristics of a highly stratified salt wedge estuary, while the head shows characteristics of a well-mixed estuary. F_{SW} in the South Slough again responds primarily to tidal amplitude. Elsewhere tidal mixing and river buoyancy forces balance well enough that a change in either has a significant affect on overall F_{SW}. The relative strengths of the two influences, however, vary by region (**Figure 3.8b** and **Table 3.2**). F_{SW} correlates significantly with both tides and river flow in the mouth region, while it correlates more strongly with river flow in the North Bend and head regions. From **Figure 3.8b**, river affects on F_{SW} appear only after the three heavy flow events occurring around 2/20 (up to 131 m^3/s), 3/8 and 3/22 (both up to ~275 m^3/s). The 2/20 flow event occurs during a spring tide, which may mute the expected salt decrease. The other two flow events correspond to neap tides,

which amplify the decreased salinity. The complex, non-linear interaction between F_{SW} and tidal amplitude and flow is apparent in scatter plots (**Figure 3.9**), which show that in all regions tidal amplitude is a poor indicator of F_{SW}, while river flow is only a mediocre indicator. The large variability in river flows, especially the three big flow events, is the primary reason flows influence any of the regions, especially in the mouth.

The interfacial Froude dimensionless number helps explain the low-flow correlation between summer F_{SW} and increasing flow, and the lack of correlation to tidal variations. **Figure 3.12** shows that F_i at the first 8 points (covering the first 15 km from the mouth) remains near or above the critical value of 1 for the duration of the run, meaning that frictional forces at these points are stronger than buoyant forces during both spring and neap tides. The effect of the lower F_i centered on the neap tide around 9/24 can be seen in **Figure 3.10**, which shows the time averaged (24.8 hrs) salinity, residual velocity and mean velocity magnitude transects where F_i values are well above 1, and where F_i values dip below 1. In both cases the estuary is fairly well mixed, so the difference is not striking. The primary difference is in the slumping of salinity isolines in the lower F_i case. Both cases lack the region of high salinity gradient characteristic of strong baroclinic gravitational circulation, but the lower F_i case shows evidence of some baroclinic circulation.

During the winter 2003 run F_i values range from 0.15 to 0.60 at the mouth and are generally lower towards the head. These F_i values well below 1 indicate a dominance of buoyant, stratifying, forces over turbulent, mixing, forces. F_i values in the mouth respond primarily to tidal influences, as indicated by the higher correlations in **Figure 3.13**. Salinity transects in **Figure 3.11** show slumped isolines and a salt wedge surrounded by a high salinity gradient characteristic of a stratified estuary. In this region when buoyant forces are significantly stronger than turbulent forces (i.e. low F_i), exchange flow is likely to develop. **Figure 3.14** shows a strong positive correlation between F_i at points 1-4 and F_{SW} in the mouth. It appears, then, that in terms of salt volume in the mouth region, increased exchange flow during neap tides does not compensate for the lower tidal salt flux.

As expected, the influence of river flow on F_{SW} increases towards the head. The North Bend F_{SW} correlation to amplitude drops to 0.31, while the negative correlation to

river flow increases to -0.76. The difference is similar for the head, at 0.39 to -0.75. The lower F_{SW} correlation to tidal amplitude from North Bend to the head may be due to increased exchange flow during neap tides compensating for the decreased neap tide tidal dispersion. The F_i to river flow correlation coefficient is low (between 0.25 and -0.23) for all points, but from **Figure 3.13a** it appears that F_i does respond to the 3/8 and 3/22 high flow events. Any increased salt intrusion through baroclinic circulation is overwhelmed, however, by the greatly increased river flow. The periods of the model runs are not particularly long, and factors that would increase or decrease stratification sometimes occur at roughly the same time (e.g. decreasing tidal amplitude coupled with increasing flow around 3/8). Thus, this type of analysis would benefit greatly from the long term record that would come with a persistent forecasting system.

3.4 Discussion

The classification numbers presented here focus on quantifying the estuary's salt content, salt structure and circulation, as well as approximating the time required to flush effluents from the estuary. The uses include some general benefits from simplified quantification of estuarine processes, potentially more refined and less ambiguous regulation of effluent discharge, and understanding the relative influence of circulation from the main channel vs. small input flows on circulation and salinity structure in peripheral bays. Note again that the Coos Bay classification numbers are based on the reference model runs, and their applicability to the Coos Bay estuary should be viewed in light of model errors (section 2).

The F_{SW} and F_i results for the low flow summer 1982 run show an estuary that is tidally dominated, creating a well-mixed state in which differences between spring and neap tides have little practical effect on the total salt and salinity structure. Small changes in river flow (on the order of 1 m^3/s, or ~9% of the maximum flow for the low flow run or ~0.3% of the maximum flow for both runs), however, can have significant affect on F_{SW} and F_i. In this environment the estuary's salt content responds to river flow in a nearly linear fashion. In the higher flow winter 2003 run F_{SW} responds to both tidal amplitude and river flow throughout the estuary, and the interaction between the two is non-linear. Model runs do not extend to a period when the transition from tidally dominated to mixed occurs, but full deployment of the Coos Bay EMS and the collection

of a long-term data set may provide insight into the conditions that precipitate this transition. The role of stratification in this transition can be investigated in part by using F_i, which can provide the basis for a real-world extension of the theoretical investigations carried out by MacCready (1999, 2006).

An important use of an EMS is to provide information on the flushing of effluents. The US EPA (2001) notes that the main factors influencing flushing times are freshwater inflow rates, tides, wind, mixing, stratification and topography, and that the variability of these factors requires attention to the relevance of flushing time calculations made under particular conditions. All of these factors but wind and topography are addressed in this study, and expansion to wind and (to a lesser extent) bathymetry would be straightforward. Tidal exchange assumes complete mixing of estuarine and ocean waters during each flood tide and no re-entry of estuarine water after each ebb tide (Dyer 1997 and Sanford, 1992, among others, discus methods to account for this return flow), and thus is more meaningful for shorter estuaries (as measured by the ratio between tidal excursion to estuary length) during well-mixed conditions with strong upwelling. Although Coos Bay is well mixed during the strongest upwelling period (summer), it is quite long compared to modeled tidal excursions (see section 2). Coos Bay filling time (T_F) results suggest that little meaningful river-based flushing will occur during low flow periods (T_F values from ~200-500 days - far longer than the low-flow season), but medium to high-flow periods may expect nearly complete flushing in ~10-70 days.

Regression analyses for all T_E and T_F vs. tidal prism or river flow (as appropriate) result in lines with high degrees of correlation. For T_F applying a full year's flow climatology provides a general sense of the parameter's values throughout a typical year (applied to filling time in **Figure 3.15**). The periods of strong river-based flushing occur from roughly mid November to early April, there is little river-based flushing in the summer, and the transition period is a fairly precipitous rate decrease in the fall and a relatively gradual rate increase in the spring.

Although many of the results presented here primarily quantify expected behaviors, the widespread use of classification numbers also holds the possibility of illuminating more complex, and even unexpected, behavior.

One such moment occurs when looking at the freshwater flushing time parameter applied to the entire Coos Bay estuary. **Figure 3.6** shows that T_R usually has strong inverse relationships to flow, but that the exact relationship changes during different periods. This phenomenon is clearly related to volume of saltwater response to changes in flow. During the low-flow, well-mixed periods increases in river flow do not necessarily result in increased flushing. While this may be due to the magnitude of the changes in flow, the flow rises ~300% from its initial value during the summer months, which is comparable to the percentage increases seen in the winter flow spikes. During the summer, Coos Bay T_R is between 25 and 45 days, while during the medium-high flow period it is between 5-50 days.

The reason for the distinct T_R responses to increased river flow is likely the different Coos Bay responses to increased river flow during low flows vs. medium-high flows. During low flow periods the increased river flow initially compresses the horizontal salinity isolines but the horizontal salinity gradient remains fairly large. The result is that salt water is pushed out of the estuary rather the fresh (presumably polluted) water riding over the top of a stratified saline lower layer.

The effect can be seen in Coos Bay's linear F_{SW} response to increased flow during the summer. During high flow periods, however, most of the salt is in a stratified lower layer and the fresh water flows over the top with little mixing. Furthermore, in stratified estuaries increased river flow is partially compensated by an increase in baroclinic circulation, meaning increased river flow moves fresh water out of the estuary almost immediately under higher flows.

While it has been generally understood that the strength of baroclinic circulation has a significant affect on the timing and method of estuarine flushing, this use of classification numbers shows that effect may actually be to create distinct flushing regimes. The T_R classification number provides one possible mechanism for identifying and quantifying these regimes. Although the conditions for the transition from low flow T_R to medium-high flow T_R cannot be deduced from the current model runs, they could possibly be determined using a longer model record and an analysis of T_R, F_{SW}, and F_i.

A simple example of the kind of analysis imagined with the flushing numbers helps illustrate some of their potential. It is determined that for a given estuary the worst-

case freshwater flushing time T_R during a season is F and an industrial plant spews X g/s of effluent E. There is a requirement that estuary-wide concentrations of E not exceed C g/m^3. The mean (or minimum) volume of the estuary is V m^3. The plant, then, can release effluent at a rate of $X = \frac{CV}{F}$ (g/s). During well mixed periods the volume V is simply the volume of the estuary, while during stratified periods (when the polluted river water mixes little with the ocean water) V is the freshwater volume $V(1\text{-}F_{SW})$, and F_i can be used to determine stratification. No effluent data that would be useful for this purpose exists for the periods of the current model runs, but validation could be done with a dye study, or by using a conservative effluent from an existing source (or sources) with measurable input.

Knowledge of the stratification and its relation to forcings, derived from numbers such as F_{SW} and F_i, can provide insight as to which flushing time estimate is the most appropriate during specific seasons. In Coos Bay, where T_E is always much less than T_F or T_R, when the estuary is well mixed (i.e. F_i values are consistently above 1), the true flushing time may be well approximated (but certainly underestimated) by T_E because ocean water will mix with estuarine water during each tide. However, the water exchanged at each tidal cycle in a well-mixed estuary comes primarily from the mouth, suggesting that T_R may be a more useful approximation in longer estuaries (as measured by the tidal excursion). T_R values may also be more appropriate when the estuary is less well mixed and baroclinic circulation is significant (F_i values are consistently below 1). If it is essential to know when nearly all of an effluent has been flushed, T_F can be a useful estimate under most conditions. The specific relationship between the flushing of an effluent, the various flushing time measurements and circulation information derived from F_{SW} and F_i remains to be explored using real world data.

The relationship between Coos Bay's peripheral bays and conditions in the main estuary can be investigated with some of the classification numbers and correlations presented here. The South Slough, for example, is fed by six small streams (aggregated to two in the model) whose input is ~25 times smaller than the combined freshwater input into Coos Bay. The South Slough R_F is on the order of 0.001 in low-flow conditions, 0.01 in medium-flow conditions, and 0.1 in high flow conditions, which suggests very

well mixed conditions at all times. The tidal exchange (T_E) ranges from ~0.7 to 1.3, suggesting frequent replacement of estuarine water with ocean water.

South Slough F_{SW} correlations to tidal amplitude (at Charleston) and river flow (**Figure 3.7-8**) show that South Slough F_{SW} responds far more to changes in tidal amplitude than river flow during both low and medium-high flow periods. F_{SW} for all other regions respond non-linearly to both tides and river flow during medium-high flow periods. South Slough F_{SW} during the summer 1982 run (mean value of 78%) is much lower than F_{SW} in the estuary mouth (mean of 96%). Such a large F_{SW} difference suggests that although the T_E is very low (frequent), in the summer most of the water that leaves during ebb comes from relatively near the mouth, leaving the water at the head of the slough to build up fresh water even under low river flows and making true flushing times significantly higher than T_E. During higher flow periods, when stratification in the mouth causes the surface water to be considerably fresher, mean F_{SW} in the mouth and slough become much closer (55% to 49%).

The existence of distinct mixing regimes from the mouth of the main channel to the South Slough head can be seen in salinity and temperature (S & T) plots in **Figure 3.16**. Different shaped S & T plots indicate either different water sources (e.g. different rivers) or different mixing characteristics. During both summer and winter runs surface plots show similar patterns for the points around the mouth (channel points 1 and 2, and chawq). The valwq point (middle of the slough) looks noticeably different than chawq, and winwq (head of the slough) is clearly distinct. The difference is most noticeable in the winter run, when cold water at the head of the South Slough is always from a (fresh) river source, while in the mouth relatively cold water sometimes has an oceanic (salty) source.

3.5 Conclusion

A preliminary suite of MECCS classification parameters have been implemented. In the long run, end users such as physical oceanographers, biologists, resource management agencies and private entities will determine the uses of characterization and classification parameters, as well as the choices of new parameters, through feedback and independent development. The parameters presented here are designed to illustrate some

of the types of numbers available, with a focus on circulation, salinity structure, salt content and the flushing of effluents. Only Coos Bay and a few Columbia River results are presented, but as the number of environmental modeling systems increase inter-estuary comparison is envisioned as an important function of MECCS.

Some of the Coos Bay salt content and mixing processes discussed above are unsurprising in light of basic knowledge of estuarine dynamics. In this case, the utility of the classification numbers lies in the quantification of generally understood phenomena for purposes of comparison between EMS and with other processes within the estuary. Effluent flushing illustrates the intra-estuary utility. Human requirements for effluent flushing change based on effluent type, and flushing processes change based on source and mixing. Knowledge of a variety of flushing calculations, their behavior and relevance under different circulation and stratification regimes, and the forcing conditions that produce these different regimes can meaningfully inform estuary management.

Chapter 3 Figures and Tables

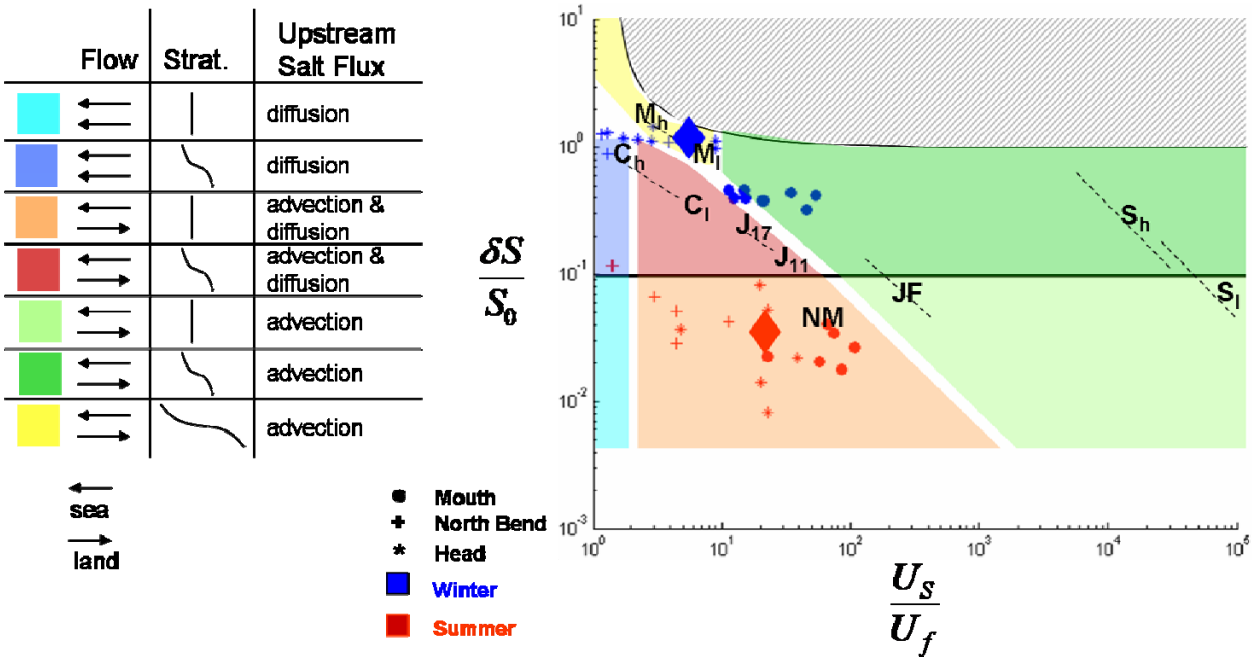

Figure 3.1: Coos Bay plotted on the classic Hansen and Rattray (1966) stratification diagram. The Coos Bay calculations were made on a weekly basis at a point in the mouth ('o'), a point in North Bend ('+') and a point in the head ('*'), and seasons are color coded. Regions represent classifications according to layered flow, stratification and the dominant method of upstream salt flux. The large diamonds reflect summer and winter run averages for the entire run at North Bend. Compared to the other estuaries, Coos Bay experiences a large range of conditions, which is in part due to the difference in stratification between the extremely well mixed summer conditions and stratified winter conditions. It is also due to the fact that MECCS allows categorization by estuary region, while the traditional classification methods rely on observations which may only allow for broader scaled characterization. From the top of the Table to the bottom, the regions are described in Hansen and Rattray as: 1a) net flow seaward at all depths, slight salinity stratification, 1b) net flow seaward at all depths, some salinity stratification, 2a) net flow reverses at depth, diffusion and advection both contribute to salt intrusion, slight salinity stratification, 2b) net flow reverses at depth, diffusion and advection both contribute to salt intrusion, some salinity stratification, 3a) net flow reverses at depth, advection accounts for 90% of upstream salt intrusion, small stratification, 3b) net flow reverses at

depth, advection accounts for 90% of upstream salt intrusion, some stratification (fjord type estuaries, thick bottom layer), and 4) salt wedge estuary.

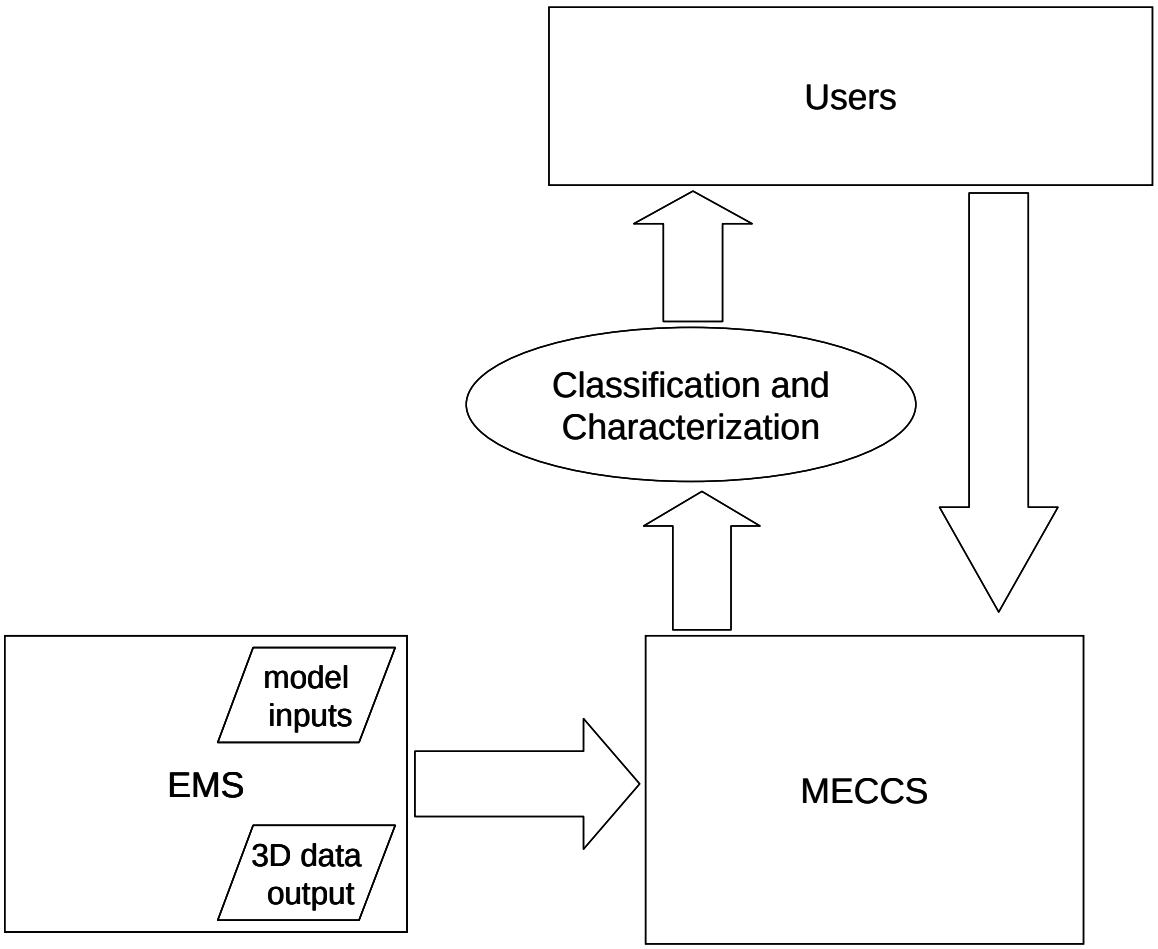

Figure 3.2: Diagram of the Model-based Estuarine Characterization and Classification System. MECCS provides a filter between the large volume of data generated by EMS and users. MECCS produces classification and characterization parameters over a range of temporal and spatial scales, as well as comparisons between parameters, between parameters and other EMS data (e.g. model inputs or forcings), and between EMS. Users gain information that encapsulates phenomena of interest. Users can also provide feedback to MECCS that can lead to new parameters and comparisons that can further the goals of science, industry and ecosystem management.

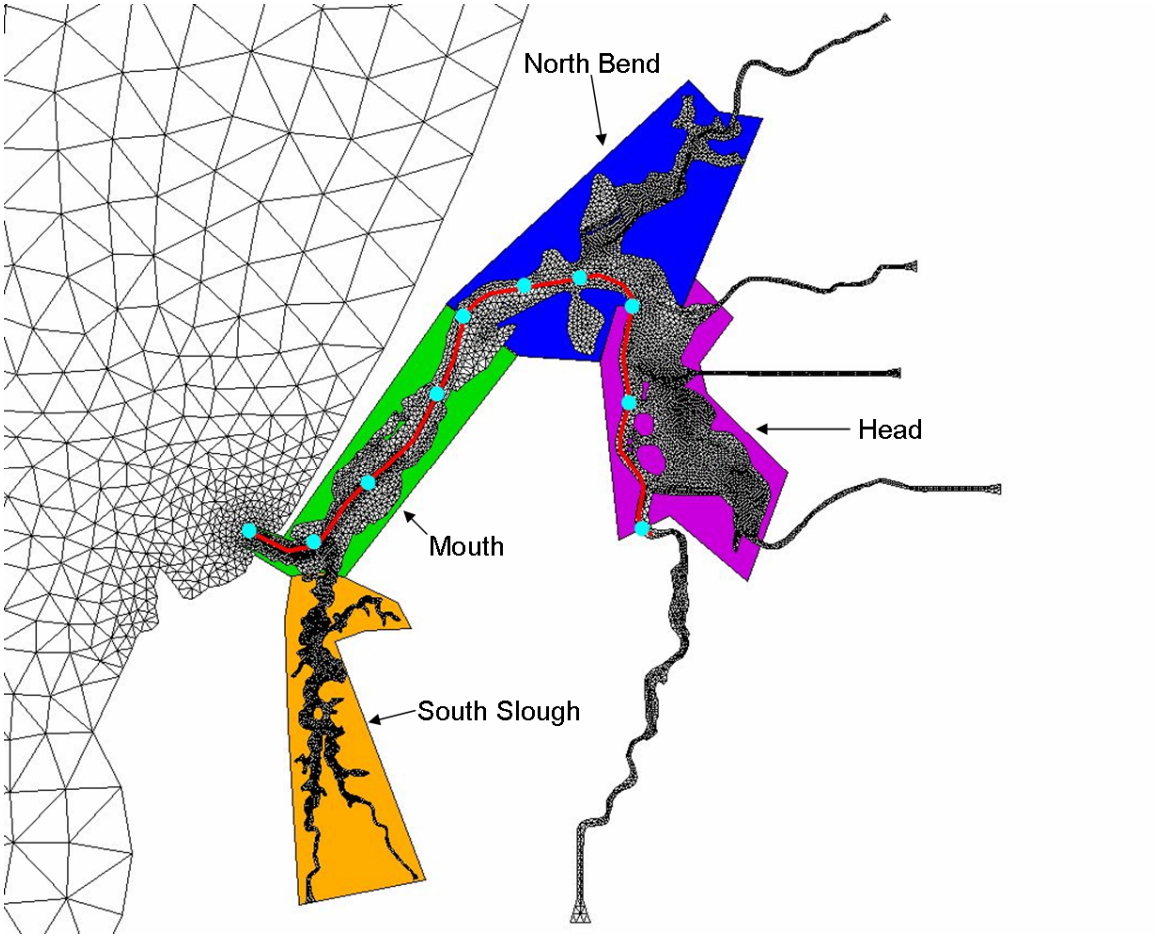

Figure 3.3a: Regions and points for the classification parameters. Coos Bay is divided into the displayed regions and excludes the five detached rivers on the eastern side of the map, which are the artificial mixing pools as described in section 2. The "All Estuary" region is composed of the four named regions plus the mixing pools. The "No Pools" region is composed of the four named regions. The "Channel" region follows the transect line. The points represent locations for the calculation of the interfacial Froude number.

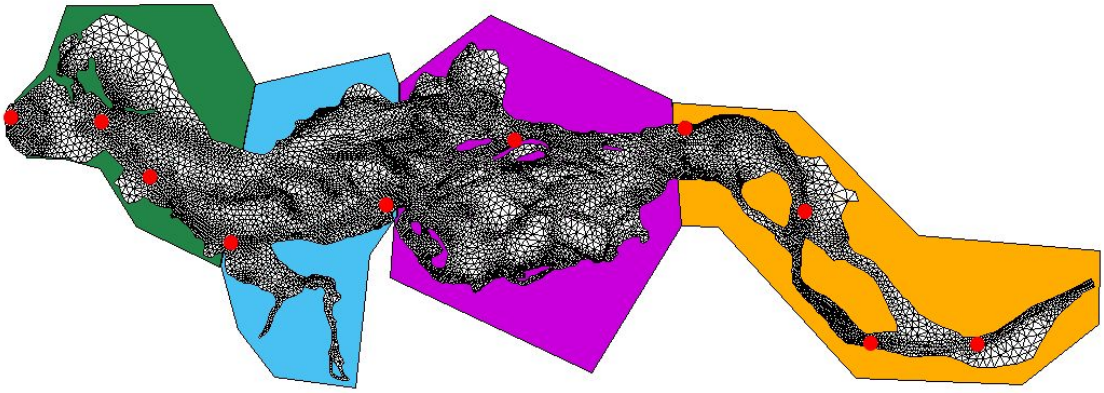

Figure 3.3 b: Regions and points for the Columbia River Estuary. "All Estuary" is all four regions, the "mouth" is the western (leftmost) region, the regions "mouth-1" and "mouth-2" are the blue and purple regions, and the "head" is the eastern region.

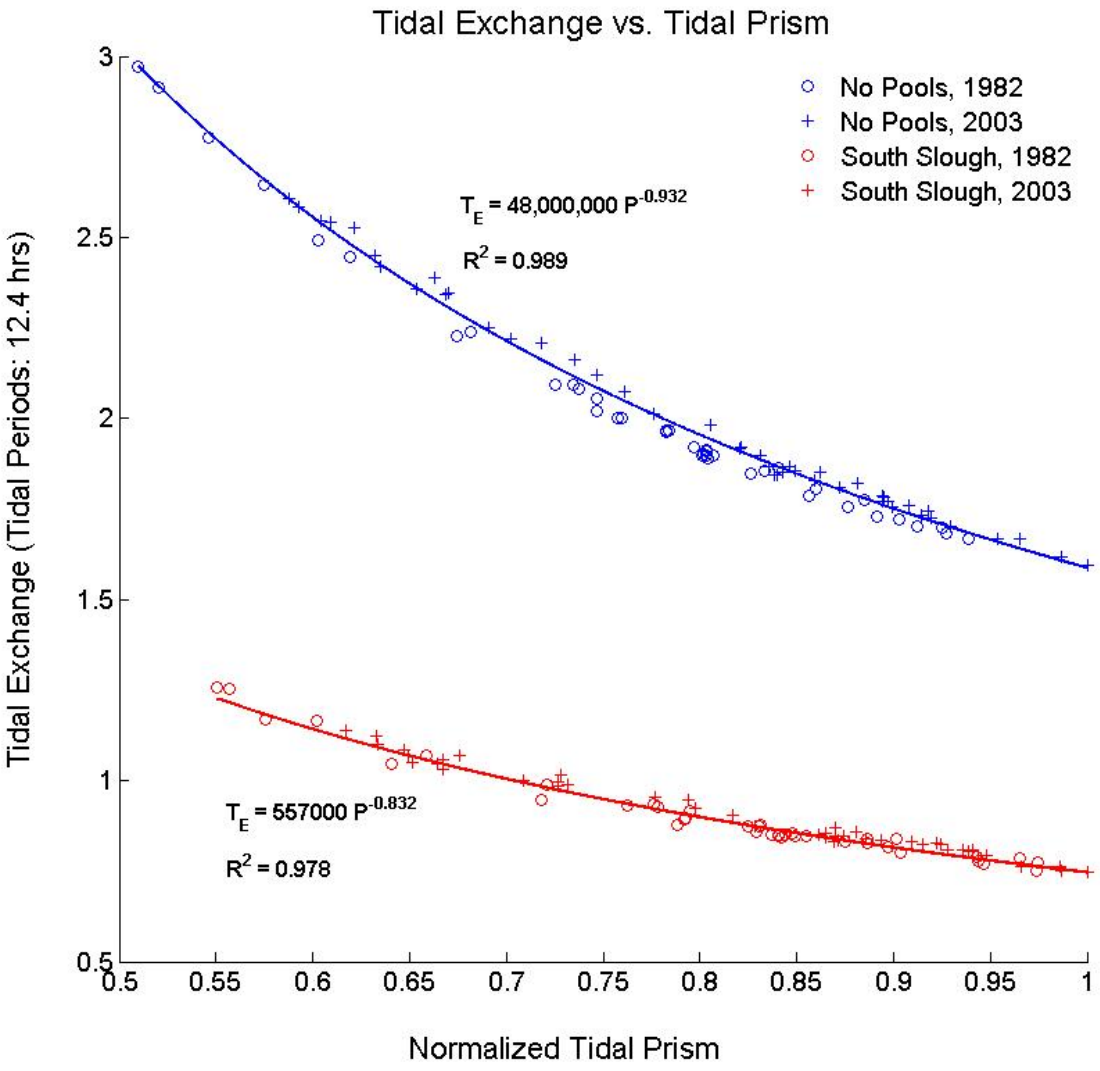

Figure 3.4a: Tidal exchange vs. tidal prism for the estuary and for the South Slough. The plot has been normalized using the maximum tidal prism for each region: 106,265,200 m^3 for the entire estuary, 11,446,234 m^3 for the South Slough. Tidal exchange is in M2 tidal periods (12.4 hrs).

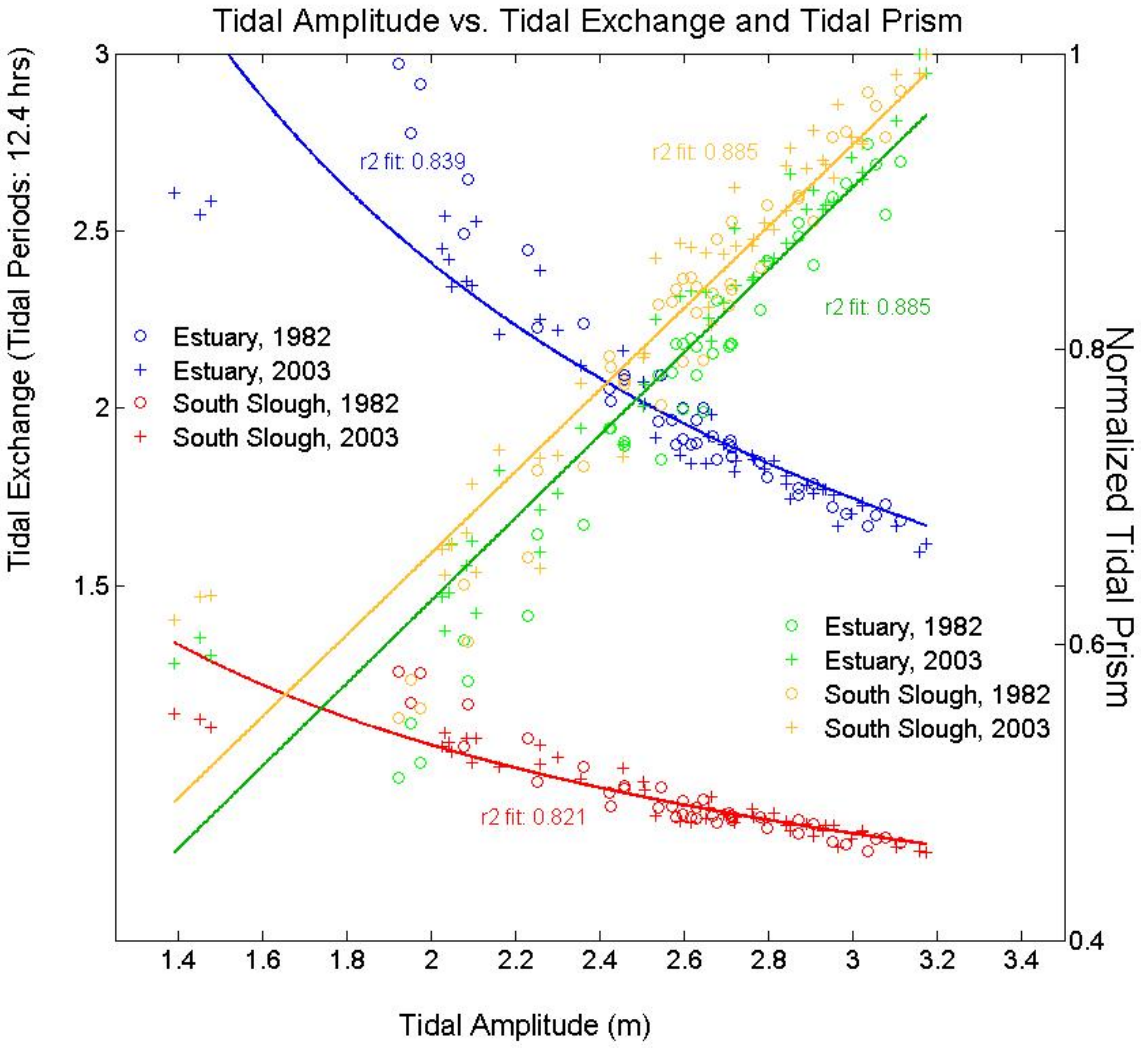

Figure 3.4b: The correlation between tidal amplitude and prism and tidal exchange. Because amplitude is a more readily available datum than tidal prism, this type of graph provides important practical information.

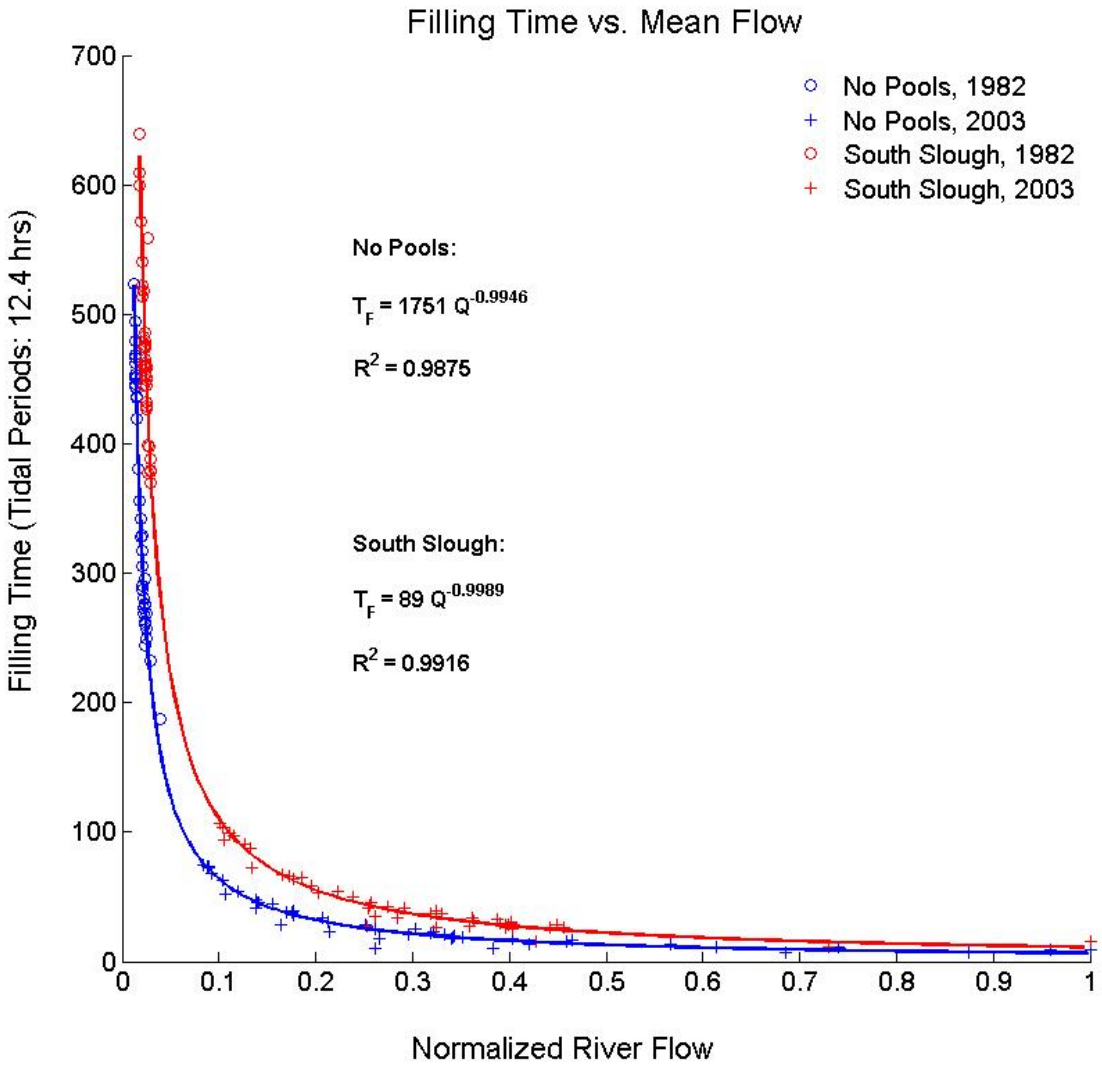

Figure 3.5: Filling time vs. mean flow for the entire estuary and for the South Slough. Regression equations and associated R2 values are included. The plot has been normalized using the maximum river flow into each region: 280 m^3/s for the entire estuary, 8 m^3/s for the South Slough. Filling time is in M2 tidal periods (12.4 hrs).

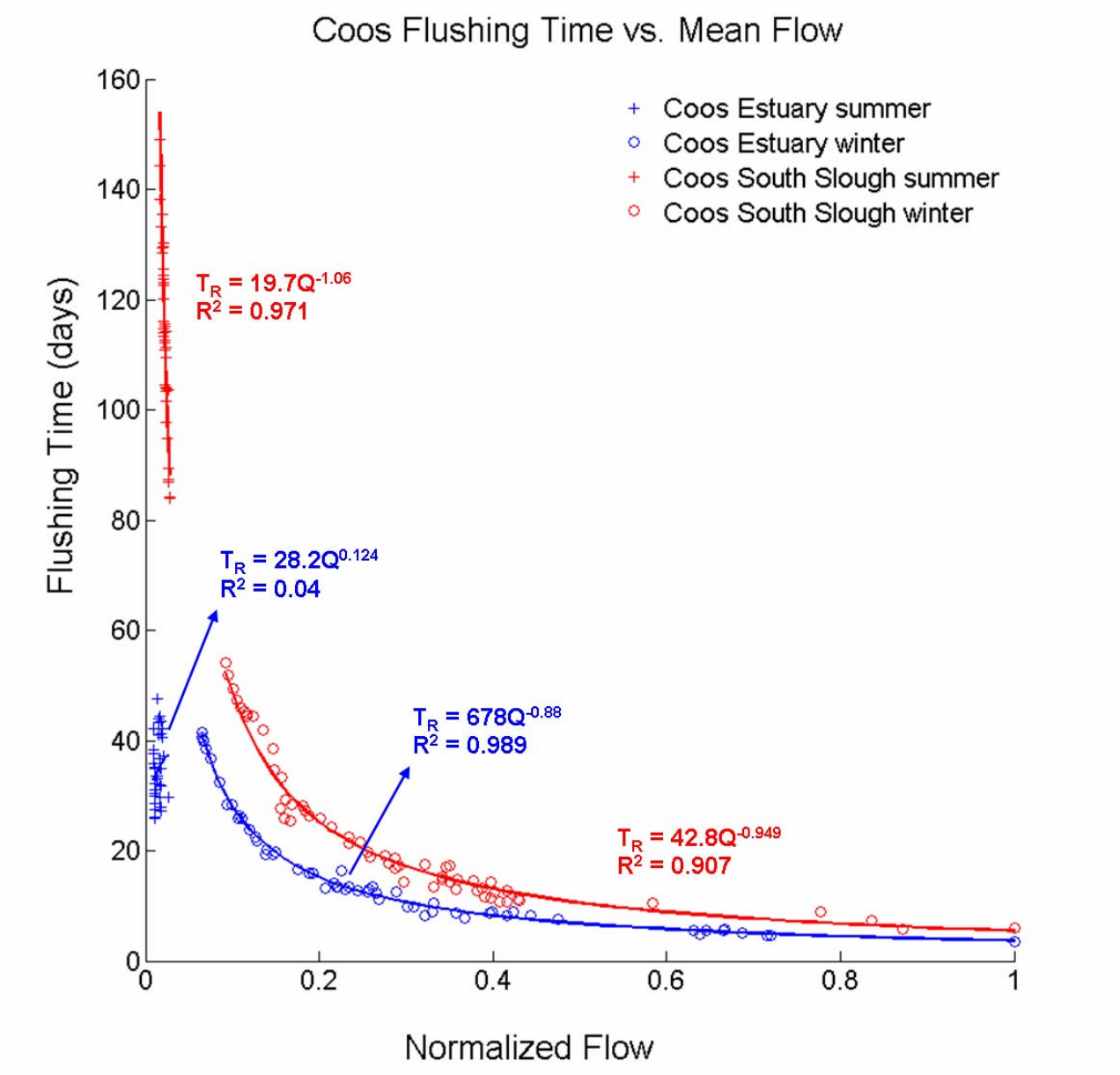

Figure 3.6a: Freshwater flushing time vs. river flow for two regions in the Coos Bay estuary. Mean flow is normalized by estuary using the maximum values for each region (374 m^3/s for the entire estuary, 8.8 m^3/s for the South Slough). The Coos Bay estuary (no mixing pools) flushing time shows distinctly different low flow (blue crosses) and medium to high flow (blue circles) behavior. This is the only region with a well mixed period. The other regions and periods show similar qualitative but distinct quantitative responses to flow across seasons.

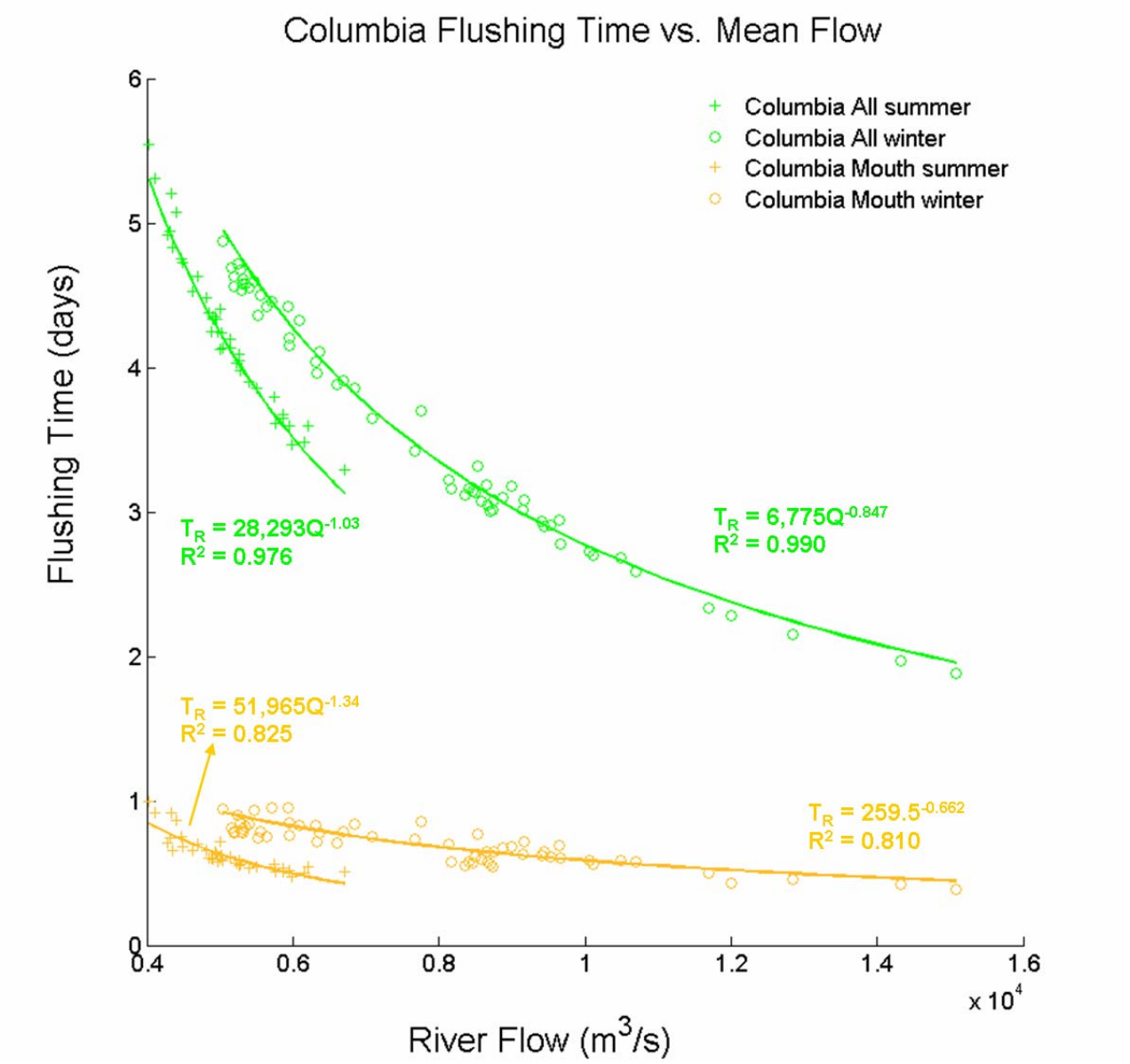

Figure 3.6b: Freshwater flushing time vs. river flow for two regions in the Columbia River estuary.

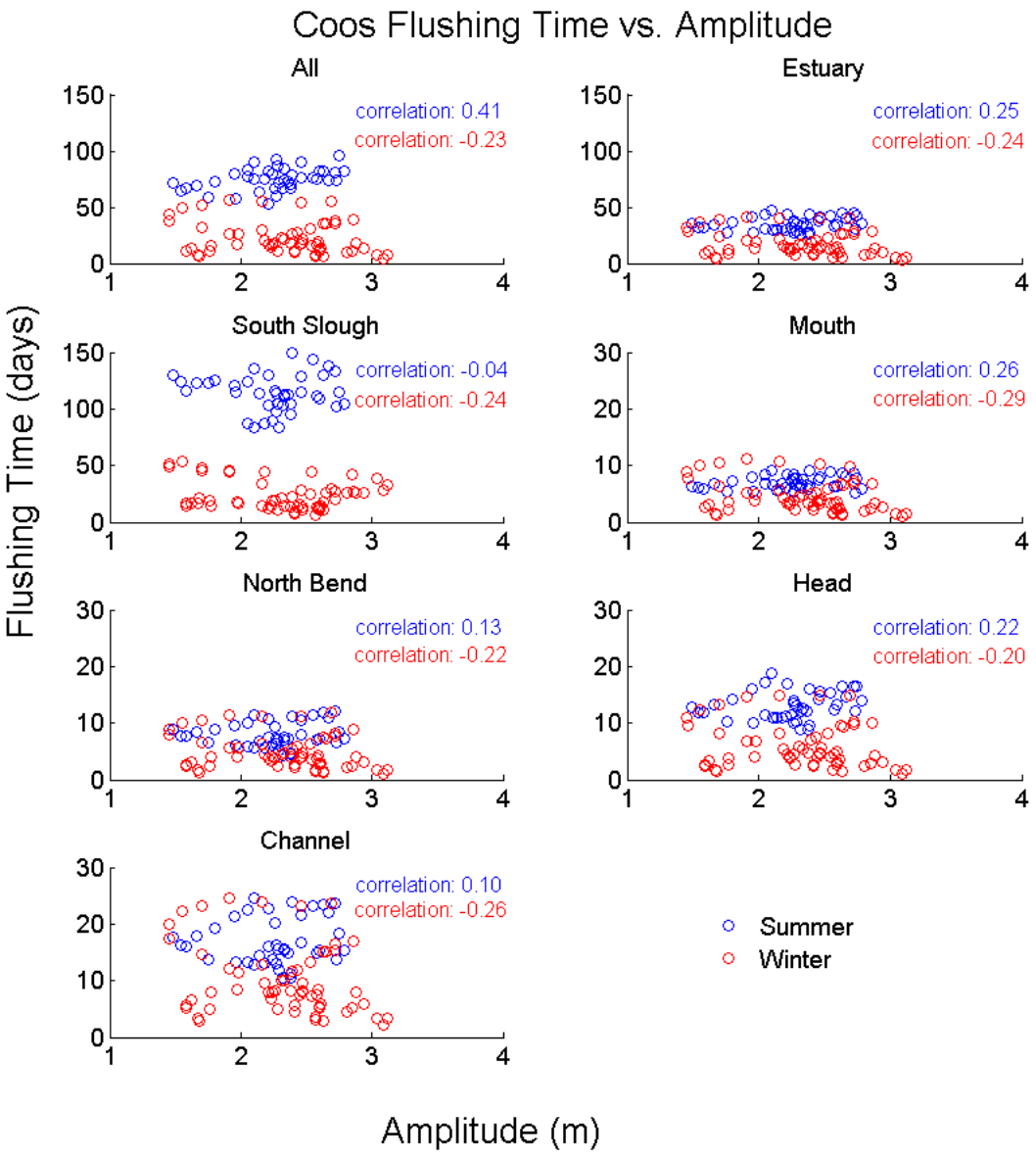

Figure 3.6c: Freshwater flushing time vs. tidal amplitude in Coos Bay. Little correlation is evident. Note that the y axis range is reduced for the mouth, North Bend, head and channel regions.

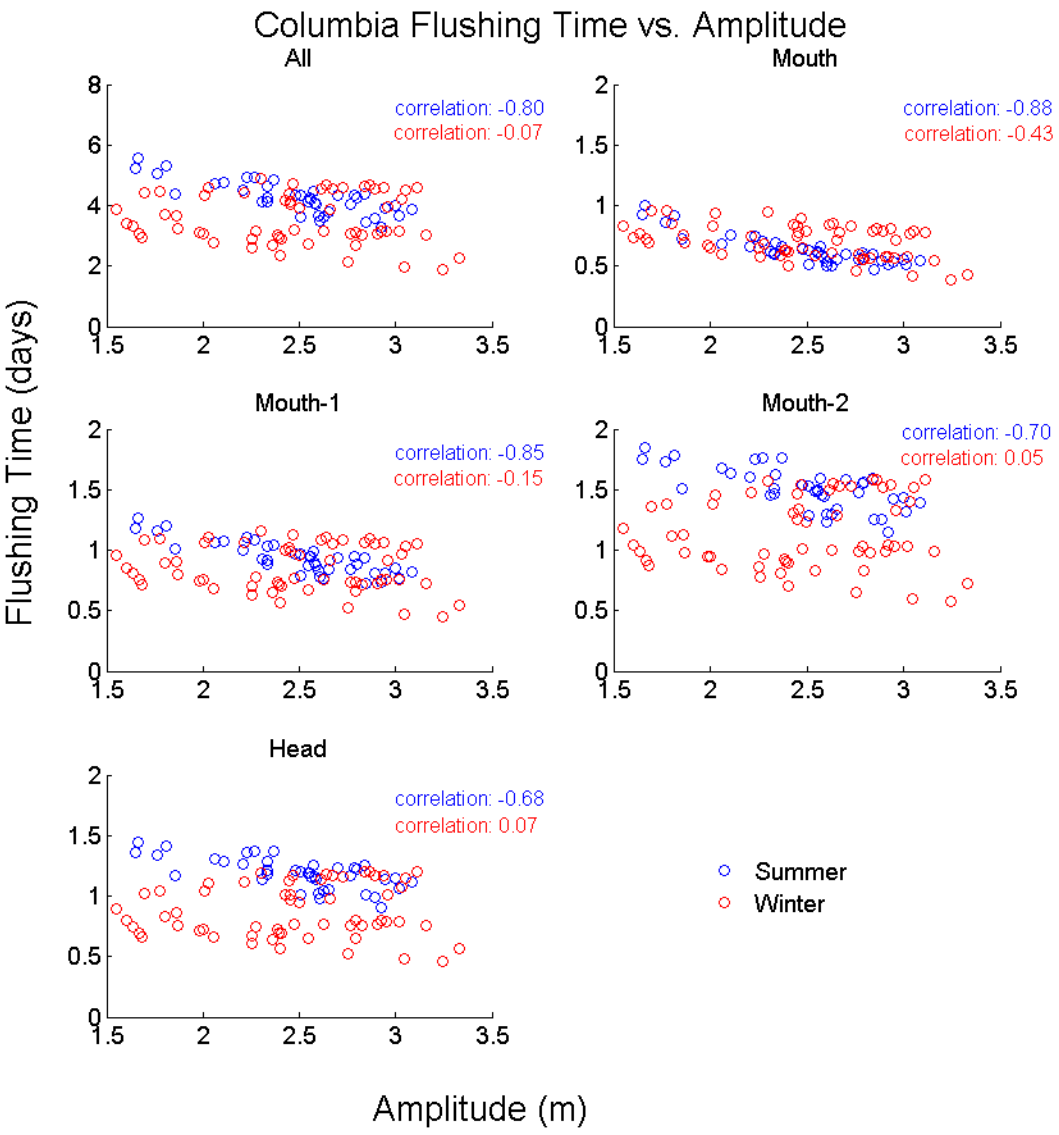

Figure 3.6d: Freshwater flushing time vs. tidal amplitude in the Columbia River Estuary. There is significant correlation between amplitude and T_R in the summer run, but not in the winter run. Note that y axis range is reduced for the sub-regions.

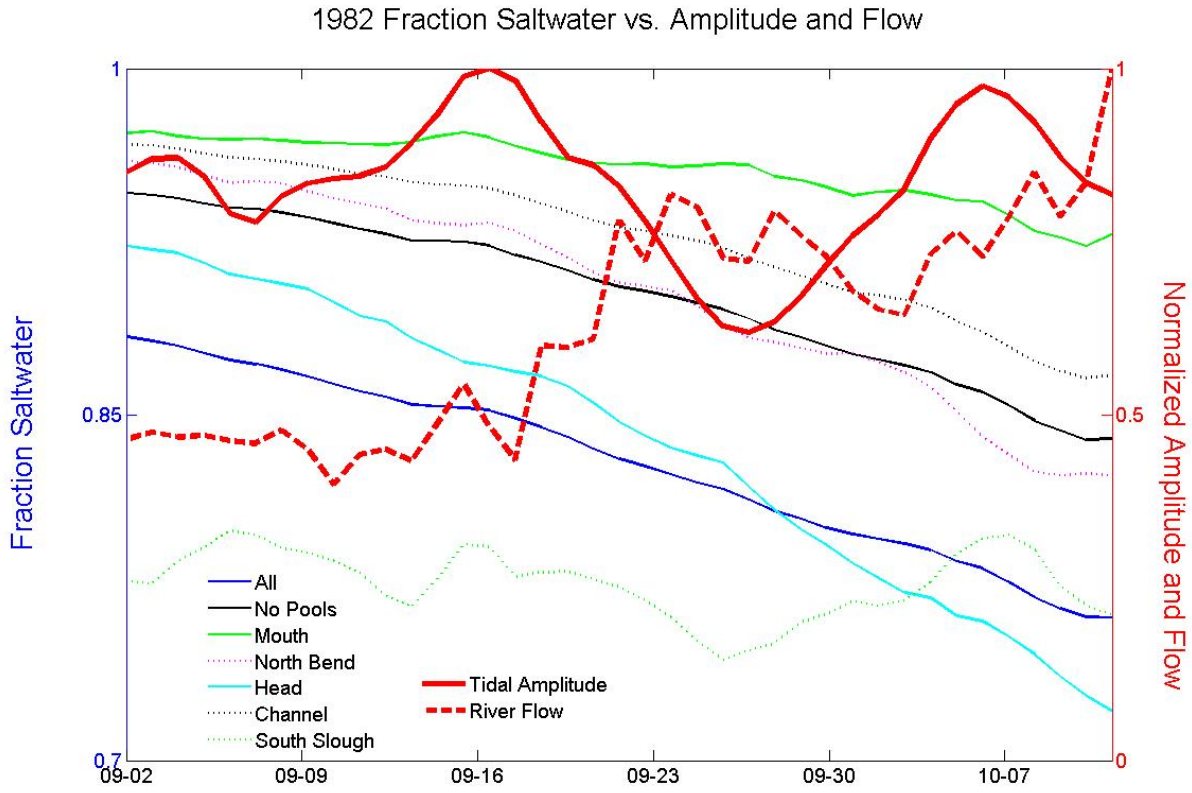

Figure 3.7a: Summer 1982 Fraction of Saltwater vs. river flow and amplitude, by region. Correlations appear in **Table 3.3**. F_{SW} (24.8 hr averages) for all the regions except the South Slough show a strong correlation with river flow and a very weak correlation with tidal amplitude. The South Slough correlations, on the other hand, are much stronger with tides than with river flow.

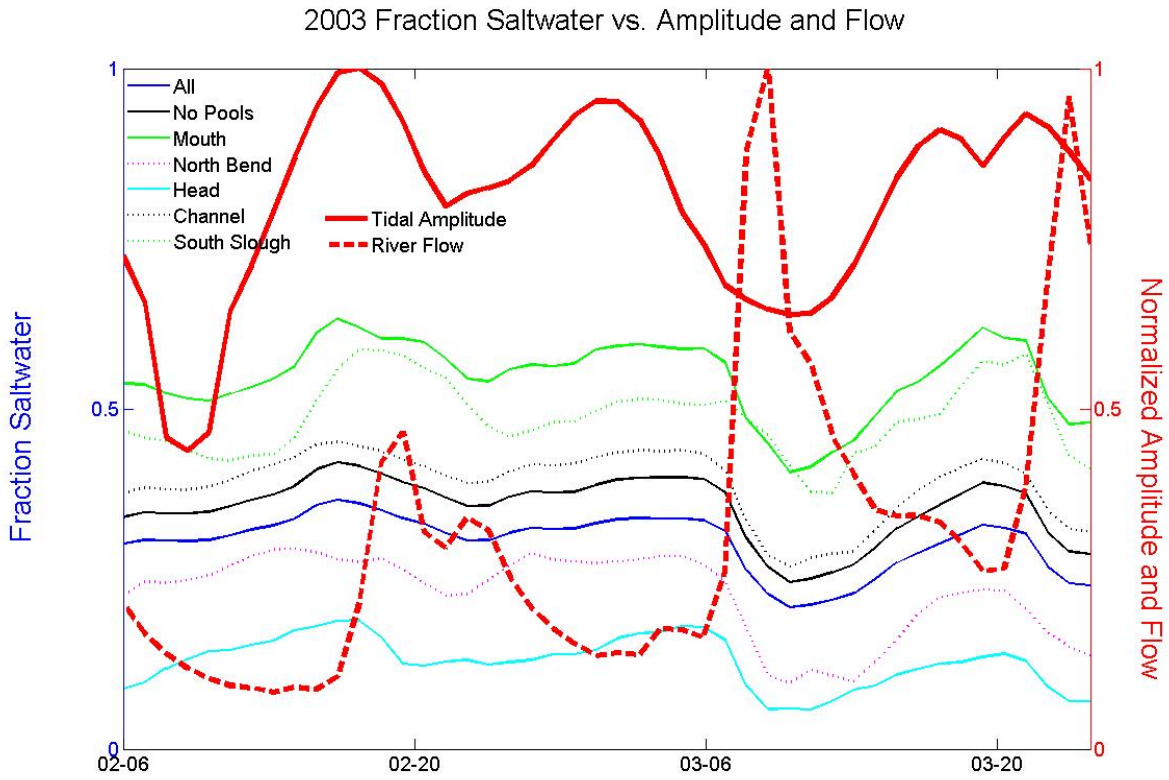

Figure 3.8b: Winter 2003 Fraction of Saltwater vs. river flow and amplitude, by region. Correlations appear in **Table 3.3**. F_{SW} shows some correlation to tidal amplitude in the mouth, North Bend and South Slough regions, and significant correlation to river flow in all regions except the South Slough. During this period baroclinic circulation has been established, complicating the estuarine response to changes in river and tidal forcings.

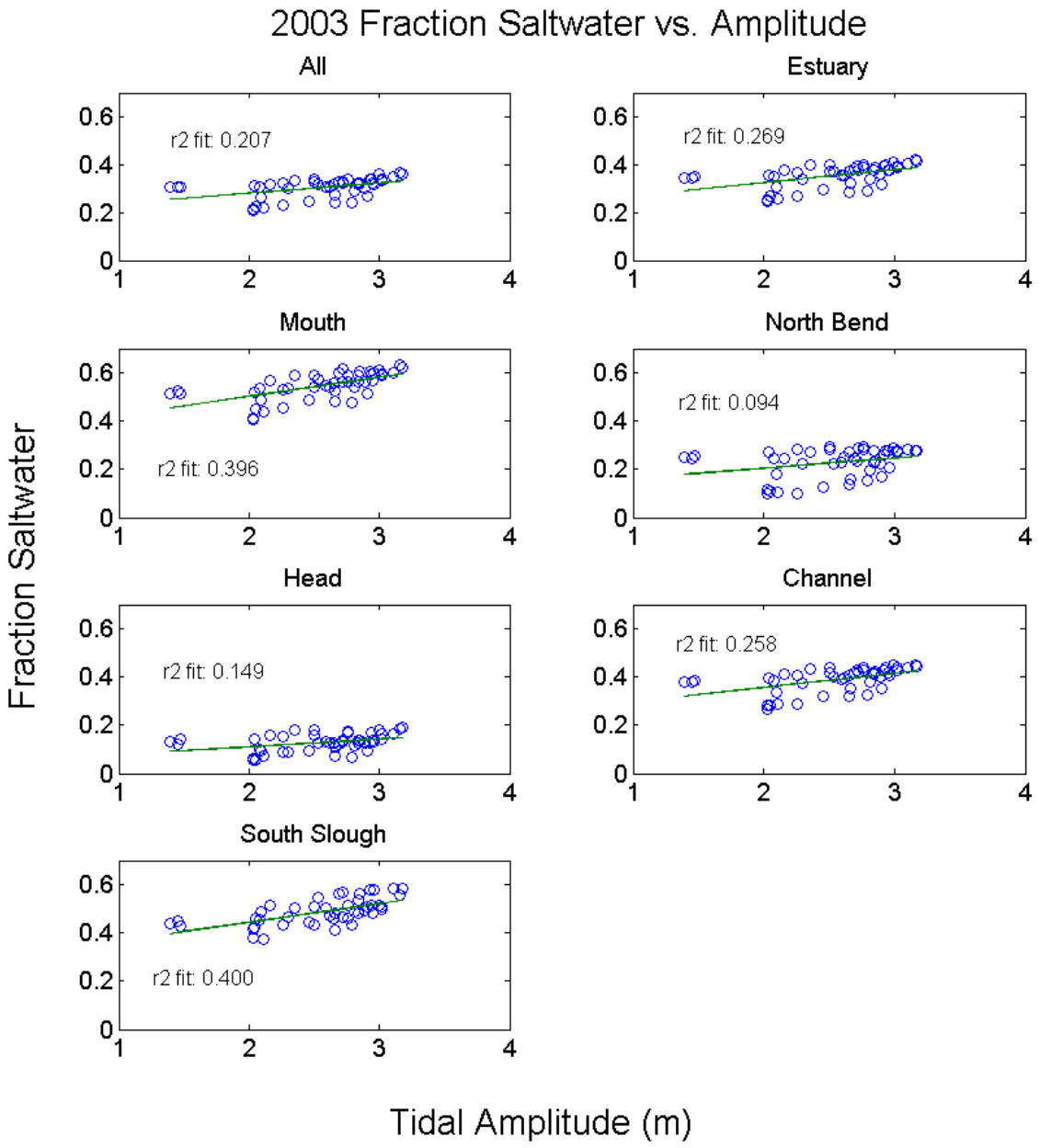

Figure 3.9a: Coos Bay winter 2003 Fraction saltwater vs. tidal amplitude at the mouth. It appears that *FSW* generally increases with tidal amplitude, but not in any consistent, reliable manner. The tightest correlations are in the mouth and South Slough. Unlike the summer case, there is enough balance between mixing and buoyant forces that any change in mixing (tidal in this case) forces have a noticeable effect.

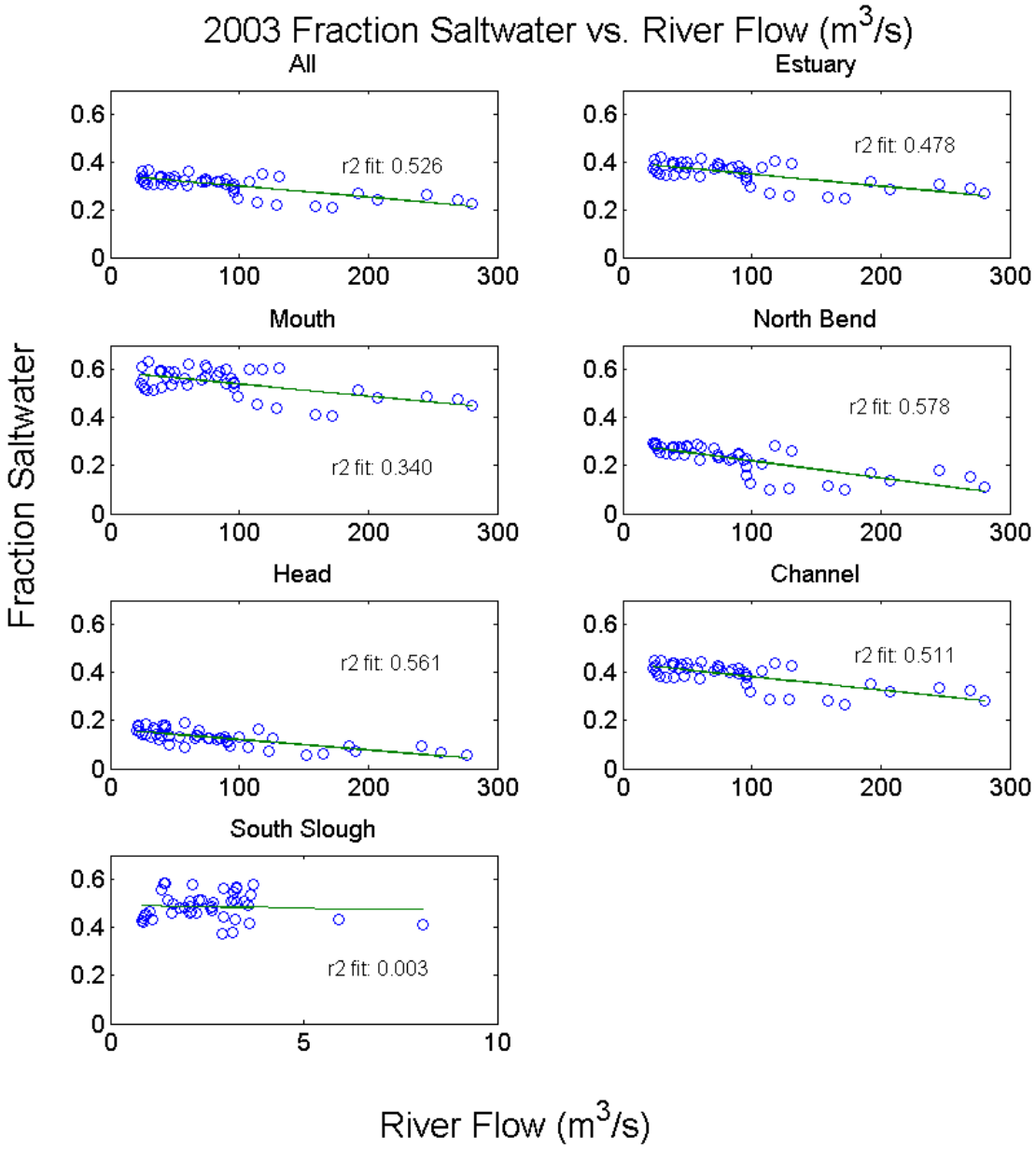

Figure 3.9b: Coos Bay winter 2003 fraction saltwater vs. net river flow. While the general trend is for less salinity with increased fresh water, the correlations are highest towards the head. Again, mixing and buoyant forces are roughly balanced. The correlation between river flow and decreased fraction saltwater seems to be primarily evident during the three large flow spikes. Without the flow events over 150 m^3/s river flow would have a far less noticeable affect on F_{SW}.

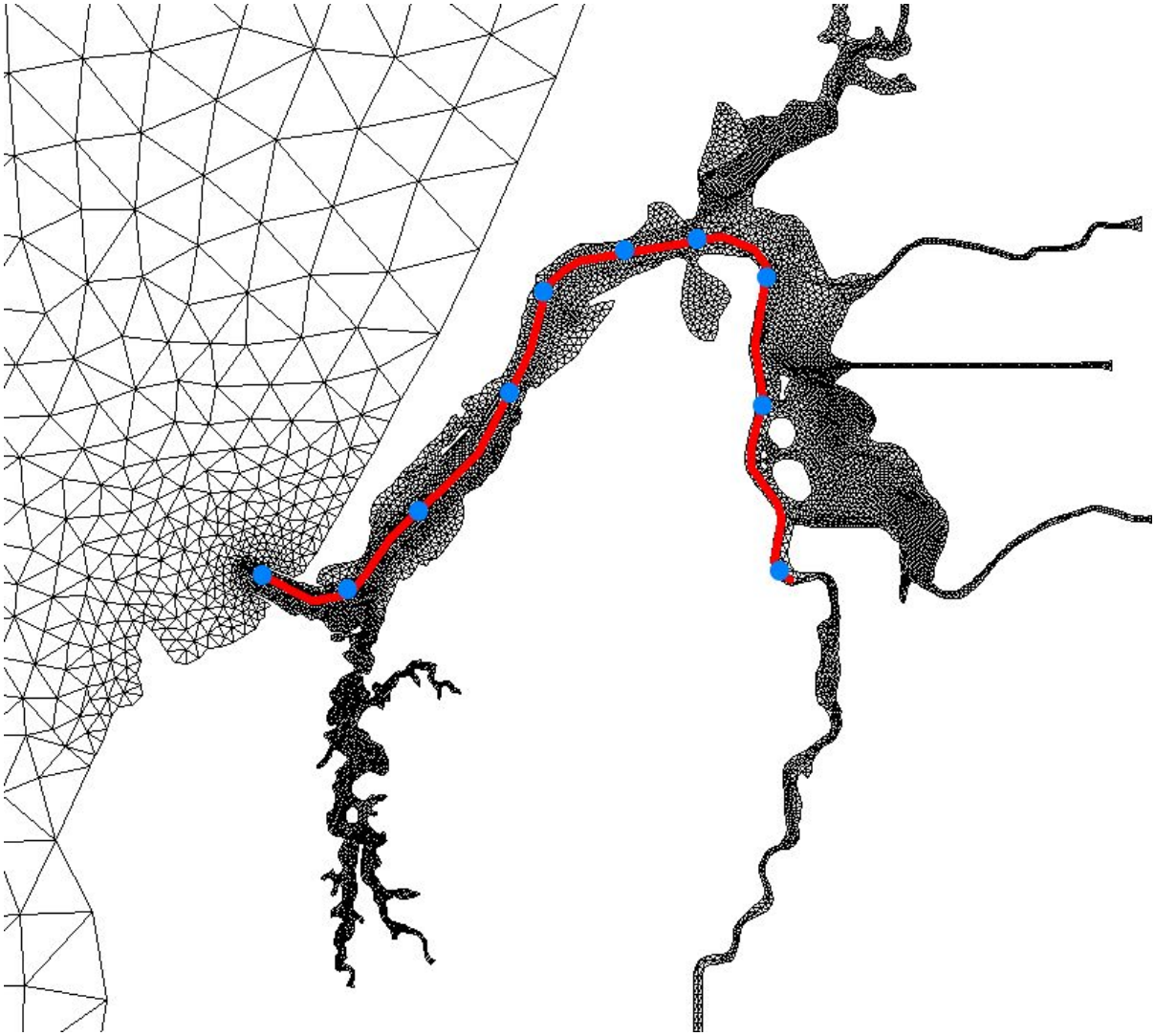

Figure 3.10 a: Path of the transect used to make the images in **Figure 3.10-11,** as well as the points for the interfacial Froude number calculations in **Figure 3.12** and **3.13**. The points are numbered from 1 to 10 from the mouth to the head.

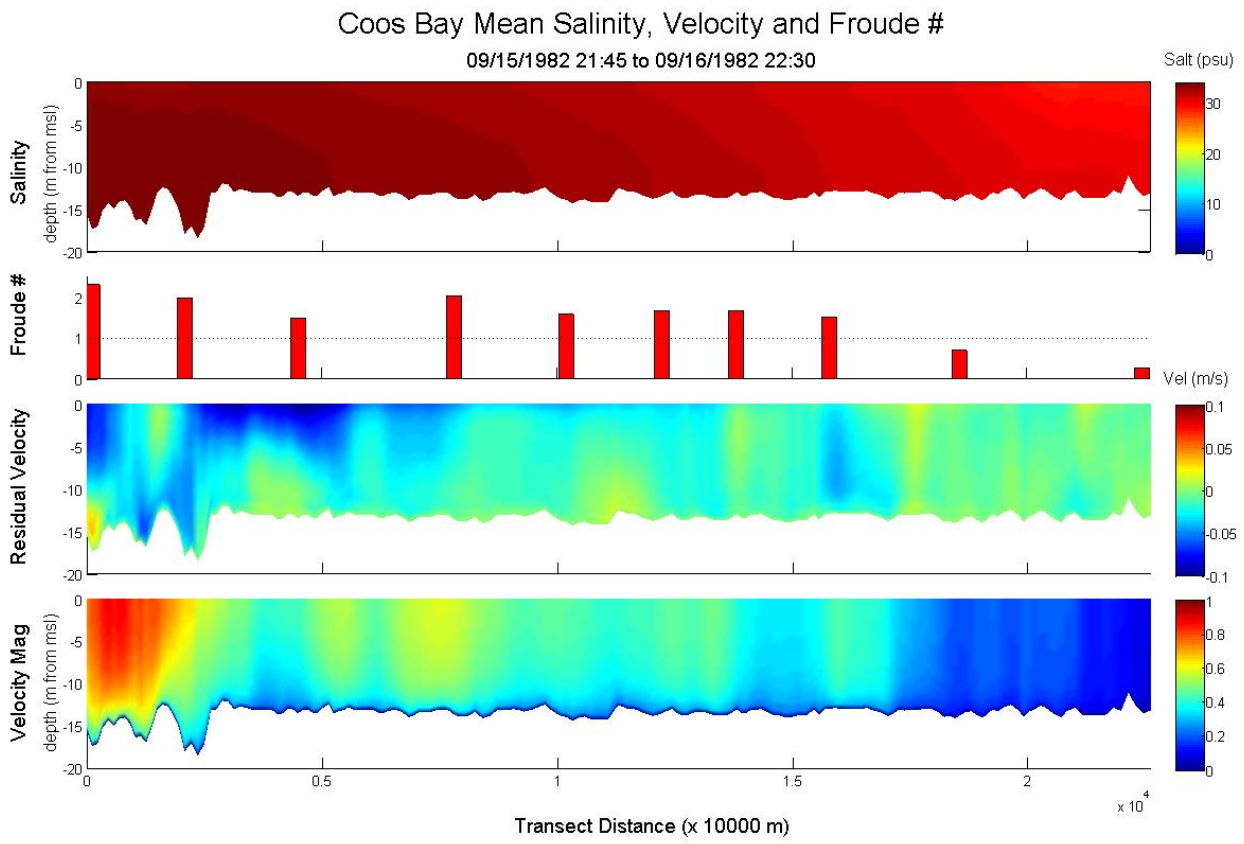

Figure 3.10b: The time averaged (2 tidal periods: 24.8 hrs) salinity, residual velocity and mean velocity magnitude transects for a period when the interfacial Froude number > 1 (9/15). This higher F_i case shows a smaller horizontal salinity gradient and residual velocity that is out or near zero throughout the transect.

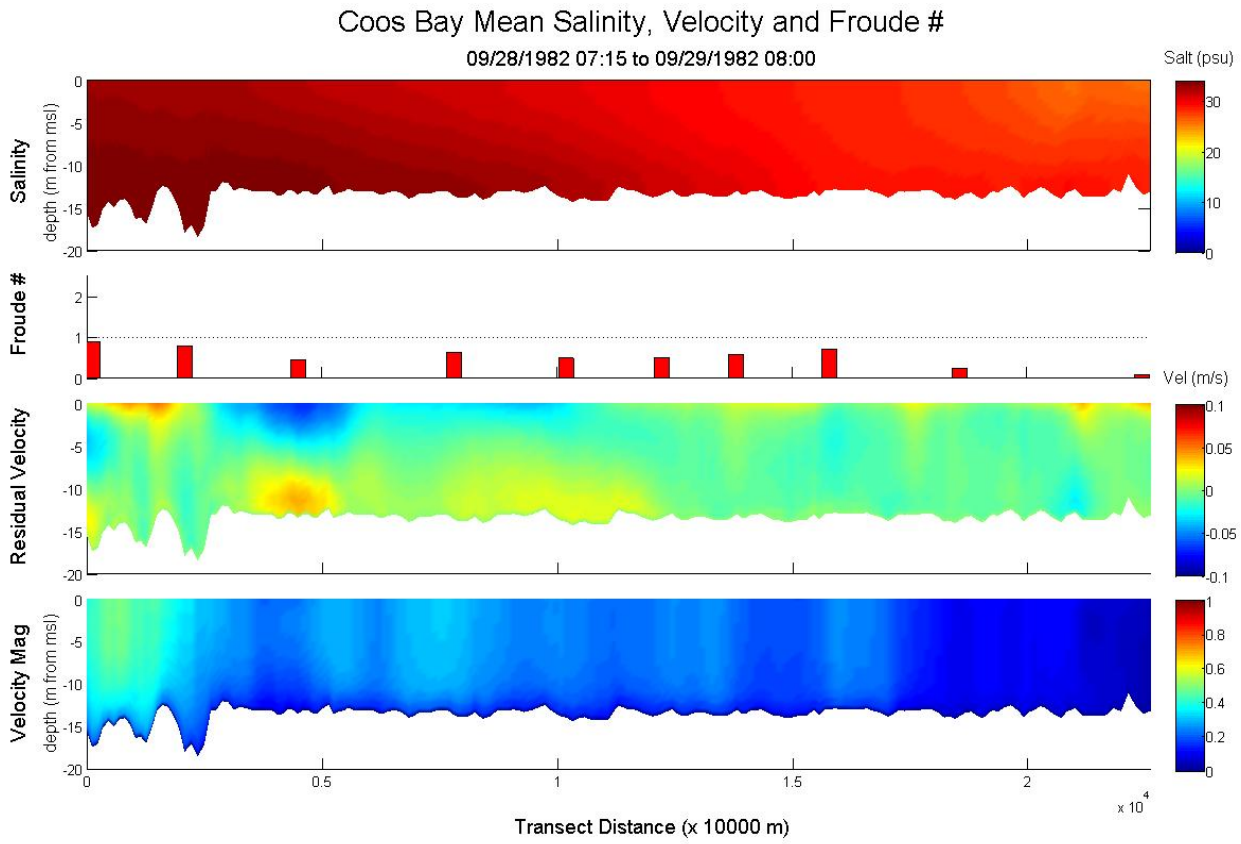

Figure 3.10c: The time averaged (2 tidal periods: 24.8 hrs) salinity, residual velocity and mean velocity magnitude transects for a period when $F_i < 1$ (9/28). This lower F_i case shows a significantly higher horizontal salinity gradient, more slumped salinity isolines, and shows evidence of a developing baroclinic circulation at about 4500 m.

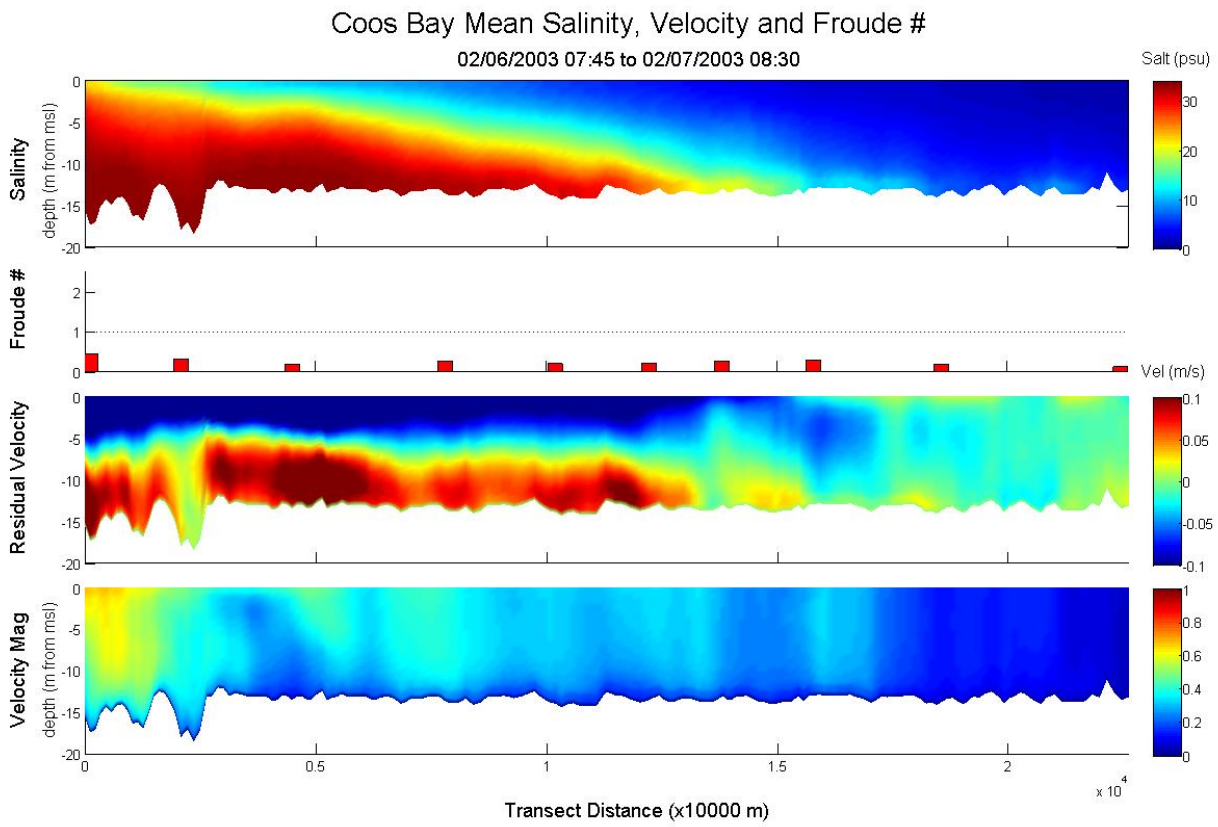

Figure 3.11a: Time averaged (2 tidal periods: 24.8 hrs) salinity, residual velocity and mean velocity magnitude transects for a period when F_i is relatively low (2/6). F_i is well below 1 and the estuary is clearly stratified. In this lower F_i case the salt wedge extends deep into the estuary, and has much sharp and significant baroclinic circulation. F_i values fall in the head of the estuary primarily due to very low velocity magnitudes and a modeling artifact from wetting and drying that can cause high salinity in rewetted elements.

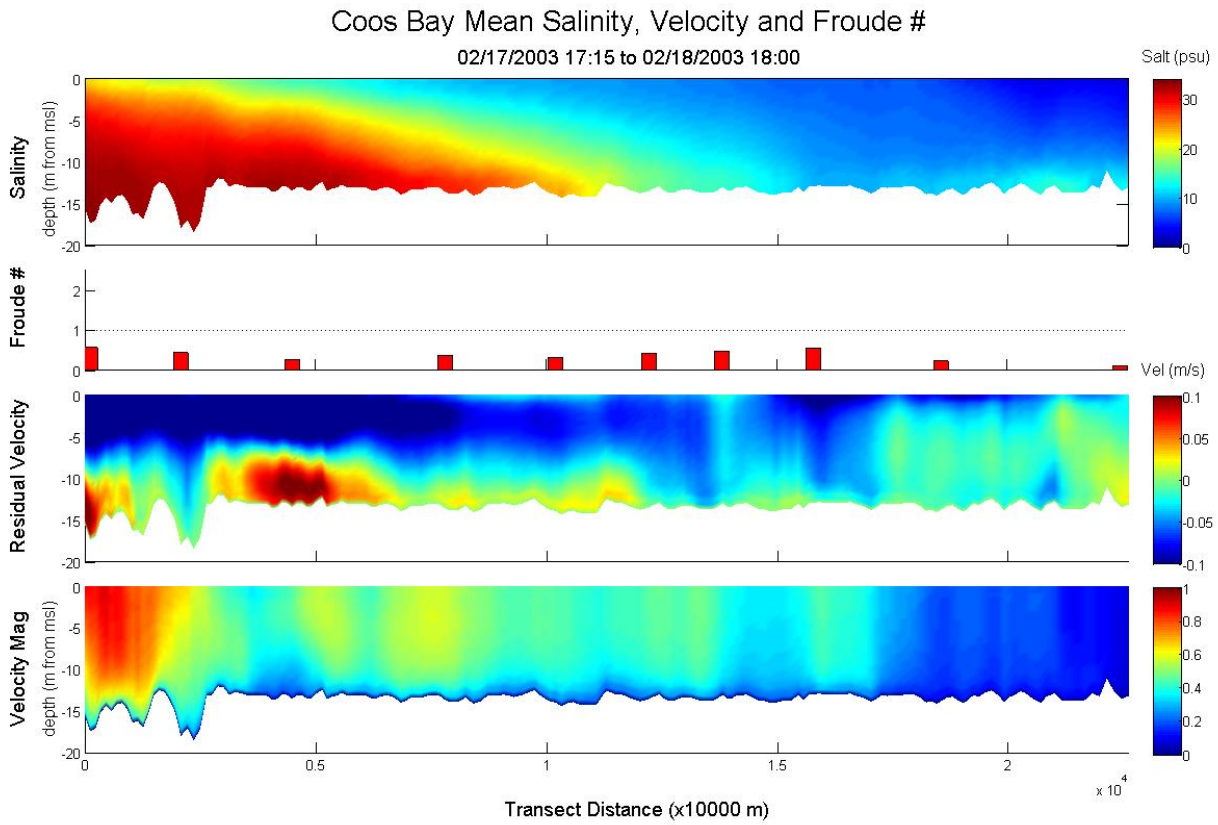

Figure 3.11b: Time averaged (2 tidal periods: 24.8 hrs) salinity, residual velocity and mean velocity magnitude transects for a period when F_i is relatively high. In both winter cases F_i is well below 1 and the estuary is clearly stratified. In this F_i case, however, the salt wedge extends less deep into the estuary, has a less sharp salinity gradient than the lower F_i case, and has significantly less baroclinic circulation.

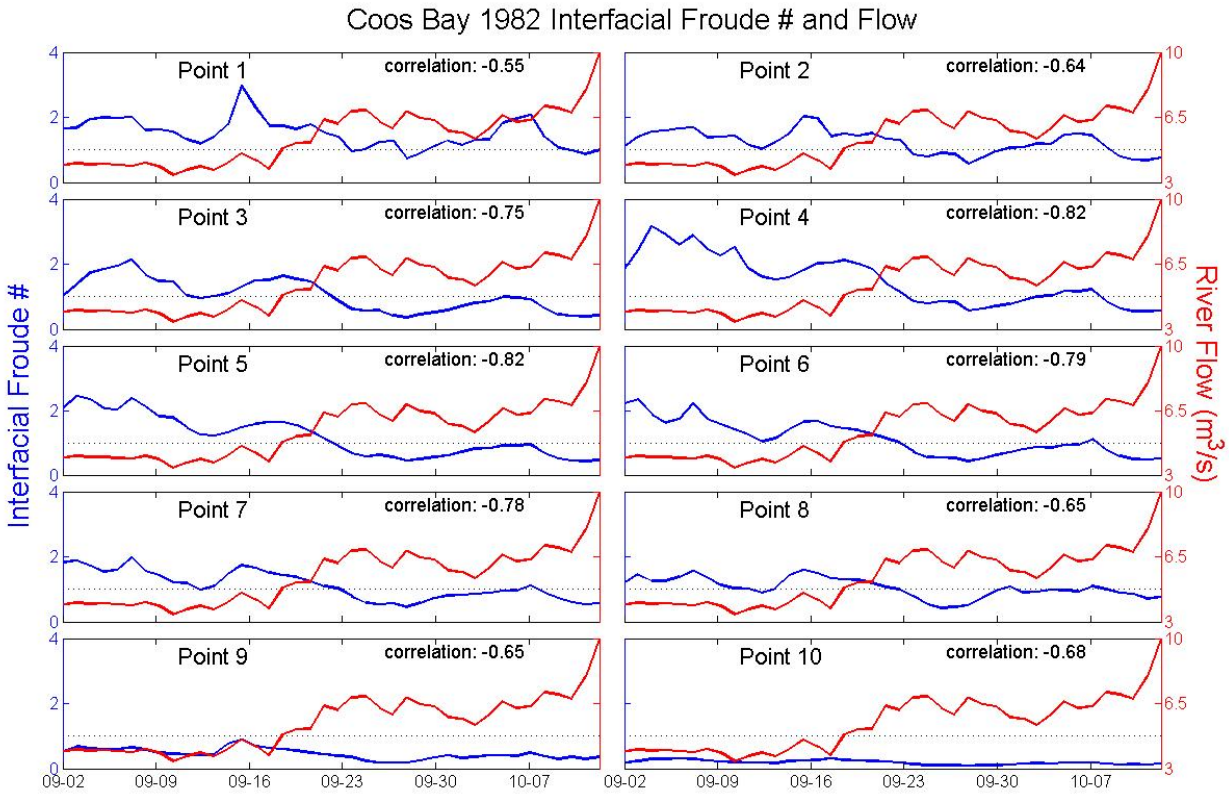

Figure 3.12 a: Coos Bay summer 1982 interfacial Froude number correlation with river flow. F_i shows significantly less correlation to river flow at points one and two, but at points 3-7 F_i shows a strong negative correlation with river flow. This higher correlation with river flow is largely due to the estuary going through the early stages of a transition from well mixed to partially mixed estuary, with more slumped salinity isolines, stronger salinity gradients and thus greater bottom-to-top density differences. Points 9-10 are difficult to interpret due to the wetting-drying salinity artifact described in section 2. Low velocities in this region mean that even small additions to the mean salinity at the bottom results in very low F_i.

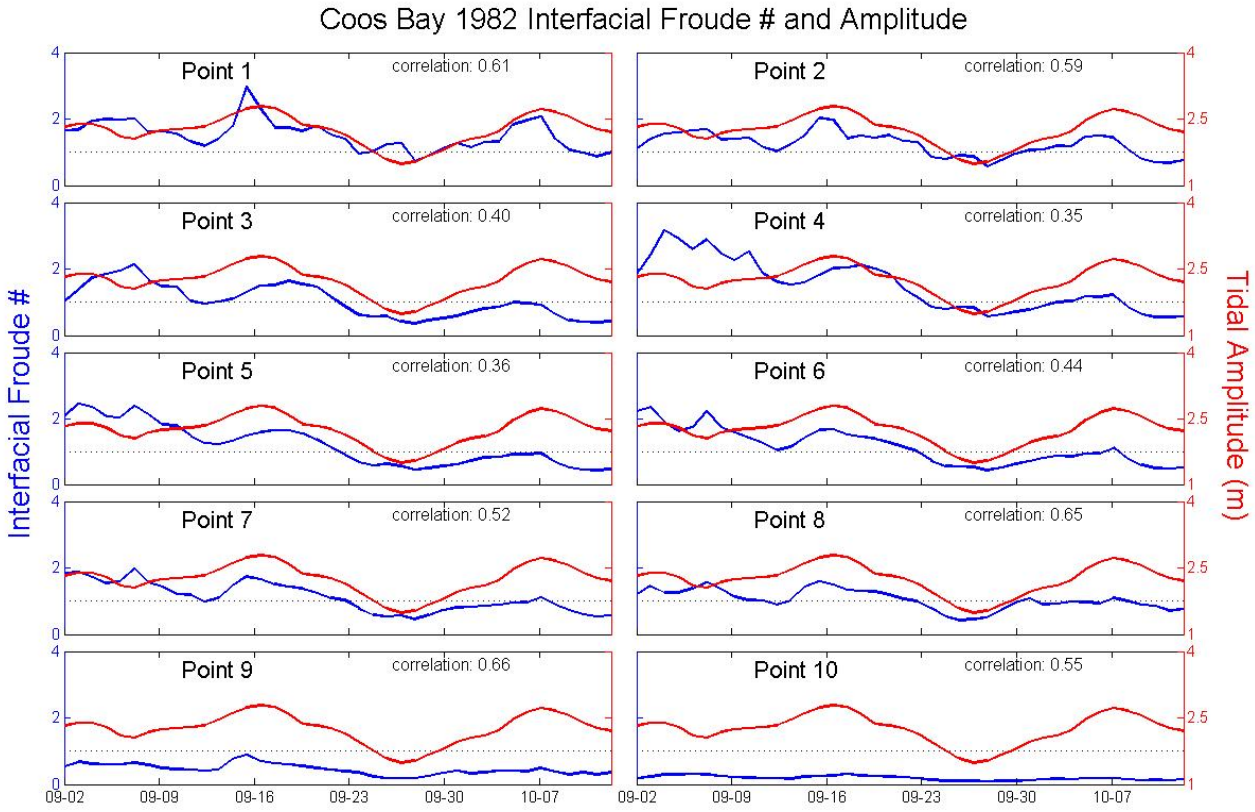

Figure 3.12 b: Coos Bay summer 1982 interfacial Froude number correlation with tidal amplitude. F_i shows slightly more correlation to amplitude than to river flow at points one and two, but at points 3-7 F_i is clearly dominated by river flow.

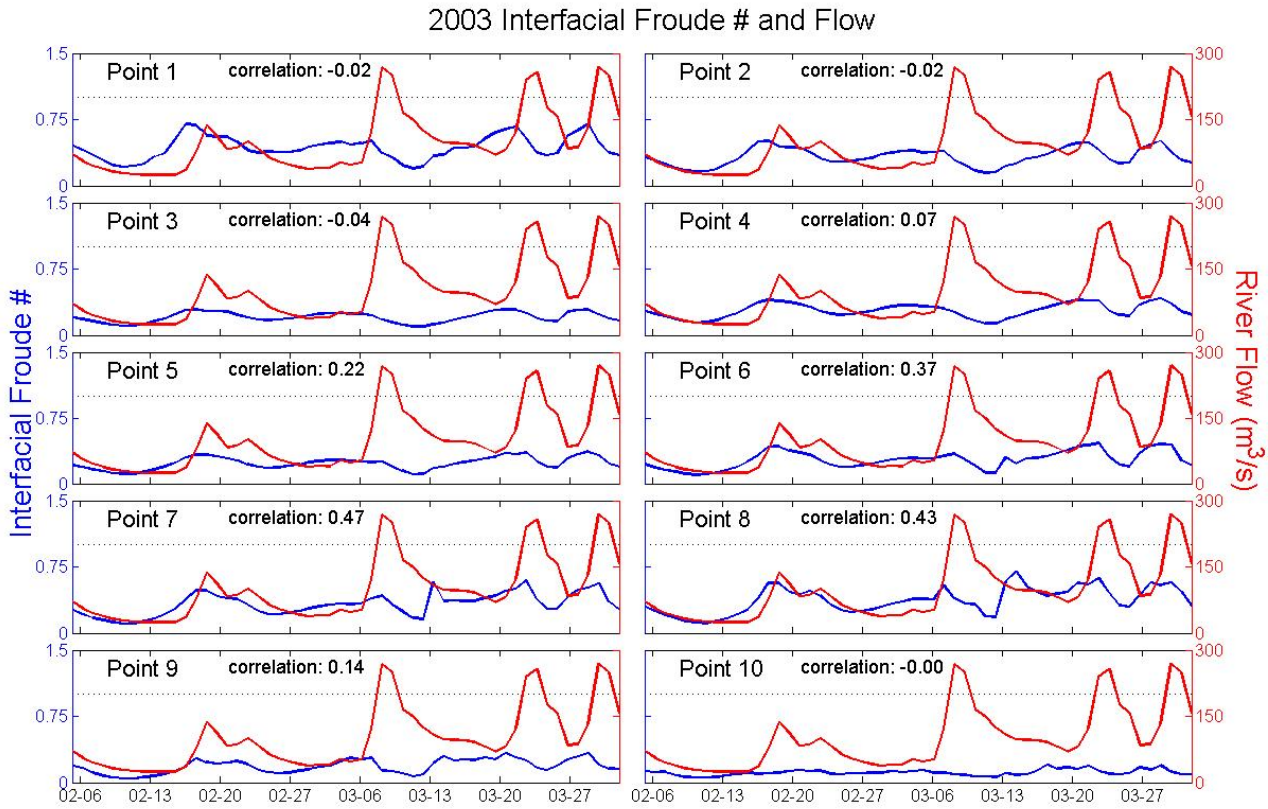

Figure 3.13a: 2003 Interfacial Froude number vs. net river flow. Although correlations are quite low, F_i clearly responds to the large flow peaks around 3/8, 3/24 and 3/30. During this period it takes very large river flow increases to have a large affect on F_i. For example, the expected F_i drop from the relatively small flow increase round 2/28 was partially overcome by the rising tidal amplitude at the same period. For the 3/24 flow increase, however, tidal amplitudes were still relatively high.

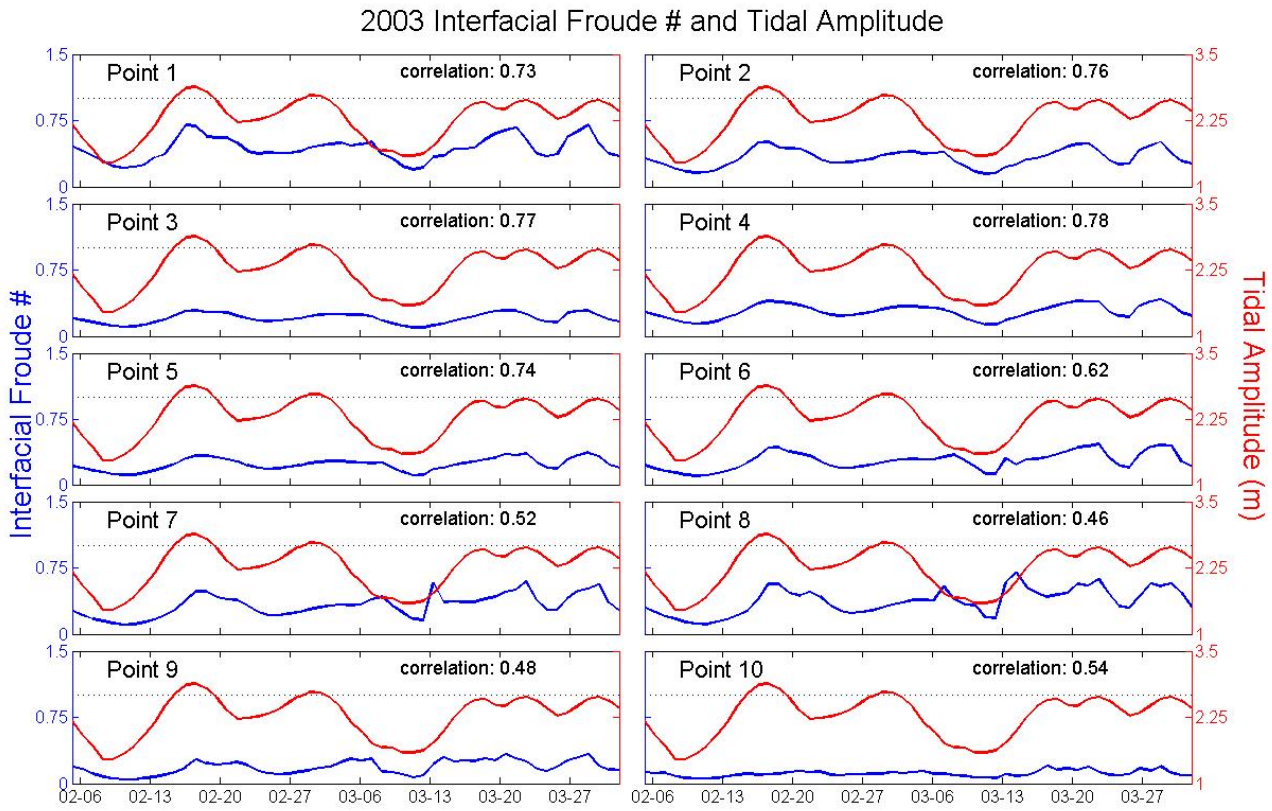

Figure 3.13b: Coos Bay winter 2003 interfacial Froude number vs. tidal amplitude. In the front part of the estuary the F_i responds consistently but slightly to changes in tidal amplitude. The large river flow spikes in **Figure 3.13a** interrupt this trend by producing sharp decreases in F_i as the increased river flow creates increased stratification and deeper salt wedge penetration.

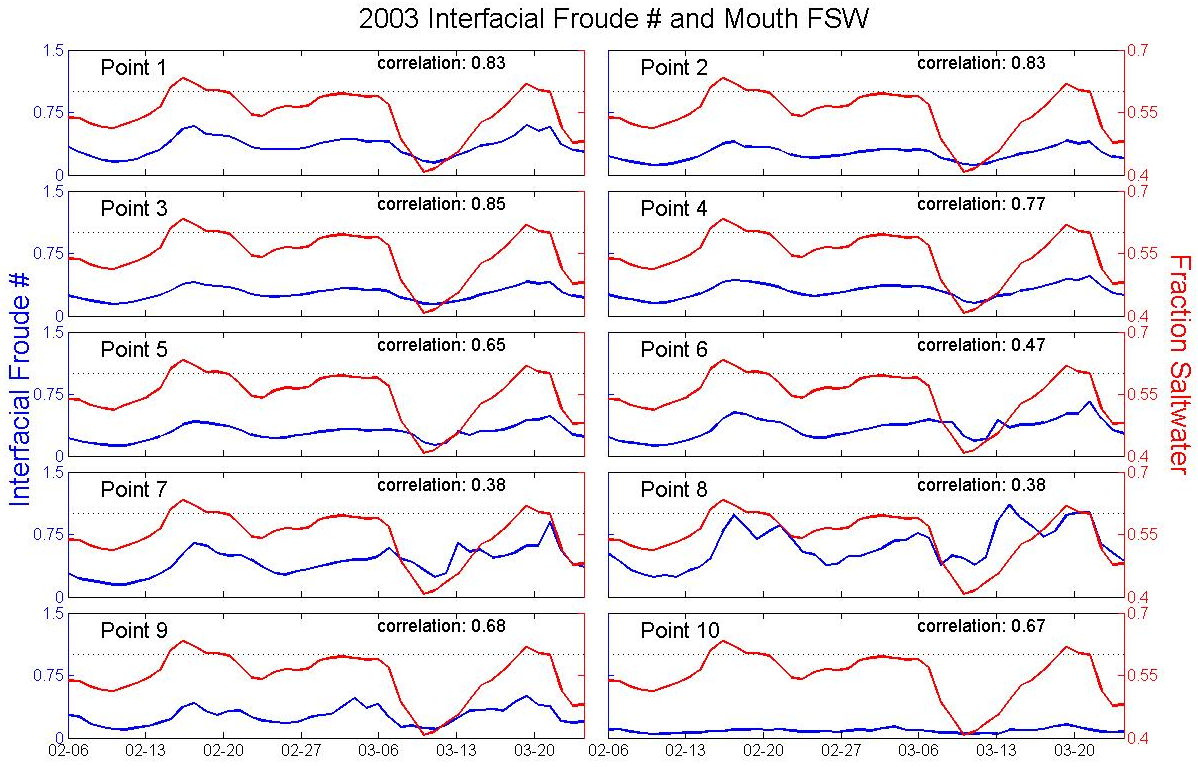

Figure 3.14: Interfacial Froude # and F_{SW} in the mouth

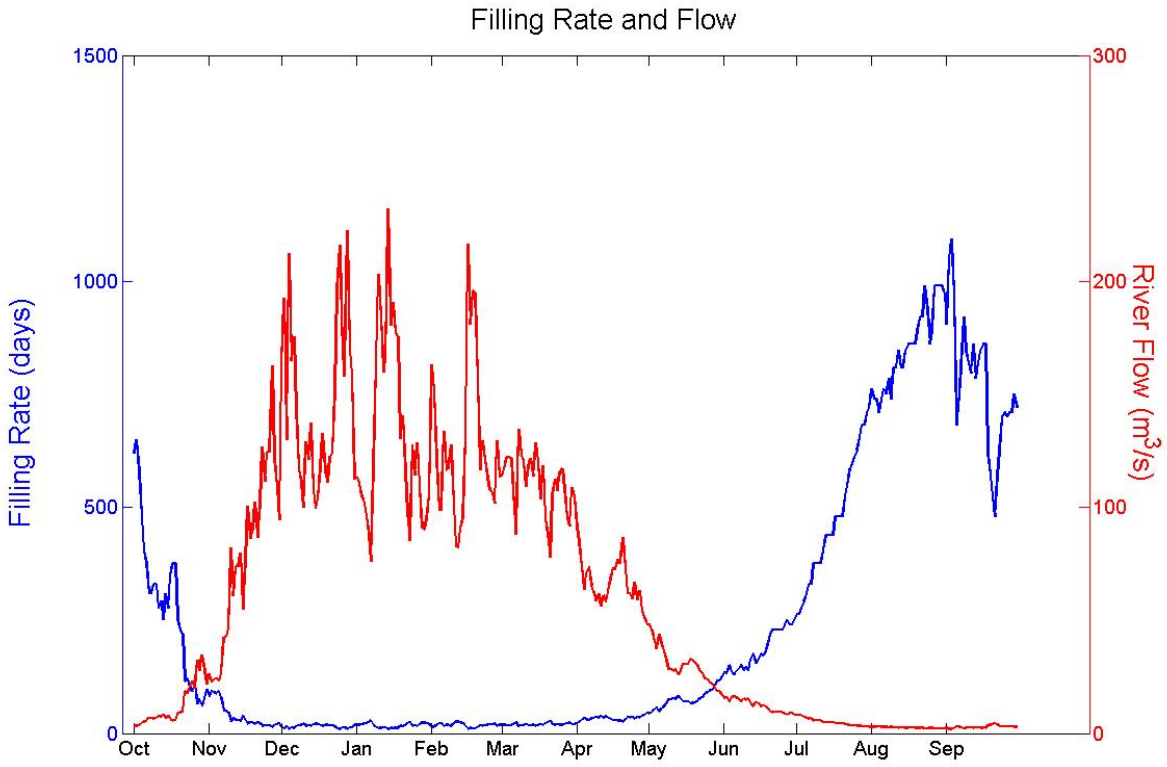

Figure 3.15: Filling rate from river flow (using the total Coos watershed river input 50th percentile climatology) and the regression equation in **Figure 3.6a**.

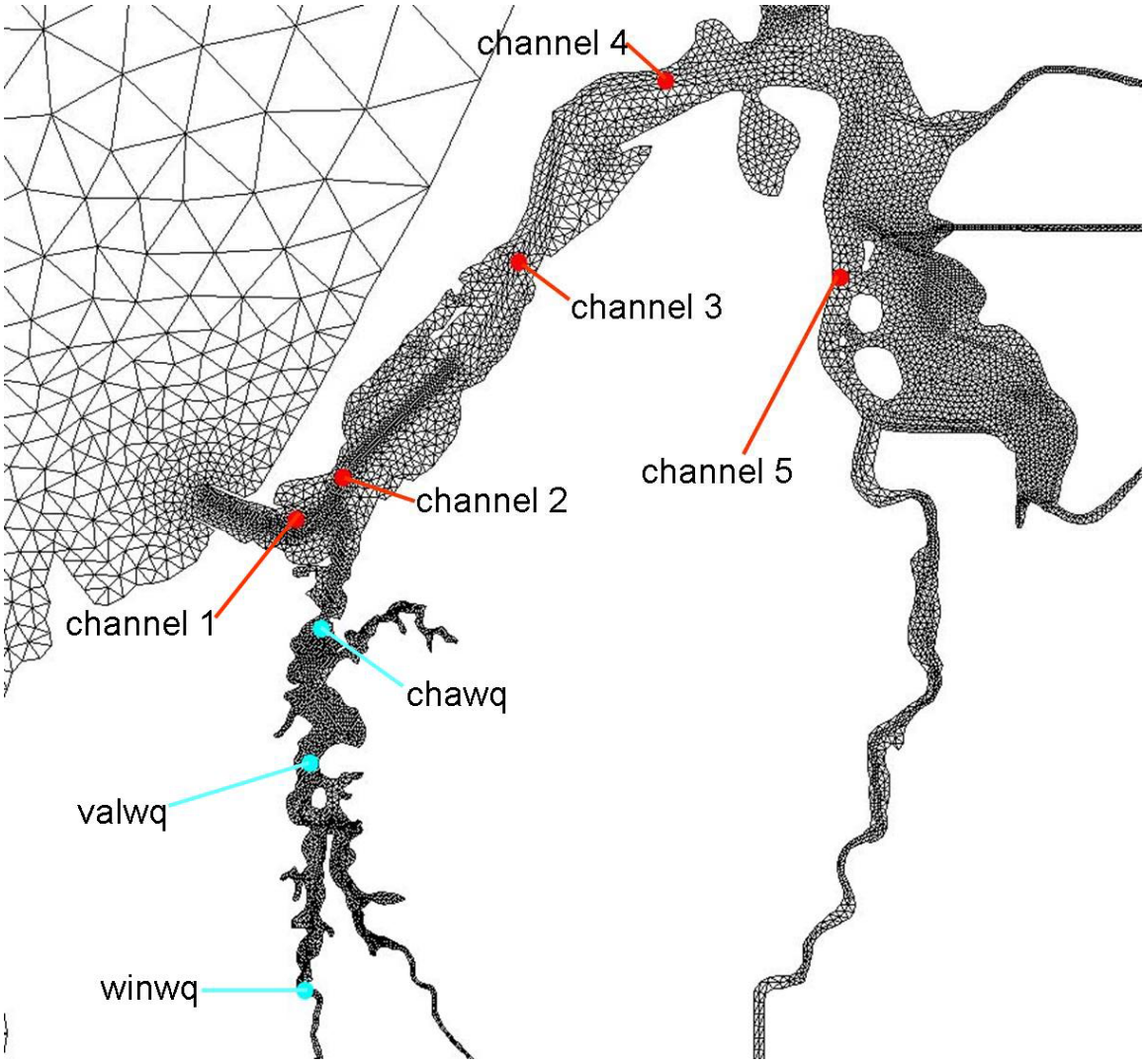

Figure 3.16 a: Sample locations for Salt and Temperature diagrams.

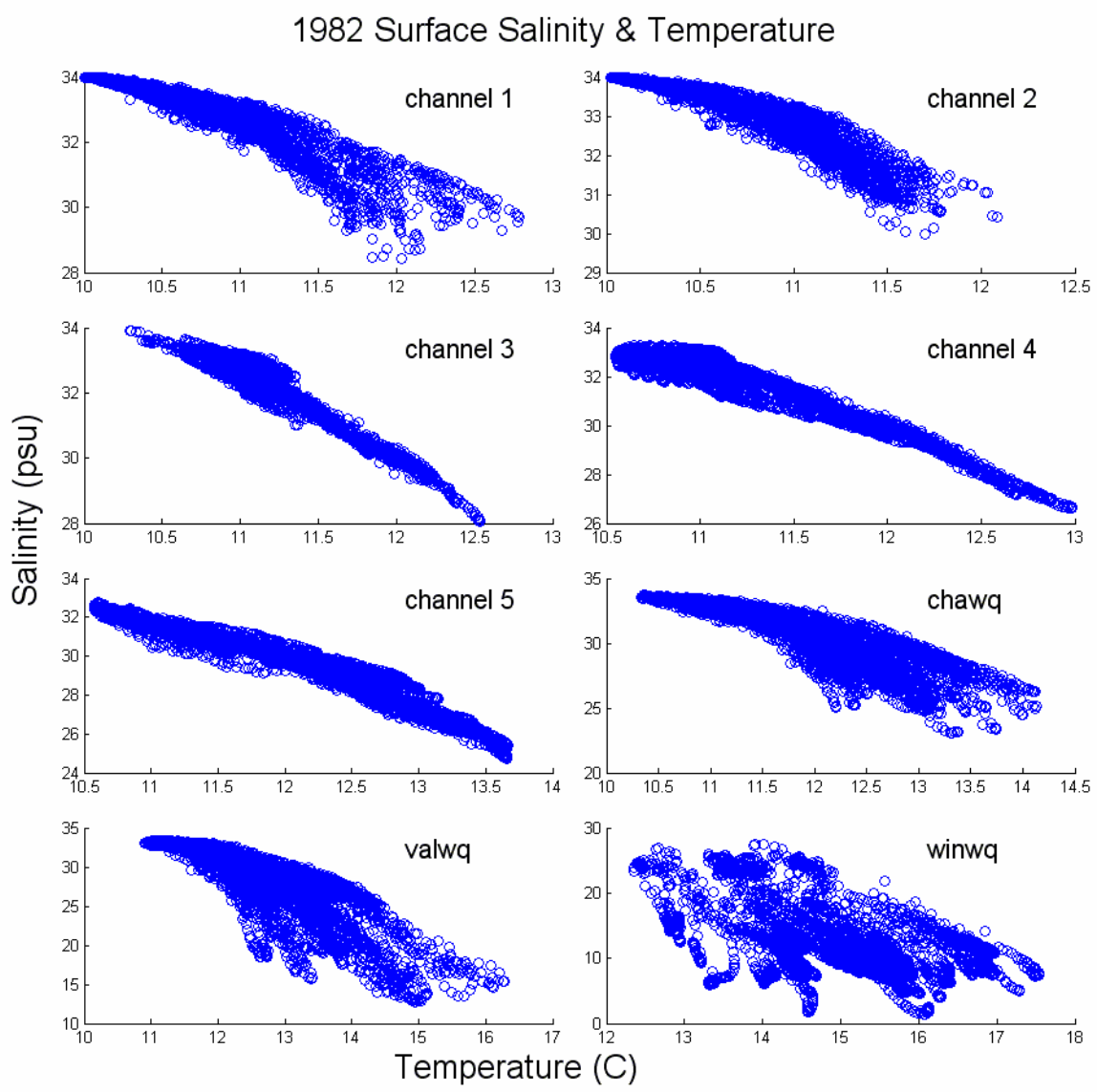

Figure 3.16 b: Model salinity vs. temperature plots for the summer 1982 model run show moderately distinctive mixing characteristics in the mouth, South Slough and estuary head.

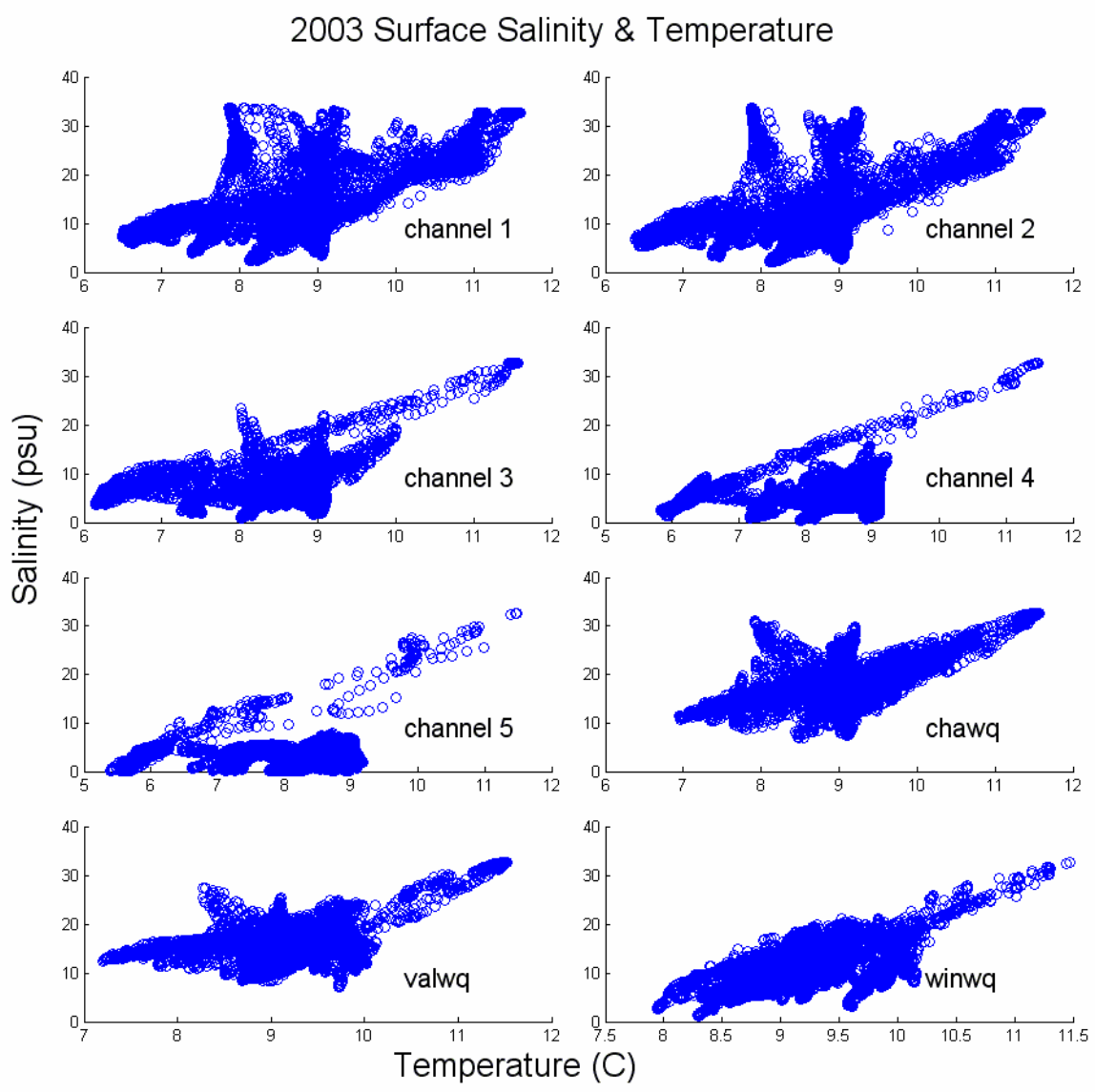

Figure 3.16 c: Model salinity vs. temperature plots during the winter 2003 run show significantly distinctive mixing characteristics in the mouth, South Slough and estuary head, especially between the Valino Island and Winchester Creek stations.

Chapter 3 Tables

	Low Flow (5 m^3/s)	**Medium Flow (50 m^3/s)**	**High Flow (300 m^3/s)**
Spring Tides (prism = 11 x 10^7)	0.002	0.02	0.12
Neap Tides (prism = 7 x 10^7)	0.003	0.03	0.19

Table 3.1: Flow ratio numbers for typical spring and neap prisms and river flows. Simons (1955) found that flow ratios above 1 indicate a stratified estuary, rates around 0.25 indicate a partially mixed estuary, and rates below 0.1 indicate a well mixed estuary. These numbers suggest that Coos Bay will be a well mixed estuary in all but the highest flows.

Region	Season	River Flow (m^3/s) Correlation	Amplitude (m) Correlation
All	Summer (1982)	-0.88	0.10
No Pools	Summer (1982)	-0.87	0.06
Mouth	Summer (1982)	-0.84	0.04
North Bend	Summer (1982)	-0.88	0.06
Head	Summer (1982)	-0.87	0.06
Channel	Summer (1982)	-0.87	0.05
South Slough	Summer (1982)	-0.46	0.75
All	Winter (2003)	-0.74	0.45
No Pools	Winter (2003)	-0.69	0.52
Mouth	Winter (2003)	-0.58	0.63
North Bend	Winter (2003)	-0.76	0.31
Head	Winter (2003)	-0.75	0.39
Channel	Winter (2003)	-0.72	0.51
South Slough	Winter (2003)	-0.17 (-0.06 to 2 direct inflow streams)	0.63

Table 3.2: Fraction saltwater correlations to river flow and tidal amplitude. Correlations to river flow are higher during the well mixed summer period, when ocean water permeates the estuary at the end of the very low flow summer period. During the winter medium-high flow period F_{SW} correlations to river flow decrease, while correlations to tidal amplitude increase. This is especially the case in the mouth. South Slough correlations are with the total freshwater flow into Coos Bay, but F_{SW} correlations with the two (modeled) streams flowing directly into the slough are even lower.

4. Conclusion

With the modeling advances made through CORIE and other modern modeling efforts, widespread monitoring of rivers by the USGS and other agencies, availability of atmospheric data sets from models such as Eta/NARR, and the expansion and integration of coastal and ocean monitoring systems, the time is right for the expansion of continuous estuarine modeling systems to estuaries with fewer resources available for long-term research. These individual forecasting systems can provide fully 3D physical data for science, industry and regulation, form the basis for deeper analysis through the calculation of an expanding suite of characterization and classification parameters, and may eventually be integrated into a National Estuarine Modeling System.

The Coos Bay pilot EMS provides evidence that RDFS is a feasible method for laying the foundation of management quality forecasting systems and of a future NEMS, but significant hurdles particular to each estuary will remain. Based on the hypothesis that local stakeholder interest and support is essential for the development and maintenance of a forecasting system, the Coos Bay RDFS leveraged local interest to gain awareness of, and collect resources that contributed to, an improved hydrodynamic model. The Coos Bay pilot RDFS moved through multiple calibration/validation cycles. Results indicate that with the support of an established forecasting system such as CORIE, a moderate quality model can be developed through stakeholder contributions that involve little additional cost. The movement to a high quality model will likely require additional investments in data collection as well as some sort of expert system or assistance. The Coos Bay experience suggests that the highest priority investments in time and data should focus on grid construction (particularly bathymetry collection throughout the entire estuary), monitoring of major tributaries, continuous deployment of appropriate environmental sensors, and development of the expertise to go from model-data analysis to correct diagnosis and remedy.

In addition to raw model data, an EMS should provide useful automated data analysis. A step towards this has been taken with MECCS, which can provide useful tools for summarizing and interpreting model results. The relationship between classification parameters and basic forcings (e.g. tides, winds and rivers) and other

parameters can provide important insight for the end users of an EMS. Finally, the use of classification parameters can allow quick, meaningful comparison between estuaries.

5. References

Banas, N.S., B. M. Hickey. "Mapping exchange and residence time in a model of Willapa Bay, Washington, a branching, macrotidal estuary." *Journal of Geophysical Research*. **110**, C11011, 2005.

Baptista, A.M. "CORIE: the first decade of a coastal-margin collaborative observatory," Oceans'06, MTS/IEEE, Boston, MA, 2006.

Black, Thomas L. "The New NMC Mesoscale Eta Model: Description and Forecast Examples." *Weather and Forecasting,* **9**, 265-278, 1994.

Blanton, J. "Energy dissipation in a tidal estuary," *Journal of Geophysical Research,* **74**, 5460-5466, 1969.

Blanton, J. "Distortion of Tidal Currents and the Lateral Transfer of Salt in a Shallow Coastal Plain Estuary." *Estuaries*, **24**, 467-480, 2001.

Borrego, J., J. Morales, M. de la Torre, J. Grande. "Geochemical characteristics of heavy metal pollution in surface sediments of the Tinto and Odiel river estuary (southwestern Spain)." *Environmental Geology*, **41**, No 7, 785-796, March 2002.

Center for Operational Oceanographic Products and Services. *Physical Oceanographic Real-Time System*. National Oceanic and Atmospheric Administration. http://tidesandcurrents.noaa.gov/ports.html (viewed October 10, 2006).

Crossett Kristen M. et. al. *Population Trends Along the Coastal United States: 1980 – 2008*. National Ocean and Atmospheric Administration. 2004. http://marineeconomics.noaa.gov/socioeconomics/Assesment/population/welcome.html (viewed February 4 2006).

Dettmann, E. "Effect of Water Residence Time on Annual Export and Denitrification of Nitrogen in Estuaries: A Model Analysis." *Estuaries*, **24**, 481-490, August 2001**.**

Dyer, K. *Estuaries: A Physical Introduction*. John Wiley & Sons, New York, 1997.

Edinger, John, Edward Buchak and Ventkat Kolluru. "Modeling flushing and mixing in a deep estuary." *Water, Air, and Soil Pollution*. **102**, 345-353, 1998.

Emery, William and Richard Thomson. *Data Analysis Methods in Physical Oceanography*. Elsevier Science, 1997.

Foreman, M.G.G**.** 1977 (revised 2004). Manual for tidal heights analysis and prediction. *Pacific Marine Science Report 77-10*, Institute of Ocean Sciences, Patricia Bay, 58 pp.

Garcon, V., Solzenbach, K., Anderson, D., "Tidal flushing of an estuarine embayment subject to recurrent dinoflagellate blooms." *Estuaries*, **9**, p. 179-187, September 1986.

Geyer, W.R. and R. Signell. "A Reassessment of the Role of Tidal Dispersion in Estuaries and Bays." *Estuaries*, **15**, 97-108, June 1992.

Grell, G., J. Dudhia, D. Stauffer. "A Description of the Fifth-Generation Penn State/NCAR Mesoscale Model (MM5)." NCAR Technical Note, NCAR/TN-398 + STR, 1995.

Hansen, D.V., and M. Rattray. "Gravitational Circulation in Straits and Estuaries." *Journal of Marine Research*, **23**, 104-122, 1965.

Hansen, D.V., and M. Rattray. "New dimensions in estuary classification." *Limnology and Oceanography*, **11**, 319-326, 1966.

Hickey, B.M. and N.S. Banas. "Oceanography of the U.S. Pacific Northwest coast and estuaries with application to coastal ecology." *Estuaries,* **26(4B)**, 1010-1031, 2003.

Hodur, R.M. "The Naval Research Laboratory's Coupled Ocean/Atmosphere Mesoscale Prediction System (COAMPS)." *Monthly Weather Review*, **135**, 1414-1430, 1997.

Ippen, Arthur T, and Donald Harleman. "One-dimensional analysis of salinity intrusion in estuaries," *Technical Bulletin 5, Committee on Tidal Hydraulics,* U.S. Army Corps of Engineers, Vicksburg, Miss., 7-48, 1961.

Jay, David and Dungan Smith. "Residual Circulation in Shallow Estuaries 2. Weakly Stratified and Partially Mixed, Narrow Estuaries," *Journal of Geophysical Research*, **95**, 733–748, 1990b

Kanamitsu, M., W. Ebisuzaki, J. Woollen, S-K Yang, J.J. Hinilo, M. Fiorino, and G. L. Potter. "NCEP-DEO AMIP-II Reanalysis (R-2)." *Bulletin of the American Meteorological Society,* **83**, 1631-1643, 2002.

Kantha, L., C. Clayson. "An improved mixed layer model for geophysical applications." *Journal of Geophysical Research*. **99**, 235-266, 1994.

Lane, A., D. Prandle. "Random-walk particle modeling for estimating bathymetric evolution of an estuary." *Estuarine, Coastal and Shelf Science*, **68,** 175-187, 2006.

Luketina, D. "Simple tidal prism model revisited." *Estuarine, Coastal and Shelf Science* **46**, 77–84, 1998.

MacCready, P. "Estuarine Adjustment to Changes in River Flow and Tidal Mixing." *Journal of Physical Oceanography*, **29,** 708-726**,** 1999.

MacCready, P. "Analysis Tools for Numerical Simulations of Estuaries For the NANOOS-IOOS Pilot Study", private communication, 2006.

MacCready, P. "Estuarine Adjustment." *Journal of Physical Oceanography.* In press.

Malone, T. C. "The coastal component of the U.S. Integrated Ocean Observing System," *Environmental Monitoring and Assessment* **81**, 51-62, 2003.

Martin, P.J. "Description of the Navy Coastal Ocean Model Version 1.0." Naval Research Laboratory. **85,** 2000.

Mesinger, Fedor, Geoff Dimego, Eugenia Kalnay, Perry Shafran, Wesley Ebisuzaki, Dusan Jovic, Jack Wollen, Kenneth Mitchell, Eric Rogers, Michael Ek, Yun Fan, Robert Grumbine, Wayne Higgins, Hong Li, Ying Lin, Geoff Manikin, David Parrish, Wei Shi. "North American Regional Reanalysis." *Bulletin of the American Meteorological Society* **87**, 343-360, 2006.

Monsen, N.E., Cloern, J.E. and Lucas, L.V. "A comment on the use of flushing time, residence time, and age as transport time scales." *Limnology and Oceanography* **47(5)**, 1545–1553, 2002.

National Geophysical Data Center. *GEODAS Search and Data Retrieval System*. National Oceanic and Atmospheric Administration. http://www.ngdc.noaa.gov/mgg/gdas/gd_sys.html (viewed January 1, 2005).

Oceans.US. *Implementation of the initial US Integrated Ocean Observing System, Part I: structure and governance*. 2003. http://Ocean.us/documents/docs/ioos_plan_6.11.03.pdf.

Oliveira, A., and A.M. Baptista. "Diagnostic modeling of residence times in estuaries." *Water Resources Research*, **33**, 1935-1946, 1997.

Oregon Department of Environmental Quality. *Laboratory Analytical Storage and Retrieval (LASAR)*. http://deq12.deq.state.or.us/lasar2/ (viewed January 17, 2005).

Oregon Geospatial Enterprise Office. *Oregon Geospatial Clearinghouse*. Oregon.gov. http://www.oregon.gov/DAS/EISPD/GEO/alphalist.shtml (viewed January 13, 2005).

Oregon Water Resources Department. *Oregon Surface Water Resources*. Oregon.gov. http://www.wrd.state.or.us/OWRD/SW/index.shtml#Surface_Water_Data_Links (viewed February 4, 2005).

Pawlowicz, R., B. Beardsley and S. Lentz. "Classical Tidal Harmonic Analysis Including Error Estimates in MATLAB using T_TIDE," *Computers and Geosciences*, **28**, 2002.

Pickard, GL. "Physical features of British Columbia inlets." *Transactions of the Royal Society of Canada*, **50**, 47-58**,** 1961.

Pritchard, DW. "Estuarine hydrography." *Advanced Geophysics,* **1**, 243-280, 1952.

Sanford, L.P., Boicourt, W.C. and Rives, S.R. "Model for estimating tidal flushing of small embayments." *ASCE Journal of Waterway, Port, Coastal and Ocean Engineering*, **118**, 635–654, 1992.

Simmons, HB. "Some effects of upland discharge on estuarine hydraulics." *Proceedings of the American Society of Civil Engineers*, **81** No. 792, 1955.

Socioeconomic Data and Applications Center. *National Aggregates of Geospatial Data Collection*. Center for International Earth Science Information Network. 2003. http://sedac.ciesin.columbia.edu/plue/nagd/place (viewed February 3, 2006).

Speer, P.E. and D.G. Aubrey. "A study of non-linear tidal propagation in shallow inlet/estuarine systems, part II: Theory." *Estuarine, Coastal and Shelf Science*, **21**, 207-224, 1985.

Umlauf, L., H. Burchard. "A Generic Length-Scale Equation for Geophysical Turbulence Models." *Journal of Marine Research*. **61**, 235-265, 2003.

US Army Corps of Engineers. *Portland District Coastal Surveys.* https://www.nwp.usace.army.mil/op/nwh/coast.asp (viewed January 17, 2005).

US Environmental Protetion Agency, Office of Water. *Nutrient Criteria Technical Guidance Manual: Estuarine and Coastal Waters*. October 2001. http://www.epa.gov/waterscience/criteria/nutrient/guidance/marine/ (viewed August 23 2006).

Wang, C, M. Hsu, A. Kuo. "Residence time of the Dansuei River estuary, Taiwan." *Estuarine, Coastal and Shelf Science,* **60**, 381-393, 2004.

Williams, B.L. "Flushing time calculations for the Upper Waitemata Harbour, New Zealand." *New Zealand Journal of Marine and Freshwater Research*, **20**, 455-465, 1986.

Willmott, C. "On the validation of models." *Physical Geography*, **2**, 184-194, 1981.

Zhang, Y., A.M. Baptista and E. Myers. "A cross-scale model for 3D baroclinic circulation in estuary-plume-shelf systems: I. Formulation and skill assessment." *Continental Shelf Research*, **24**, No. 18, 2004.

Zhang, Y.L., and Baptista, A.M. (submitted) " SELFE: A semi-implicit Eulerian-Lagrangian finite-element model for cross-scale ocean circulation," *Ocean Modelling*, 2007.

Biographical Information

Nathaniel Hyde grew up in southeast Portland, Oregon. He obtained a Bachelor of Arts degree in philosophy from the University of Notre Dame (1993). Training in the rigorous logic inherent in philosophy, combined with a desire to put bread on his table, lead naturally to computer science. Nate earned a Bachelor of Science in Computer Science from Portland State University (2002). A love of nature and an appreciation of mankind's dependence on healthy ecosystems caused Nate to jump at the opportunity to combine his computer science skills with environmental science by joining the Environmental Information Technology program at Oregon Health and Science University. He was awarded his Master of Science degree in Environmental Science and Engineering in June of 2007.